DESGIN AND MODELLING OF THE CLEAN ENERGY ROUTER WITH ADVANCED ADIABATIC COMPRESSED AIR ENERGY STORAGE SYSTEM

by

NI, CHENYIXUAN

A thesis submitted to

The University of Birmingham

for the degree of

DOCTOR OF PHILOSOPHY

Department of EESE

School of Engineering

The University of Birmingham

February 2023

Dedicated to

My Wife, Songyi Lee

My Mother, Ping Ni

and

My Father, Yunhao Chen

My Uncle， Shengwei Mei

ABSTRACT

The advanced adiabatic compressed air energy storage (AA-CAES) technology naturally has the flexibility of multi-energy storage and supply, which is discussed in this doctoral study as a demand for the current power system to provide more flexibility under the high proportion of sustainable consumption of renewable energy. The clean energy router (CER) can be suggested as a scheme based on the properties of AA-CAES. This thesis systematically studies the design, modelling, and operation methods of AA-CAES typical application forms, providing technical support for the operation control optimization planning of modern power systems (MPSs).

An overall architecture scheme of the CER based on AA-CAES is constructed to store and convert abandoned wind and solar energy to heating, cooling, and electricity, it offered a crucial technical solution for coordinating and fully utilizing a variety of clean energy sources. The thermodynamic model of AA-CAES can also be used to examine the CER scheme efficiency and transformation mechanism.

Based on the CER with high-temperature medium thermal storage and high-speed turbine power generation, a solar thermal collection and storage (STC) can be integrated to use the natural solar energy to further improve the overall efficiency. Combining the STC technology with AA-CAES, it can improve the capacity of multi-energy storage and supply. From the aspect of system design, it can ensure the flexible multi-energy storage joint supply capacity and high energy conversion efficiency of the system. Exergy efficiency can be applied to reflect the efficiency of the system to further analyze the performance of each subsystem and the overall system. For the economy of the system, an artificial intelligence algorithm – particle swarm optimization algorithm (PSO) is applied to obtain the minimum cost of the system through multi-objective optimization of heat and power supply units.

ACKNOWLEDGEMENT

Prior to anything else, I would like to thank and truly appreciate my supervisor, Prof. Xiao-Ping Zhang. He provided me with a lot of support and encouragement as I worked on my PhD thesis and research. He looks after my daily needs as a revered elder.

I would like to thank my wife, Mrs. Songyi Lee for her sincere love and support. I also would like to thank my parents, Mrs. Ping Ni and Mr. Yunhao Chen for their love, moral and financial support since I born.

I would like thank Prof. Shengwei Mei from Tsinghua University, China. With his guidance and support, I can get opportunity to participate and study about energy storage projects with his group. I also would like to particularly mention the following names: Prof. Xiaotao Chen, Dr. Xiaodai Xue, Prof. Laijun Chen, Dr. Xueling Zhang, Dr. Tong Zhang and Dr. Weiqi Zhang. Thank you.

Last but not least, I would like to thank my colleagues and friends: Dr. Junyi Zhai, Dr. Ying Xue, Dr. Cong Wu, Dr. Min Zhao, Dr. Jianing Li, Dr. Nan Chen, Dr. Conghua Yang, Mr. Longmao Fan, Mr. Kai Lin, Miss. Xin Ma and Mr. Shuailong Dai.

CONTENTS

LIST OF FIGURES

LIST OF TABLES

LIST OF ABBREVIATION

A-CAES	adiabatic compressed air energy storage
AA-CAES	advanced adiabatic compressed air energy storage
BESS	battery energy storage system
CAES	compressed air energy storage
CER	clean energy router
CHP	combined heat and power
CHPED	combined heat and power economic dispatch
CTS	cascade thermal storage system
D-CAES	diabatic compressed air energy storage
ED	economic dispatch
EH	energy hub
EI	energy Internet
ESS	energy storage system
ESSs	energy storage systems
EXE	electric-to-electric efficiency
HEX	heat exchanger
HTF	heat transfer fluid
IES	integrated energy system
LAES	liquid air energy storage

MPSs	modern power systems
MSTS	molten salt thermal storage
PHS	pumped-hydro energy storage
PTC	parabolic trough collector
PSO	particle swarm optimization algorithm
REN	regional energy network
RTE	round-trip efficiency
SMES	superconducting magnetic energy storage
STC	solar thermal collection and storage

LIST OF NOMENCLATURE

A	the heat exchange coefficient
A_{ab}	absorber surface, m^2
A_c	cavern wall surface area, m^2
A_g	glass tube surface, m^2
a_k	heat-only unit cost coefficient
A_T	heat-transfer tank surface area, m^2
A_{TES}	external surface area of heat reservoir, m^2
A_{SF}	mirror field area of the solar thermal collection system, m^2
a_z	cost coefficient for CHP units
b_0	constant, 0.3
b_1	constant, 1.8 or 0.36
b_2	constant, 1.4 or 1.06
b_k	heat-only unit cost coefficient
b_z	cost coefficient for CHP units
c_1	learning component, 5.94
c_2	learning component, 5.94
c_k	heat-only unit cost coefficient
c_p^a	constant pressure specific heat of air, J/(kgK)
c_p^{HTF}	constant pressure specific heat of HTF, J/(kgK)

C^{HX}	heat capacity ratio of the heat exchanger
c_p^{TES}	constant pressure specific heat of TES, J/(kgK)
c_z	cost coefficient for CHP units
C^{min}	minimum heat capacity of the heat exchanger
C^{max}	maximum heat capacity of the heat exchanger
C^{HX}	heat capacity ratio of the heat exchanger
c_R^p	heat capacity ratio of the air storage tank surrounding rock
C_v	constant volume specific heat, J/(kgK)
D_1	outer glass tube diameter, m
D_2	inner glass tube diameter, m
d_z	cost coefficient for CHP units
Ex	exergy
e_z	cost coefficient for CHP units
f_{tub}	the focal line length of the trough collector, m
f_z	cost coefficient for CHP units
$\dot{G}$	dimensionless reduced order flow
$g_{best_{i,n}}^{iter-1}$	entire swarm best position of ith particle
h	specific enthalpy of the air, J/kg
h_c	heat transfer coefficient, W/m^2K
H_d	heat demand, MW
H_k^h	heat-only generation, MW
H_z^c	combining heat and power units heat generation, MW
I_{AM}	incident angle correction coefficient

I_{DNI}	the surface of direct solar radiation, W/m^2K
k	adiabatic index, 1.4
$L_{endless}$	endless heat loss of the collector tube, J
L_{tub}	collector length, m
L_{Row}	the groove collector of row spacing, m
Lx	energy destruction
$\dot{m}_c$	air mass flow during charging, kg/s
$\dot{m}_e$	air mass flow during discharging, kg/s
$\dot{m}^{HTF}$	heat transfer fluid mass, kg/s
N	total number of decision variables
$\dot{N}$	reduced order speed
N_c	the stage of the compressor
NTU	heat transfer unit number of heat exchangers
P	pressure, bar
$p_{best_{i,n}}^{iter-1}$	best position of ith particle in previous iteration
P_d	power demand, MW
P_{loss}	power system transmission loss, MW
P_v^p	power-only generation, MW
P_z^c	combining heating and power units power generation, MW
Q	heat transfer coefficient of the air storage tank surrounding wall
Q_{Loss}	convection loss of heat collecting link, W
Q_s	input of solar thermal power, W
Q_{SF}	absorb of solar thermal power, W

r	velocity value control component
r_1^n	random numbers, interval (0, 1)
r_2^n	random numbers, interval (0, 1)
R	specific air constant, J/kg
R_g	specific air constant for isothermal air storage tank, J/kg
R_W	radius of the air storage tank, m
s	entropy, kJ/K
t_0	initial time, h
T	temperature, K
T_0	initial air temperature, K
T_1	external glass tube surface temperature of the receiver, K
T_2	inner glass tube surface temperature of the receiver, K
T_{amb}	ambient temperature, K
T_{RW}	rock wall temperature, K
U	heat exchange size
$\mathcal{U}$	heat-transfer tank surface area, m^2
u	specific internal energy of air, W
U_{TES}	heat transfer coefficient between heat reservoir and environment
V	volume, m^3
V_i^{iter}	velocity vector
W	power, W
x_n^{min}	minimum limits of variables
x_n^{max}	maximum limits of variables

X_i^{iter}	position vector
Z	air compressibility factor, 1
Greek symbols	
α	impact factor of the influence of the change rotation speed change
α_{shadow}	performance degradation coefficient of shadow groove collector array
α_v	coefficient of power-only units cost function
β	compression ratio
β_v	coefficient of power-only units cost function
γ_v	coefficient of power-only units cost function
ε	void fraction
ε_1	chosen coating emissivity
ε_2	glass tube emissivity
η	isentropic efficiency
η_{SF}	efficiency which solar radiation is converted into heat energy
$\eta_{SF,opt}$	optical efficiency of the heat mirror field
$\eta_{SF,ab}$	absorption efficiency of trough heat collecting
η_{HX}^p	pressure retention factor of the heat exchanger
μ_{SF}	available concentrating area, m^2
ξ	solar zenith angle
ρ	density, kg/m^3
ρ_{av}	average air density during the operation, kg/m^3
ρ_R	density of the air storage tank surrounding wall, kg/m^3
σ	Stefan-Boltzmann constant

ϕ	actual heat capacity
ω	inertia coefficient

Subscripts and superscripts

a	air
AST	air storage tank
c	process of compression
cav	cavern
COM	compressor
$cond$	conduction
$conv$	convection
e	process of expansion
env	environment
i	stage
in	inlet
j	subsystem
rad	radiation
TES	thermal energy storage
TUR	turbine
TV	throttle valve

CHAPTER 1 INTRODUCTION

1.1 Research Background and Motivation

The most fundamental way to ensure energy security and facilitate sustainable development of new energy in the current context of global warming is through the scientific and effective use of renewable energy. As representative renewable energy sources such as wind and solar power have matured, their installed scale has grown over the last ten years. According to the World Wind Energy Association survey [1], since the beginning of the twentieth century, the installed capacity of wind power worldwide has increased at a rate of more than 10% per year. As shown in Figure 1.1, total installed capacity will have increased to 955.84GW by the end of 2022.

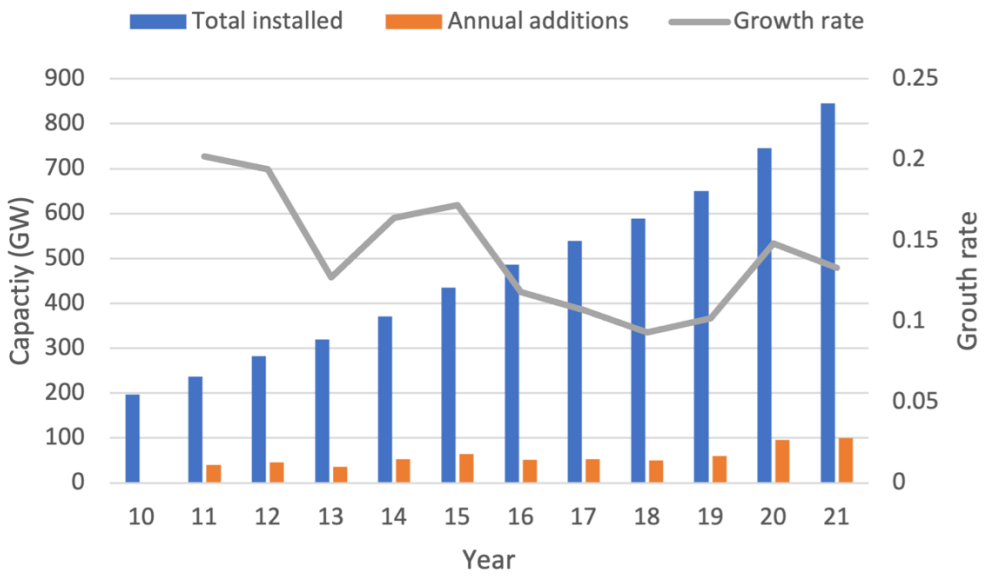

Figure 1.1. Statistics of world installed wind power capacity, 2010-2022

However, while renewable energy capacity continues to increase, renewable energy consumption also does as well, which presents a significant obstacle to the sustainable long-

term expansion of renewable energy [2]. The development of MPSs with a high percentage of renewable energy penetration has met certain challenges, mainly manifested as the lack of flexible resources for MPSs, resulting in the difficult consumption of clean energy. The efficient absorption of renewable energy requires not only the absorption of its electricity form but also the absorption of its heat form and other forms of energy [3]. It can realize the absorption of heat, electricity, and other multi-energy forms, which brings opportunities for the realization of efficient consumption of renewable energy. Therefore, it is necessary to seek new renewable energy absorption ideas from the perspective of the integrated energy system (IES).

1.11 Fluctuating Renewable Energy Sources

In the future, the use of fossil fuels and the release of carbon dioxide will be two of the biggest problems that people will have to deal with. The use of renewable energy sources creates significant problems for the long-term growth and health of renewable energy sources which are the characteristics of renewable energy (fluctuation and intermittence). The trend toward developing renewable energy like wind power generation will grow because it is better for development without carbon emissions [4]. However, the problem of how to utilize the wind power will become more and more significant, and the serious problem of wind curtailment will not only waste a lot of resources, but it will also affect the long-term development of a healthy power system in the wind power industry and in MPSs.

Numerous challenges must be overcome to create MPSs that have a high penetration of renewable energy. Because MPSs lack flexible resources, these difficulties are primarily manifested in the difficulty of clean energy use [5]. To be more precise, due to the high output instability and erratic fluctuations of wind energy, it is necessary to absorb both the thermal

and electric forms of renewable energy to fully utilize them. The primary focus of renewable energy absorption at this moment is on electric energy, which to some extent restricts the ability of renewable resources such as the absorption of energy [6]. For example, thermal power heating units are powered by combustion heat during the winter heating season. Due to the influence of the heating season with strong wind season and low load, and other factors, most of the abandoned wind power grid occurs in the winter heating season [7]. The IES in the MPEs can effectively absorb renewable energy not only in the form of electricity, but also in the form of heat and other multi-energy sources which brings the possibility of effectively absorbing renewable energy. Therefore, it is equally vital to seek for new scheme for using renewable energy from the viewpoint of an IES.

On the one hand, the growing popularity of variable renewable energy sources, as well as the resulting injection of variable power into the grid, creates several challenges that must be addressed [8]. Furthermore, the grid must account for this fluctuating power. In order to overcome the technical barriers that are impeding the growth of variable renewable energy sources, energy storage system (ESS) technologies are receiving increased attention in the form of research and application. The findings of these studies are currently insufficient to solve the complex energy fluctuation scenarios, and implementation is still in its early stages.

On the other hand, although renewable energy has great potential in solving problems such as sustainable development and environmental protection, most renewable energy has limitations such as scattered distribution and poor controllability, which makes it hard to develop and utilize in a large-scale and centralized manner under the dispatching and control mode of the traditional power grid [9]. Energy Internet (EI), a hybrid of Internet technology and renewable

energy, provides a feasible strategy for optimizing renewable energy use in consideration of Internet technology rapid development and renewable energy potential for widespread deployment [10]. EI can be conceptualized as a novel type of power network node that integrates progressive power electronics technology with information technology, intelligent control technology, distributed energy collecting and storage devices, and a wide variety of loads to establish a system of mutually beneficial energy sharing and exchange. The term "energy exchange and sharing network" is used to describe this type of power grid node.

1.1.2 Large-scale Energy Storage Systems

The method of storing energy is a crucial component of the smart grid and a key enabler for renewable energy sources. Improving the adaptability, economic feasibility, and security of conventional electricity distribution networks is a crucial responsibility. A crucial task is to increase the adaptability and affordability of the traditional power systems. It can simultaneously provide support for demand response, frequency modulation, and other services for power grid operation. Energy storage systems (ESSs) are a foundational technology that expedite the efficiency of using and storing renewable energy sources like wind and solar [11]. The utilization of ESSs also facilitate the transition from fossil fuels to renewable energy sources. Its adaptability and aptitude for sharing mean it might help build an EI premised on the expansion of renewable energy sources by drastically reducing the energy wasted during the generation of that energy.

Table 1.1 The characteristics of electrical energy storage technologies

Technology	Battery (Lead-acid)	Flywheel	PHS	CAES	SMES	Supercapacitor	Chemical storage (Hydrogen fuel cell)
Storage capacity (MW h)	0.001-40 [12], more than 0.005 [13]	0.0052 [22], 0.75 [20], up to 5 [23]	500-8000 [14], 180 Oki-nawa PHS [24, 77]	~<1000 [10], 580 & 2860 [26, 27]	0.0008 [20], 0.015 [29], 0.001 [30]	0.0005 [20]	0.312 [25], developing 39 [33]
Power rating (MW)	0-20 [14], 0-40 [15], 0.05-10	<0.25 [14], 3.6 [22], 0.1-20 [13,177]	100-5000 [14], 30 [24], <4000 [18]	Up to 300 [14], 110 & 290 [28], 1000 [20]	0.1-10 [4, 14], ~1-10 [20]	0-0.3 [14], ~0.3+ [26], ~0.001-0.1 [20]	<50, <10, 58.8
Daily self-discharge (%)	0.1-0.3 [14], <0.1 [16], 0.2 [17]	100 [14], >29% per hour [16]	Very small [14, 25]	Small [14], almost zero [25]	10-15 [14]	20-45 [14], 5 [10], 10-20 [31]	Almost zero [15, 25]
Discharging efficiency (%)	85 [18]	90-93 [18]	~87 [18]	~70-79 [18]	95 [18]	95 [18], up to~98 [32]	59 [18]
Response time	Milliseconds, <0.25 cycle [15]	<1 cycle [18], seconds [21]	Minutes [18], not rapid discharge [21]	Minutes [18]	Milliseconds, <0.25 cycle [18]	Milliseconds, <0.25 cycle [18]	Seconds, <0.25 cycle [18]
Maintenance and operating cost	~50 $/kW/year [19]	~0.004$/kWh [20], ~20$/kW/year [19]	0.004$/kWh [20], ~3$/kW/year [19]	0.003$/kWh[20], 19-25 $/kW/year [19]	0.001$/kWh [20], 18.5$/kW/year [19]	0.005$/kWh [20], ~6$/Kw/year [18]	0.0019-0.00153$/kW [34]
Commercial Maturity	Commercialized	Early commercialized	Mature	Commercialized	Demo/early commercialized	Developing/demo	Developing/demo

The three categories that can be used to classify ESSs are mechanical energy storage, electromagnetic energy storage, and chemical energy storage. The pumped-hydro energy storage (PHS), the compressed air energy storage (CAES), and the flywheel energy storage are examples of mechanical energy storage [35]. The term “chemical energy storage” is most frequently used to refer to battery energy storage system (BESS), which can refer to a range of battery types including lead-acid battery, flow battery, sodium-sulfur battery, and lithium battery. In this chapter, lead-acid battery is selected as the representative of BESS and hydrogen fuel cell as one of the chemical energy storage technologies to describe the charatersitics. Superconducting magnetic energy storage (SMES) and supercapacitor energy storage are examples of electromagnetic energy storage. The power system cannot be fully served by any one energy storage technology. Therefore, the characteristics of each technology should be fully considered while choosing the optimal choice. Table 1.1 demonstrates the capabilities and traits of several energy storage methods [36]. This chapter focused on the features and details of large-scale ESSs.

The PHS power station is equipped with two reservoirs, upper and lower reaches. When the off-peak power is surplus, the water from the lower reaches of the reservoir is pumped to the upper reaches of the reservoir for preservation. The water that is kept in the upstream reservoir can be used to produce electricity when there is a peak load gap. The PHS is the most developed and cost-effective way to store energy on a large-scale ESS technology. In addition, it is part of a group of technologies that are widely used to store large amounts of energy [37]. The total installed capacity in the world has surpassed 150,000 MW. The drawback is that it has a slow response time, is poorly able to handle load fluctuations, and is significantly constrained by geographical factors, transformation efficiency and other factors. PHS plants can be used to

black start, control grid frequency, provide reserve capacity and enhance the operational efficiency of thermal and nuclear power plants.

CAES is a kind of ESS technologic which use residual electric to store compressed air into storage tank at the off-peak time and release the high-pressure air to actuate the turbine to generate electricity when the power is needed. While the air consumption of CAES is 40% less than that of traditional air turbines with good safety factors and extended service lives, the fuel consumption can be reduced by half compared to peak-regulating air turbine units [38]. Since its creation is constrained by unique topographical circumstances like caves and mines, CAES is more suitable for large-scale systems [39]. However, with the development of CAES air storage device technology, air storage tank and steel pipe tank (SPT) for small and medium-sized CAES can be used, which will no longer affect the use and development of CAES by geographical location. Compared with PHS, CAES is not limited by geographical location and does not have an ecological impact to match the current goal of zero carbon emission. Therefore, large-scale CAES technology with clean performance can be selected as the core of the CER.

1.1.3 The Consumption of Fluctuating Renewable Energy Sources through EESs

Intermittency, fluctuation, and randomness are all characteristics of renewable energy generation that can lead to some problems for the reliability of the power grid. Grid-connected facilities that generate a high share of renewable energy provide a challenge to the transmission capacity of the power system on the generating side of the grid [39]. The proportion of reserve capacity provided by existing conventional units is insufficient due to the rapidly rising installed capacity of renewable energy, making it impossible to account for the capacity of

renewable energy and the system stability, which necessitates the use of numerous renewable energies. Under the huge challenge of peak regulation, if only the intervention of renewable energy is limited, the utilization rate of clean energy will be decreased, and the absorption capacity of renewable energy cannot be improved.

The contradiction between the peak regulating pressure which cannot be ignored and the power supply structure which cannot be adjusted in a short time, it is one of the biggest limitations of renewable energy at present. If the system power structure is improved, the impact of renewable energy on treatment can be improved, and the grid restrictions on renewable energy that is connected to the grid can be settled [3]. At the same time, the structure of the grid, the location of the power source, the grid capacity, and how the demand is distributed all affect how much power can be sent through it. In the past, the addition of a transmission line and an active/reactive power supply were the main ways to increase the amount of data sent. These two additions were both provided but it is not a very flexible solution. However, ESSs have features of high energy, flexible installation, fast charging and discharging speeds, which allow it to smooth out the fluctuations of renewable energy, improve the peak regulating capacity of generating units, and increase the amount of renewable energy used without changing the structure of the power grid. In the existing studies, the energy storage device is different from other devices in that it can consider both charging and discharging functions and can timely respond to the volatility of new energy. When the system needs power, it can respond more quickly than conventional units, not only responding to grid demands but also allowing conventional units enough buffer time. When the compound in the system cannot absorb the power in the grid, it can be stored in real-time and wait for the appropriate processing time.

At present, the research on ESS configuration is mainly focused on two aspects of energy storage planning which consider only the factors of the ESS and comprehensively consider the overall system operation. When considering only one aspect of the ESS, the power and capacity design of the ESS based on power quality is the preferred configuration [40]. In the meantime, a significant amount of renewable energy is being integrated into the grid and made fast response for usage. As a result, to enhance the regular and steady functioning of the grid, the majority of power plants should increase the flexibility of their traditional units. The emergency response equipment must be able to provide several supplemental services to promote the usage of renewable energy sources. When relying only on power-generating machinery that is powered by renewable energy sources, it is difficult to ensure the stability of the operation of the power grid. On the other hand, ESSs offer greater adaptability than more traditional power plants. It has the capacity to increase the system's overall peak-regulating capacity, assist conventional units in peak-regulating, and achieve peak loading shift on its own to better promote the promotion of renewable energy consumption.

In this thesis, the traditional CAES technology has shortcomings such as energy input and absorption forms (only electric energy), low thermal storage temperature (water is the general thermal storage medium), and the need for supplementary combustion of fossil fuels and environmental pollution caused by carbon emissions. On the basis of the AA-CAES system with a seven-stage expansion and a two-stage compression system, the research and development of integrated molten salt thermal storage (MSTS) and compression heat recovery technology is conducive to the improvement of its comprehensive energy utilization efficiency. Based on this, the system integrates the STC technology which can absorb and integrate solar

energy into thermal energy to improve the intake air temperature on the power generation side, to further promote the comprehensive energy utilization rate.

1.2 Research Objectives

1.2.1 Objectives

Based on the literature review in Chapter 2, research gaps and research directions have been identified in Section 2.4. And based on these gaps and research directions, the following research objectives are proposed:

- From the design concept of the router on the Internet and the concept of no emission, the concept and scheme of the energy router in the EI are proposed, and then the CER based on AA-CAES is designed.

- To deal with the problem of sustainable consumption of the high proportion of renewable energy, application of AA-CAES with conventional flexibility of power storage, multi-energy supply and multi-energy storage can be applied to the CER is investigated.

- To deal with the function conversion of internal components and multi-energy coupling mechanism of the CER based on the AA-CAES system, the mathematical model of AA-CAES is established, which will be the theoretical basis of this thesis.

- To further improve the overall performance of the CER, ST-AA-CAES with occasional external heat sources are proposed to further improve the comprehensive energy efficiency of the system and the mathematical model of its core STC is studied.

- To efficiently verify the economy of the CER, application of artificial intelligent algorithms the CER is investigated.

1.2.2 Scientific Contributions of the Thesis

The main contributions of the work shown in this thesis are summarized as follows:

- A new concept of the CER based on the AA-CAES system is proposed. The modelling and analysis of the AA-CAES system with 7-stage compression and 2-stage expansion is achieved.

- The efficiency of the CER's IES with a combination of cooling, heat and electricity are analysed.

- A new system of solar-thermal assisted the CER is proposed. The thermodynamics analysis and exergy analysis of this system are achieved.

- The utilization of PSO to analyse the economic characteristics of the CER is achieved.

1.3 Thesis Outlines

The outline of the thesis is described as follows:

Chapter 2 illustrates the literature review of existing different types of CAES system and their development. The corresponding reviews on CAES system of different storage and air storage methods are presented in detail. The literature on existing conventional CAES power station is also presented.

Chapter 3 proposes the concept and framework of the CER, which draws inspiration from the design concept of the processor on the internet and the concept of the energy hub (EH), and then designs the architecture of the CER based on AA-CAES. To verify the characteristic of the CER in Chapter 4 and the improved CER in Chapter 5, the mathematic model of its core AA-CAES should be presented.

Chapter 4 aiming at AA-CAES, the core problem of the CER, a thermodynamic simulation system based on AA-CAES is established, the heat exchange and adiabatic conditions of the AA-CAES system is analyzed. Combined with the proposed simulation model, the internal thermodynamic characteristics, and overall functional characteristics of the typical AA-CAES system under different operating conditions are analyzed based on the mathematic model of the AA-CAES system in Chapter 3. On the basis, the CER coupled with the STC will be presented in Chapter 5.

Chapter 5 aiming at the core problem of energy efficiency improvement of the STC. Based on the CER presented in Chapter 4, the design of the STC process combined with the external heat source is established. There are four aspects of the system that can be described, heat collection approach, heat storage medium, multi-energy storage and supply and thermodynamic simulation and exergy analysis are used to verify the performance of the system.

Chapter 6 focuses on the analysis of the improved CER in Chapter 5 and using PSO to solve the economic problem of this system.

Chapter 7 concludes this research, highlights the innovative contributions and discusses possible future works.

CHAPTER 2 LITERATURE REVIEW

2.1 Introduction

ESSs can make the energy system more effective, safe, and cost-effective [36][41]. It does this by storing electric energy in a certain medium and then using that energy to produce electricity when it is needed. ESS is one of the main elements for the renewable energy consumption because more and more renewable energy will be used. It is also a key technology for making conventional power systems, distributed energy systems, and the smart grid more efficient, safe, and cost-effective [36]. Based on this, ESS technologies are well-known area for research and investment in the energy and power industries. The creation of an electric energy storage system is essential for the widespread use of renewable energy sources, as well as a practical means of enhancing the effectiveness, security, and economics of the conventional power system. Currently, electricity storage technologies include flywheel, supercapacitor, secondary battery, flow battery, SMES, PHS, and CAES [35].

However, based on factors of capacity, energy storage cycle, energy density, charge and discharge efficiency, life span, operation cost and environmental protection, there are two kinds of ESSs that have been operated in large-scale commercial systems: PHS and CAES [42][43]. For PHS, it is strongly dependent on the geographical environment and natural resources, and will destroy the ecological environment, such as water evaporation and water freezing. For CAES, it releases high-pressure air to generate power through the turbine by releasing compressed air that has been used to store excess electric energy. It has a wide range

of applications in the generation, transportation, and consumption of electric energy and is currently a popular large-scale ESS technology for research and development.

CAES is a form of ESS that is derived from the technology of gas turbines. After the compressor squeezes the air, it is burned with the fuel in the combustor to heat it up. The heated high-pressure air then goes into the turbine to produce electricity [44]. Figure 2.1 shows the operation details of gas turbine. The gas turbine works on the idea that after the air is compressed, it is burned with the fuel in the combustor to heat up. Since about two thirds of the work done by the turbine is used by the compressor, therefore, the net amount of work done by the gas turbine is much less than that done by the turbine.

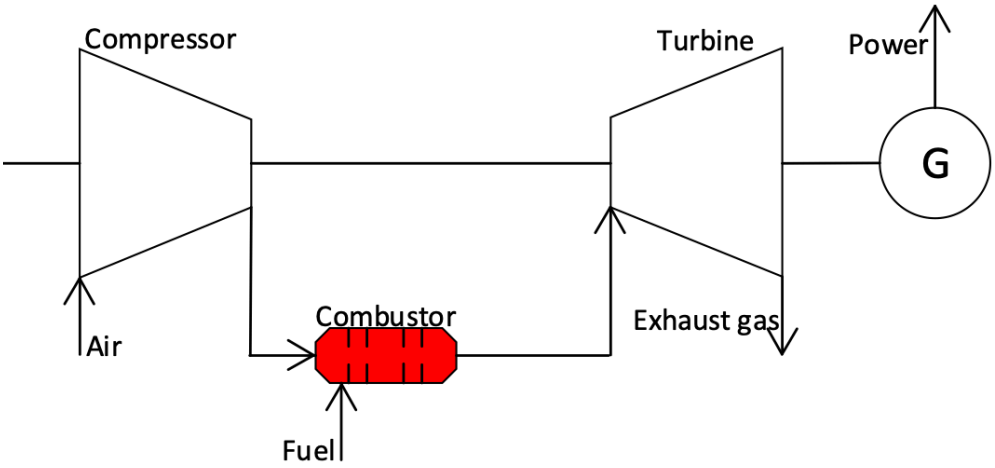

Figure 2.1. The operation of gas turbine

In Figure 2.2, the CAES system's compressor and turbine are not operating simultaneously. The CAES system uses electric energy during energy storage to compress and store air in the air storage tank. The storage compressed air from the air storage tank is discharged during energy release and enters the gas turbine combustor where it burns with fuel to drive a turbine and produce electricity [45]. Compressor will not use the output work of the turbine during the energy release period because energy storage and release are not occurred at the same time. As

a result, the CAES system may produce more than twice as much power as a gas turbine system using the same amount of fuel [46].

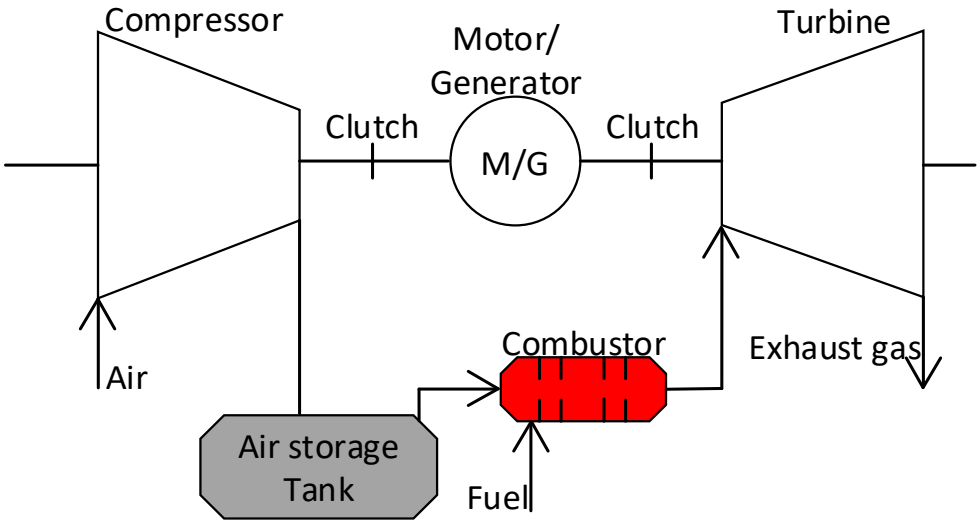

Figure 2.2. The working principle of CAES

The above is the origin and principle of traditional CAES technology. This chapter will introduce and review the principles of different types of CAES technologies for demonstration projects. Meanwhile, the application and function of CAES technology will also be reviewed.

2.2 The Technology and Current Research of the CAES System

As a physical energy storage method, CAES has the characteristics of large capacity, low cost, long life and abundant energy interface types. Since the 1940s, when the American Gay Frazer W proposed the CAES technological process [47][48], relevant research institutions and scholars have successively developed diabatic compressed air energy storage system (D-CAES), liquid air energy storage (LAES) and AA-CAES focusing on the key issue of improving energy storage efficiency.

2.2.1 Diabatic CAES System

The principle of the D-CAES works is shown in Figure 2.3 [49]. The compression heat that is lost when compressed air is stored cannot obtain used again. As part of the process of expansion, fuel is added to high-pressure air to make it full again so that the system can continue to work. D-CAES usually has a power range between 100 and 300 megawatts, and its energy storage efficiency ranges from 40% to 60% and make it suitable for large-scale energy storage [50].

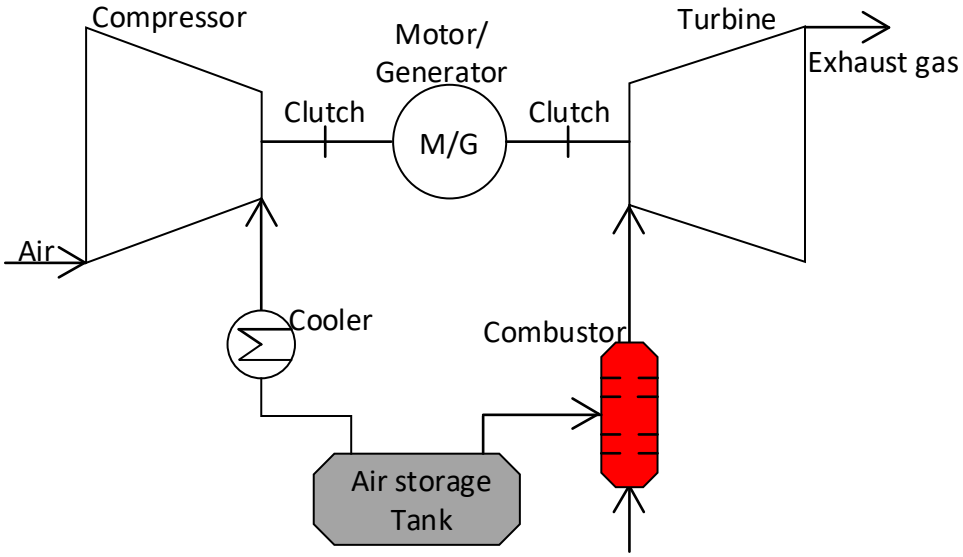

Figure 2.3. The working principle of D-CAES

D-CAES is mainly composed of compressors, coolers, air storage tank (underground cave or air storage tank), turbine and combustion chamber. Energy storage and energy release modalities constitute its fundamental operation. D-CAES operates in the energy storage mode when there is an off-peak period. The high-pressure air output is currently held in the air storage tank while D-CAES drives the compressor using off-peak period power. D-CAES runs in the energy release mode when the power demand is needed. In the combustion tank, natural air and high-pressure air are combined after being released from the air storage tank. High enthalpy

air heat flow enters the multi-stage turbine and drives the generator to produce electricity. Air compressor is generally selected with intercooler multi-stage compressor, as far as possible to reduce the intake temperature into all levels of the compressor and the power loss of the compressor. However, due to the low energy storage density of air, D-CAES require huge air storage space. In the 1940s, Stal Laval proposed the technical scheme of using underground caves to store high-pressure air [50]. Only with the support of geographical conditions such as natural air mines or salt caves, it can make CAES have more application advantages.

Table 1.2 Comparison of technical parameters of commercial CAES power station

CAES Power Station	System efficiency	Output Power MW	Range of Air Storage Tank MPa	Cave Depth m	Volume m^3	Charging /Discharging h	Respond Time min	Natural Gas Consumption m^3
Huntorf	42%	32	4.3~7	600	310000	12/3	6	100000
McIntosh	54%	110	4.5~6.6	450	560000	41/26	9	350000

Currently, Huntorf Power Station in Germany and McIntosh Power Station in the United States are the two largest D-CAES power stations in commercial operation. The main technical parameters are shown in Table 1.2. Compared with Huntorf power station, McIntosh Power Station adds a regenerator in the expansion power generation unit, which uses the flue air waste heat discharged from the low-pressure expansion machine to preheat the air released from the salt storage hole, and then enters the high-pressure combustor for combustion. McIntosh power station, which adopts this regenerative technology, saves 22% to 25% fuel compared with Huntorf power station when generating the same amount of electricity, and the efficiency increases from 42% to 54% [49]. The design and operation experience of McIntosh power

station show that increasing the inlet air temperature of the expansion generator is one of the effective means to improve energy storage efficiency.

America announced the Norton Energy Storage demonstration project in 2009. It consisted of 9 × 300MW units the CAES demonstration power station, which has a total installed power of 2700 MW [50]. The abandoned limestone mine is used for the air storage tank, the air storage volume is $9.57\times 10^6\ m^3$, the design unit power generation heat consumption is 4558 kJ, the compressed air power consumption is 0.7 kWh. However, Norton's CAES station has not been commercialized yet.

Bethel Energy Storage Center is currently building a CAES power station. The power station plans to use underground rock salt layers to build air storage caves to store compressed air and reduce emissions through advanced exhaust emission control technology [48]. The designed power of the system is 317 MW, and the startup time from the cooling standby state to full power is 0.16 h, which can quickly respond to the peak regulating demand of the grid.

It should be noted that the output power of the above D-CAES power stations, which have been built and are under construction, is usually MW level is mainly used to adjust the peak-shaving difference of the power grid, and there is a dependence on natural gas and geological conditions, which is contrary to the current zero carbon emission.

2.2.2 Liquid Air Energy Storage System

Scientists from the United States and other countries have written about the technological path of the LAES is depicted in Figure 2.4 [50]. The proposal of this system makes this technology less reliant on mines and salt caverns by increasing the density of air energy storage. During

the energy storage process, the progress of the compression and cooled, and then heated liquid air is stored in the liquid air storage tank that has been liquefied. The compression creates heat, which is stored in a tank made for high-temperature thermal storage mediums. When energy is released, the high-temperature thermal storage medium heats and vaporizes liquid air, which causes its volume to rapidly expand and power the turbine expansion generator that produces electric energy. In addition, the low-temperature thermal storage medium tank stores the cooling energy capacity produced by the expansion process, which is required to cool the high-pressure air produced by the compressor. In order to guarantee the steady and dependable performance of the device, the system energy consumption is decreased [51] [52].

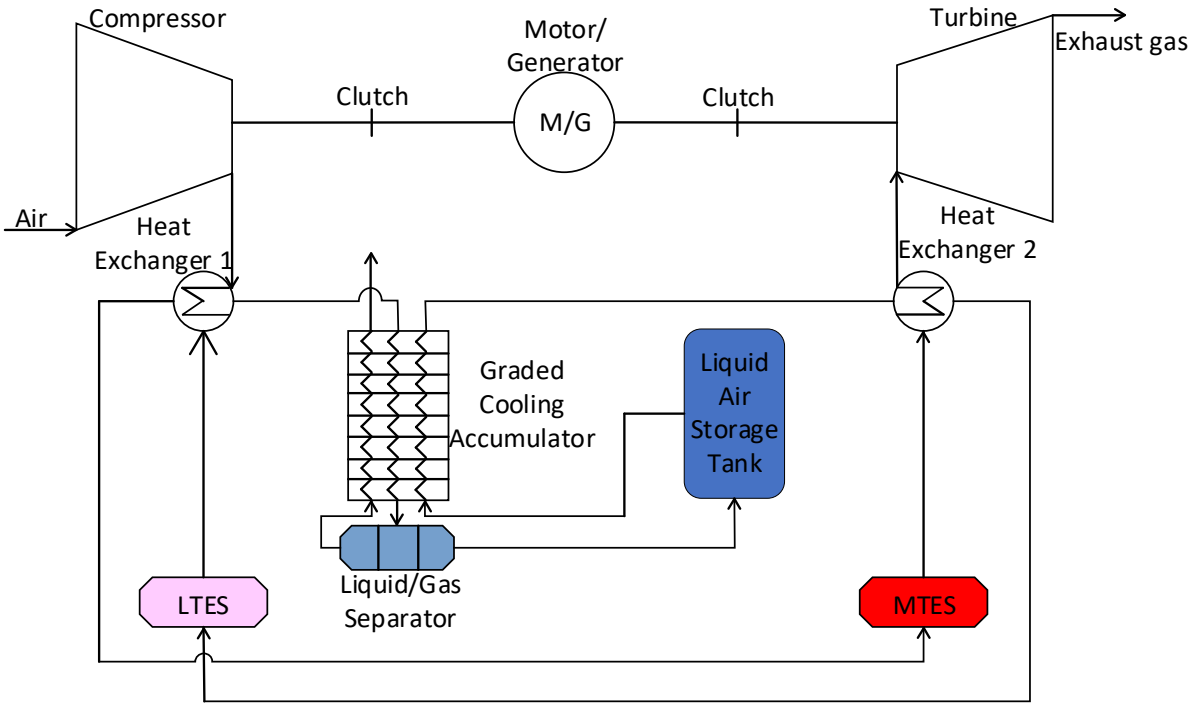

Figure 2.4. The working principle of LAES

On the other hand, the LAES technology uses liquid air at a low temperature to store energy. Liquid air has the following properties, which help to increase the amount of energy storage. 1) The energy density is high (between 60 and 120 Wh/L), it has a low storage pressure

(between 0.5 and 1 MPa), and it makes the size of storage tank smaller. The single power generation amount is between 10 MW and 200 MW, the power generation startup time is 15 minutes, and the power generation regulation time is 3 minutes. This can be used for secondary frequency modulation of the power grid; 2) To enhance the efficiency of preheating, the technology of recycling waste heat during the storage process and waste cooling energy during the generation process is used; 3) The technology of recycling waste heat in the storage process and waste cooling energy in the generation process is adopted to improve the power generation efficiency, and the expected operation efficiency can reach 50 to 60%.

LAES mainly includes four subsystems: compressed liquefaction, thermal storage system, cooling storage and expansion power generation, and key equipment that will directly determine the operational efficiency of the LAES system [53]. The main function of the compression and liquefaction subsystem is to compress and purify the air, cool it through the cooling tank and the expansion refrigerator, and liquefy the high-pressure air. The compression heat is stored by heat exchange and the cooling energy of the cooling storage subsystem is fully utilized to enhance the efficiency of the liquefaction progress.

The thermal storage subsystem is required to recover the heat of compression produced by compressed air and then meet the thermal energy demand for expanding liquid air. When releasing heat, it is necessary to maintain the original heat energy grade (the heat release temperature should be as similar to the heat storage temperature as feasible), and the temperature fluctuations of the heat release process are minimal. The thermal storage requires the storage medium to store high-quality heat energy. Therefore, the initial heat energy grade must be maintained to the greatest extent possible while releasing heat.

The cooling storage subsystem should meet the cooling capacity needs of the air liquefaction process. It also helps to recover and store the cooling energy from liquid air is turned into air during the power production process. For the progress of cooling storage, the medium that can be used to store the cooling energy must be able to meet the needs of low-temperature operations. At the same time, the stored cooling capacity should keep the original grade (the temperature during the release of cooling should be approximated by storage temperature), and the temperature fluctuation during the release of cooling should be stable. The flow of the thermal/cooling storage subsystem is shown in Figure 2.5. The expansion power generation subsystem uses high-pressure air to perform adiabatic expansion in the turbine, and the work capacity of unit mass air is improved by heating air between stages.

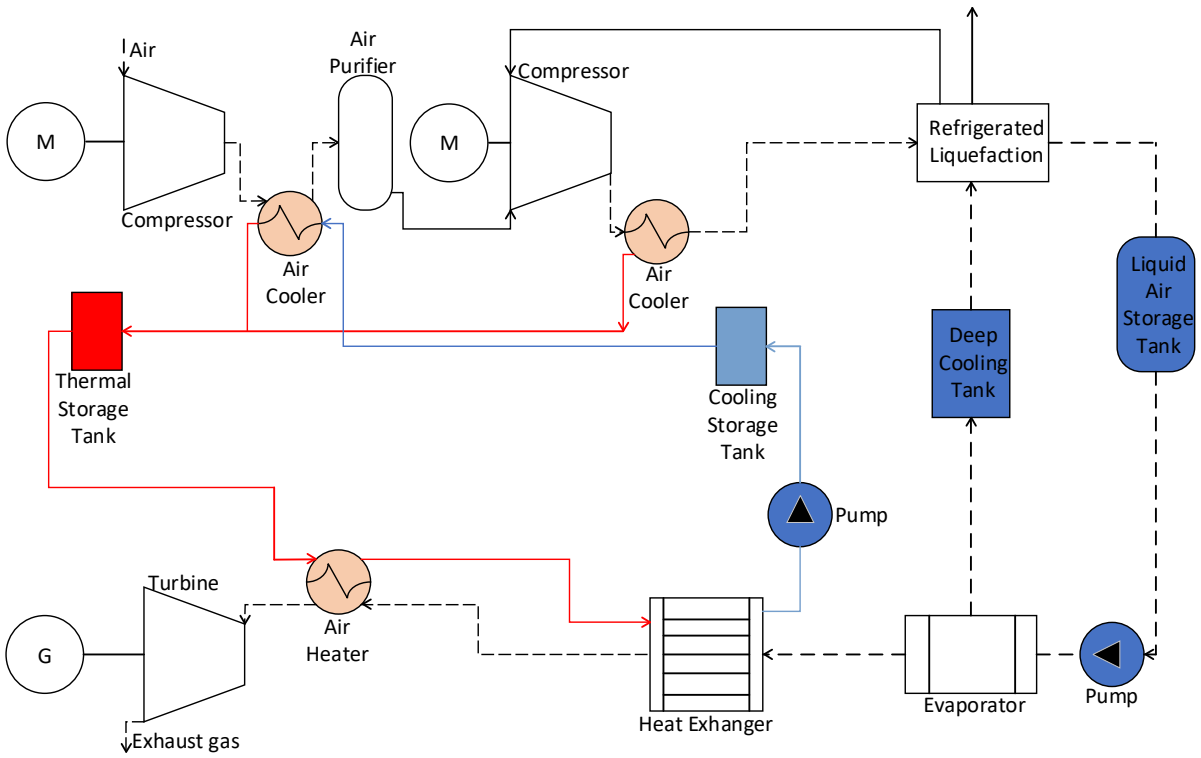

Figure 2.5. Diagram flow of cooling /heat subsystem

There have been two LAES demonstration projects in the world. One is the LAES demonstration project in London, UK, built in 2010, with a capacity of 350 kW×7 h [54]. The second is the CAES demonstration project in Manchester, UK, which is currently under construction. The capacity of the project is 5MW×3h, and the design overall efficiency is 55%. LAES technology integrated air liquefaction and gasification units, therefore, the energy release response rate of the LAES is lower than that of the conventional CAES system.

2.2.3 Advanced Adiabatic CAES System

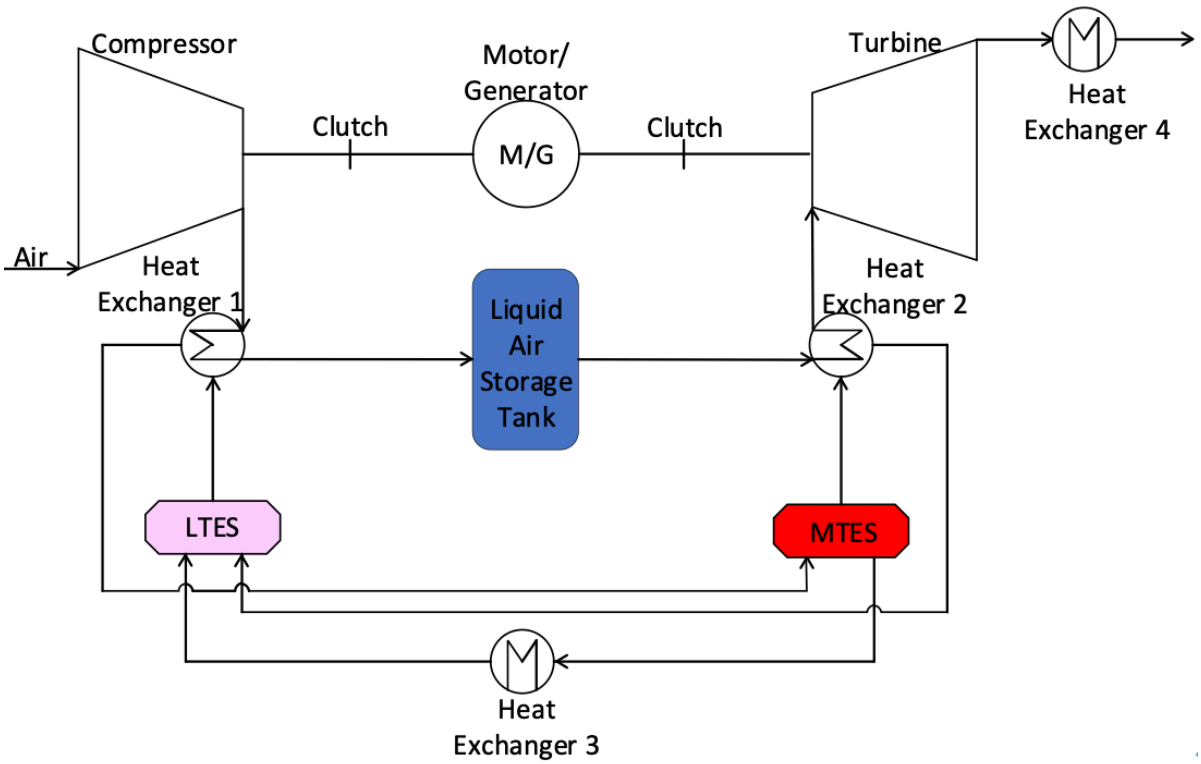

Figure 2.6. Diagram of AA-CAES

M. J. Hobson proposed AA-CAES for the first time in 1972 [55][56] in view of the shortcomings of the D-CAES system, such as its dependence on fossil fuels, lack of compression heat collection, carbon emission and low energy utilization. Its structure is shown

in Figure 2.6. Ideally, AA-CAES does not exchange heat with the environment, and the energy input and output are only electricity.

When compared to D-CAES technology, AA-CAES is distinguished by the addition of a heat regenerative mechanism. The heat recovery system is employed during compressed energy storage to gather and store the compression heat produced during the operation. The regenerative system will use the stored heat energy to storage compressed air, actuate the turbine to generate power, and it can also supply heat to local customers when the energy is released through expansion. Because AA-CAES realizes efficient conversion and exploitation of diverse energy forms of air-heat-power, AA-CAES does not require the use of fossil fuels during the entire cycle process.

The main elements influencing the energy storage efficiency of the system are thermal storage capacity, thermal storage temperature, and heat exchange efficiency of AA-CAES. Its energy storage efficiency is anticipated to reach 70% if a high-temperature compressor is utilized to increase the thermal storage temperature [57]. However, limited by the high-pressure ratio, the production process of the high-temperature compressor, efficient heat exchange and thermal storage technology of low exergy loss is not mature. Hence, there are difficulties of great technical difficulty and high realization cost. The technical scheme of high-temperature compressor has not achieved the industrial application.

In 2013, RWE Technology International GmbH started to construct a large-scale cave-type D-CAES power station with a design capacity of 90MW×4h and a design overall efficiency of 70%, which is scheduled to be put into operation by the end of 2016 [57]. However, the design

is limited by the design and manufacturing level of the high-temperature compressor and the high efficiency of heat storage and heat transfer, so the project is at a standstill at present.

AA-CAES use salt cave as air storage medium, as a good and natural large-scale air storage method, and it can be combined with CAES technology and an effective approach to figure out the issue of large-capacity air storage in large-scale CAES power stations [59][60]. The underground salt cavern has the advantages of low construction cost (the investment is only equivalent to 1/10 of the surface pressure vessel), small land occupation, good leak proofness, high air storage pressure, mature technology, safety and stability [61-64].

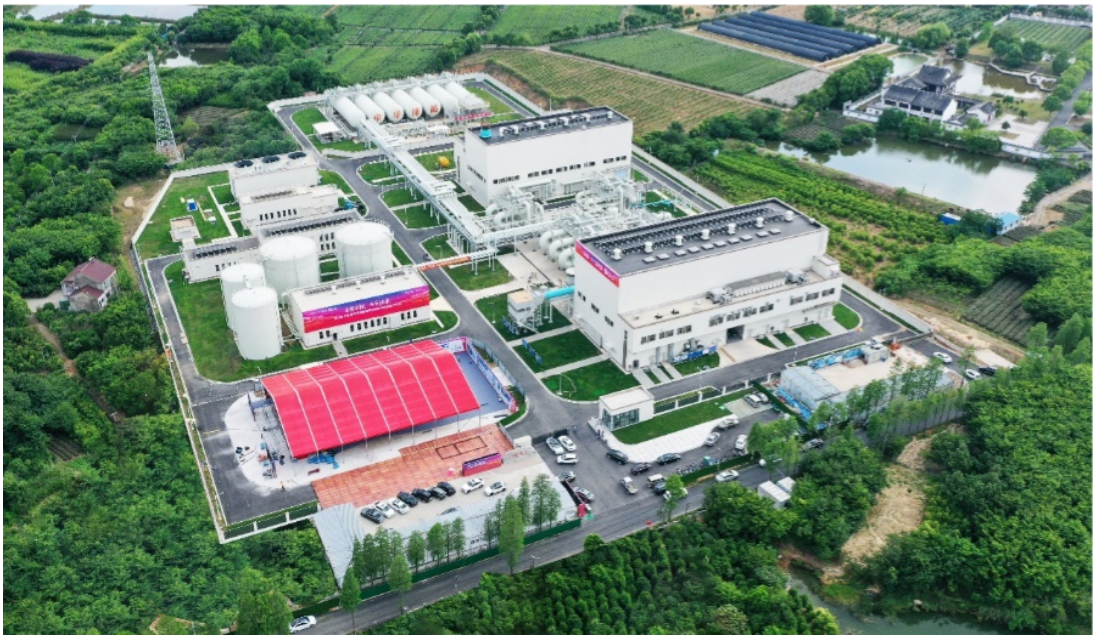

Figure 2.7. Diagram of Jintan Salt carven AA-CAES power station [65]

In May 2017, AA-CAES power station project based on salt cavern air storage was officially approved by the China National Energy Administration [65], becoming the first national demonstration project of CAES in China. The capacity of AA-CAES power station based on salt cavern air storage is 60 MW×5 h and the future construction capacity is 1000 MW. The

primary purpose of the power plant is to reduce the local power grid peak-shaving difference and smooth out the resulting lack of power supply. It is the world first non-supplementary combustion CAES power station in Jintan district, Changzhou, China, which was operated commercially on 26th May 2022, as shown in Figure. 2.7 [65]. The energy storage power and generator of the phase I project already in operation are 60 MW, and the energy storage capacity is up to 300 MWh, which can continuously compress air for 8h and generate power for 5h. The future construction capacity is 1000 MW, and its underground air storage cave is about 1000 m deep with a total capacity of $2.2\times 10^5\ m^3$ and a compressed air pressure of 14 MPa. It is worth mentioning that different from the previous two commercial power stations, this power station adopts two ways of thermal storage, namely compression heat recovery and electric heating of molten salt, to improve the power generation efficiency. It is the only commercial power station with zero carbon emissions.

To sum up, the currently has been built and under construction of AA-CAES demonstration plants depend on ascending temperatures for storing heat to improve the power capability of compressed air, but its thermal storage temperature by multi-stage compressor structure, material, adiabatic efficiency and the limitation of multi-stage compression side heat transfer efficiency. If the collection of large capacity high compression heat, it must cause the increase of the power consumption of the compressor. Thus, it becomes a technical restricting the improvement of energy storage efficiency of AA-CAES power station [65]. With the maturity of high-grade thermal storage technology and the continuous reduction of cost, AA-CAES technology coupled with external heat source can get rid of the dependence on high-temperature adiabatic compressor and enrich the consumption form of renewable energy.

2.3 The Application and Function of the CAES System

This section will focus on the application and function of CAES technology from four aspects, including the research status of thermodynamic characteristics modelling of CAES, the modelling characteristics of AA-CAES, and the research of AA-CAES modelling on renewable energy sources, the research of multi-energy joint supply characteristics of AA-CAES and the challenges of AA-CAES.

2.3.1 Modelling of Thermodynamic Characteristics of the CAES System

AA-CAES can be used for integrated heat and power supply systems, distributed energy systems in addition to power system peak shaving, frequency control, spinning reserve, reactive power support, black start, and application scenarios [66]. In the above typical application scenarios, AA-CAES may frequently operate under off-design conditions, resulting in the change of coupling state of internal compressor, heat exchanger (HEX), turbine and other components, thus causing changes in the overall operating performance of AA-CAES. At the same time, the thermodynamic characteristics of the compressor, HEX, turbine, thermal storage tank, air storage tank and other components are highly coupled, and each of them will affect the operating characteristics and efficiency of the system. In this context, it is of great significance to establish the coupling thermodynamic simulation model for each component to analyze the internal thermodynamic characteristics and overall performance of AA-CAES.

At the present, in terms of modelling and simulation analysis of thermodynamic characteristics of AA-CAES, most of them adopt a fixed efficiency model to describe the power conversion relationship of internal components, and some literatures also study the simulation model of

the impact of subsystem operating characteristics on the overall performance. In the literature, it is investigated how the major HEX parameters impress the performance of the AA-CAES system [67]. The analytical relationship between the compression ratio, expansion ratio, and isentropic entropy efficiency with the air mass flow rate is given in the literature. Based on the compressor and turbine cogeneration properties, the rated operating conditions are assessed. However, the analysis does not consider the thermodynamic characteristics of other components, like the compressor, the turbine, and the HEX. It was used in the article analysis of the energy and exergy characteristics of a micro CAES system under specified operating conditions [68]. Through using the first law of thermodynamics and the second law of thermodynamics, this thesis created a thermodynamic model of air storage subsystem and calculated how much exergy it could store. In this study, the operation parameters of a typical AA-CAES system are analyzed and will be impact on changes in temperature and pressure have on the performance of the system is considered. On the other hand, it does not consider the operating characteristics of air storage heat transfer and adiabatic.

To simplify, the current research on the modelling and simulation of the thermodynamic characteristics of air storage tank under heat transfer and adiabatic conditions is not sufficient. Without comprehensive consideration of the coupling relationship between components, it is difficult to effectively support the modelling analysis and operation of AA-CAES in various flexible application scenarios for modern energy and power system applications.

2.3.2 Research of the CAES System for Renewable Energy Sources

AA-CAES is similar to D-CAES power station to some extent, but the AA-CAES thermal storage system replaces the supplementary combustion subsystem of D-CAES, resulting in a

certain coupling between the air pressure release energy and the compressed heat energy in the system during the storage process and expansion energy release, which achieves the modelling analysis of AA-CAES.

In the system of the combined the wind power consumption and storage, the unit combination problem of the power system with the D-CAES power station is researched [69]. The operation characteristics of the D-CAES power station are presented based on the corresponding battery model. The influence of power system performance is systematically studied. The unit combination problem is also addressed and the economic dispatch (ED) problem of the D-CAES power station in the combined operation system with wind power storage. Literature [70] shows that the equivalent battery model and combined with the thermodynamic model of D-CAES, which considers the influence of dynamic characteristics of air storage on the operation characteristics of compressors and turbines and evaluates the specific influence of wind power consumption before and after the use of D-CAES power station in Ireland new energy power system. The results are optimistic using the equivalent battery model. In addition, for the CAES system, literature [71] proposed a new bilinear model of air storage based on two parameters: air temperature and air pressure in air storage. The advantages of this model are not only in high accuracy, but also in low computational complexity. Based on the literature [72], the bilinear model was used in [73] to study the unit combination problems caused by operating CAES power stations in the MPSs, and the consumption of wind power after the introduction of CAES was discussed. However, the model used in this paper is more complicated, which is not conducive to the popularization of scheduling operation research in the future. In addition, in view of the characteristics of CAES that can alleviate the fluctuations of renewable energy output, [74] proposed a two-layer programming method for islanding

microgrids in a pioneering way. Specifically, the upper and lower layers of CAES are fixed capacity problems and unit combination problems based on the requirement of spinning reserve respectively. However, in [74], in this literature, there is little investigation on the specific impact of the operation characteristics of the CAES power station with consideration of heat transfer of air storage tank. Hence the research conclusions in this paper are too optimistic. [75] pointed out that the CAES system has the ability of phase regulation and can support the stable operation of the power system more flexibly on the power supply side. On this basis, [76] discusses the phase regulation operation mode of the AA-CAES system, which provides a preliminary basis for constructing the optimal dispatching model of modern energy and power system considering the reactive power support capacity of AA-CAES.

For the current stage, the CAES operation characteristics is mainly realized through the equivalent battery model, and the significant influence of heat transfer of air storage tank has not been fully investigated. Therefore, the power system operation with AA-CAES is too optimistic. Moreover, these studies only focus on the traditional CAES power stations, but do not adequately research on the system performance related to AA-CAES power stations, which is not conducive to the conventional flexibility of AA-CAES.

2.3.3 Research of the CAES System as an EH

AA-CAES uses the thermal storage system to recover and reuse the heat energy from the air compression. The remaining heat in the thermal storage system can be used to heat the compressed air in the turbine and it can be further heated by temperature cascade utilization, and the turbine can also provide cooling energy after low temperature exhaust, thus improving the comprehensive utilization efficiency of energy. The combined heat and power (CHP)

storage and supply capacity of AA-CAES power station enable it to be applied in the CHP energy system.

At present, cogeneration units are regarded as the main research objective in the dispatching and operation of the IES. The following first introduces the modeling of cogeneration units, and then introduces the scheduling and operation of cogeneration units in the IES. If the modelling is based on CHP units, CHP units mainly include two types [77]: one is the CHP units that mainly generate steam, and the other is the CHP units that match the heating load demand. In the modelling of steam-generating CHP units, it is assumed that the steam generated by CHP units can be directly used in other production, so the production capacity of steam flow can be defined as thermal load boundary conditions. In the modelling of cogeneration units that match the heating load demand, unit thermal power rating can be defined as unit thermal load boundary conditions. For the second type of cogeneration unit, the modelling principles usually consider the following two points: First, the modelling is based on the definition of an EH [78-80]. The cogeneration unit can be regarded as an EH connecting fuel and power and heat output. However, an EH has not fully realized the function of combined cooling, heat and electricity. Therefore, the CER with the function of combined cooling, heat and electricity will be introduced in detail in Chapter 3.

Literature [81] establishes the relationship between input energy and output energy based on the efficiency matrix, and this method can be chosen for the analysis of multi-energy systems. However, for the CHP unit model based on the EH, the coupling of electric heating output is usually not considered. Secondly, based on the investigation of thermal output and electric output, the relationship between them is modelled. Generally, it can be divided into two types

of turbine structure as the standard: first, it is the back pressure type unit; second, the suction type unit. The former model is mainly based on the linear relationship between power and thermal output, while the latter model is based on the operational feasible region (convex and non-convex) [82]. Literature [83] points out that the convex feasible region can be described and Linearized by a group of linear inequalities or a convex combination of fixed points of the feasible region. Literature [84] points out that the non-convex feasible region can be composed of multiple convex feasible regions, and the mixed integer programming model of the extraction unit is established by introducing 0-1 variables.

In summary, the existing modelling and optimal operation models of cogeneration units are constructed only from the perspective of energy conservation constraints, but the heat transfer process constraints have not been investigated. If the heat transfer capacity is insufficient, it is difficult to be consistent with the energy conservation constraints.

While cogeneration units are frequently employed in MPSs from a power system perspective, research on the ED of the power system of cogeneration units has been significantly increased. In particular, the given cogeneration units should meet the heat load demand, the target of system scheduling is primarily to reduce the total cost of operations. Literature [85] systematically studies the process of efficiently solving a single cogeneration heat load balance equation. [86] is efficient to solve multiple cogeneration system studied heat load balance equation. [87] based on the perspective of cogeneration climbing rate on the efficient solution of the heat load balance equation in-depth study. The large-scale access of wind power cogeneration units to rolling scheduling situation is discussed in literature [88]. However, in the process of dispatching, the use of the rule of “determining power by heat” restricts the

flexibility of the power system. Therefore, there are more and more studies on the rational use of thermal system components to promote the significant improvement of the regulating capacity of cogeneration units and effectively solve the consumption problem. To significantly improve the peak-shaving capacity of cogeneration units, literature [89] uses the combination of a thermal storage device and a cogeneration unit to convert excess electric energy into heat energy for storage. In reference [90], the surplus wind power resources are utilized by means of electric heating boilers to meet the demand of heat load. Literature [91] promotes the enhancement of regulation capacity using thermal storage devices. Moreover, no matter which form, the goal of scheduling is always to meet the given heat load to find the thermal power of each component as the form of presentation. Literature [92][93] study the utilization of the heat storage capacity of the heating pipe network of the thermal system and the thermal storage capacity of the heat user building envelope to facilitate the coordinated operation of the IES of wind power consumption. Literature [94][95] proposes a solution strategy of decomposition coordination to settle the scheduling problem of the IES. In reference [96], the flexibility of the thermal system can be as the research perspective, and the coordination of different heat sources is deeply discussed. Therefore, the current coordinated operation research only focuses on the power system, but the thermal system is simplified, and the coordinated operation analysis of the IES is deficient.

For the heating supply system, its coordinated operation is mainly based on the heat source of the heating supply system and achieves the maximization of economic benefit in the dispatching process [97]. The coordinated operation optimization of heating supply system has local characteristics and does not involve the coordination among CHP. Literature [98] has conducted research on the specific influence of temperature and flow rate and other parameters

in the heating supply system and discussed the specific influence of pump coordination mode and other factors in the heating supply system. References [99][100] discuss the use of renewable energy sources as heat sources to achieve the operational demand for thermal system. The above studies basically do not consider the impact of the power system, it has not achieved the purpose of integrated heat and power energy system operation coordination.

In addition, the IES can be regarded as the CER, are in the process of IES modelling, can be on any form of power and energy storage (cogeneration units, heat pump and thermal storage devices) in direct modelling, it can consult the EH concept in IES application [86][101]. However, the economic performance of the system will be analyzed by using the artificial intelligence algorithm with good convergence and accuracy based on the system demand for heat and power energy in Chapter 6.

2.3.4 Research of the CAES System for Power Grid

By conducting research on the flexibility of both the power side and the load side of AA-CAES, it is possible to promote the operating reliability and efficiency of MPSs. In contrast, the availability of clean energy will bring a significant amount of operational uncertainty into the current energy and power system. This will result in a considerable change in the power flow condition and operation mode of the power grid, necessitating new requirements for the upgrading and expansion of the transmission system. The production simulation of the power system is an integral part of the power systems overall planning [36]. The production simulation seeks to identify the issue in power transmission and assess the impact of this issue on the operational efficiency of the power network by simulating the operational condition of the power network for an appropriate period. This is performed by identifying the issue that

have the most detrimental effect on operational efficiency. At the same time, production simulation can also be used to verify the feasibility of power grid upgrade schemes and evaluate the economy of these schemes from the perspective of operation [102]. Production simulation has emerged as a crucial tool for examining the effects of clean energy fluctuation on power grid operation and assessing the capacity of the power grid for clean energy, particularly in the case of widespread access to clean energy.

The application of deterministic production simulation in power system includes the following two fields: the first is the simulation study of daily operation, and the second is the simulation study of medium and long-term operation. The main goal of the deterministic production simulation is to investigate the peak regulating capacity restriction of the system power structures. In this thesis, the 24-hour operation of AA-CAES will be simulated. AA-CAES can reduce transmission line traffic, increase the rate at which transmission lines are loaded, and delay the expansion of transmission and distribution lines, which is expected to reduce the limitation of flexible resources in the high-proportion MPSs [103]. Meanwhile, the thermal storage system enables the AA-CAES to supply heat and power simultaneously. In other words, this enables the power grid to be flexible and provides heat energy to meet the need for heating. On the other hand, different from BESS and PHS, thermal storage system enables AA-CAES to provide CHP supply and storage. However, there is a lack of research on the comprehensive energy utilization capacity and principal analysis of AA-CAES in these studies. Therefore, the concept of the CER based on the AA-CAES will be described in detail to provide the flexibility of power grid in Chapter 3 and the economic performance analysis of the system will be performed in Chapter 6.

2.4 Research Gaps and Directions

Based on the literature review in Section 2.1 – 2.3, the following research gaps and directions can be identified:

1) The research on the internal energy conversion mechanism and energy efficiency improvement strategy of the AA-CAES system is needed for the development of AA-CAES technology and achieving the goal of efficient consumption of renewable energy.

2) More research is needed on the modelling and simulation of heat exchange and adiabatic conditions of AA-CAES components and the thermodynamic characteristics of the system under off-design condition. It is challenging to support AA-CAES in a variety of variable application scenarios, such as modelling analysis without sufficient considering the coupling relationship between components in its whole.

3) Although there has been the concept and design of the EH, zero emission and no pollution have not been fully considered. Therefore, the concept of the CER with no emission and no pollution should be proposed and applied.

4) The current research is lacking the mutual restriction relationship between different energy flows in the AA-CAES system which is not conducive to exploring the supporting role of AA-CAES in achieving the sustainable high proportion renewable energy supply with multi-energy storage and multi-energy supply as the core energy supply flexibility.

These research gaps and directions lead to the research objectives in Chapter 1.

CHAPTER 3 THE CLEAN ENERGY ROUTER CONCEPTIONAL DESIGN

3.1 Introduction

With the development of science and technology, the single energy network cannot meet the higher requirements for the power system. Different energy networks and different energy forms begin to combine with each other gradually, making the results of the whole network more and more complex [104]. This situation makes the EI and the traditional energy network have a great change. Therefore, the concept of the EH is proposed. However, the EH cannot fully realize the function of combined cooling, heat and electricity with zero carbon emissions. As a result, this chapter proposes a CER based on the AA-CAES. Energy is a crucial resource for the global economic development and society will lose the ability to advance if there is no energy supply in the world. Progress and the amount of energy available are closely related concepts in the development of humans and the remarkable economic development of human society all started with the great development of energy [105]. With the development of the economy, society needs more and more energy, so the use of fossil energy on Earth is much more than the natural abundant energy. In addition, due to the exploitation and waste of exotic energy in the world, the gas produced when fossil energy is burned usually violates the zero carbon emission in various indicators. In this process, unqualified gas is directly released into the atmosphere, thus causing serious damage to the environment. From the perspective of sustainable development of human beings, the renewable energy usage and its replacement of

traditional energy is the way to adjust the energy structure of the whole society and ensure sustainable development [3]. The United States, China, and India are the three largest energy consumers in the world, so the three countries have a significant influence on how the world consumes energy. Recently, due to the rapid development of the entire planet and human science and technology, our method of energy consumption has undergone significant change.

In terms of renewable energy, nuclear power plant capacity grows yearly. Until 2021, there are 440 nuclear power plants installed globally, with a combined amount of 390 GW. The capacity of wind power plants throughout all EU member states has surpassed 236 GW, including 207 GW onshore and 28 GW offshore facilities. The UK installed the most wind power capacity is 2.6 GW in 2021 (88% of that was offshore wind) [106]. In recent years, due to the gradual decline of traditional energy and the increasingly serious pollution, various countries have paid more and more research on renewable energy, and the development of renewable energy has been supported by the world. Until 2022, renewable energy will account for 8% of the total energy consumption worldwide. Because of the combustion of fossil energy and serious pollution, it is against the goal of zero carbon emission in the world.

Although renewable energy has tremendous potential in addressing issues such as sustainable energy development and environmental protection, it often faces limitations such as distributed and intermittent, and poor controllability. Under the traditional dispatch and control mode of the power grid, it is difficult to achieve large-scale centralized development and utilization. With the rapid development of information technology, the integration of information technology and renewable energy has provided a feasible technological approach - EI for the efficient utilization of renewable energy. EI can be seen as the integration of advanced power

electronic technology, information technology, and intelligent control technology, connecting many power network nodes consisting of distributed energy harvesting devices, distributed energy storage devices, and various types of loads. It enables energy flow in both directions and facilitates energy exchange and sharing within the network.

The generation, transmission, and consumption of electricity use in the current power system are independent of one another, and plug-and-play support for distributed energy is insufficient. Renewable energy sources including solar and photovoltaic power generation are used as the primary energy sources in the EI, which integrates the production, transmission, and consumption of energy. At the same time, the consistency of the energy supply is inconsistent with the variety of energy demand (power, heat, and cooling) on the user side (power). One of the main issues to be resolved in EI is how to actualize the positive consumption and thorough exploitation of renewable energy [107].

The Internet integrates a variety of communication modes and provides great convenience for the enrichment and utilization of information. It is quietly changing the way people communicate with each other, overturning the business models of more and more traditional industries, and providing reference and information support for the construction of the EI [108]. The router is the main node device of the Internet, also known as the gateway device, which plays the role of connecting the local area network and the wide area network on the Internet. Referring to [109] the design concept of switching equipment on the Internet and AA-CAES, the architecture of the CER is designed. To realize the wide area network with the large power grid as the backbone and the local area network composed of distributed energy (or micro grid) and other units of two-way energy flow and information flow connection. At the same time,

the Internet has many terminals as producers and consumers of information, the core component of which is the processor. In this chapter, the concept and scheme of "energy processor" in the EI are proposed, and then the CER architecture based on AA-CAES is designed.

3.2 The Design Scheme of the CER

In the 1940s, Turing proposed the "universal computer", and Von Neumann proposed the logic framework of stored programs as shown in Figure 3.1a. They respectively built the computing experimental platform for both scientific and engineering research purposes, which laid the theoretical foundation of the modern computer or information processing unit. Currently, various information processing units on the Internet such as large computing servers, personal computer, mobile terminals are the continuation and development of the experimental platform built by Turing and von Neumann. The idea of energy processors should be present in the EI by referring to the advancement of information processor and network technology, as indicated, it can realize active consumption and IES in the future EI as shown in Figure 3.1b.

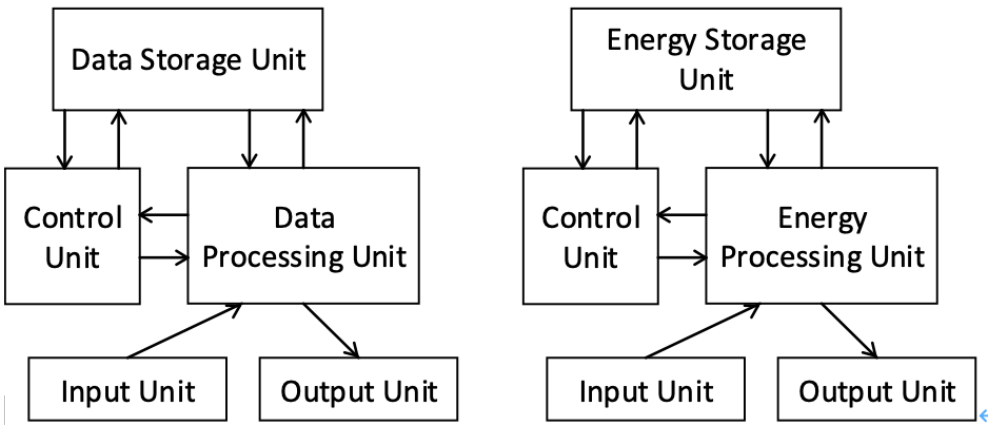

a) Information router b) Energy router

Figure 3.1. Information router and energy router schematic

In the information Internet, the information processor can realize much repeated complex acceptance, conversion, computation, storage, and output, which is one of the key technologies that constitute the Internet. Similar to the information router, the CER in the EI should also have similar functions, mainly including the following four aspects:

1) Through the energy input unit, it can realize the absorption of fluctuating wind and solar energy, and through the energy processing unit, the input electric energy can be converted into the smooth power required by the user for output.

2) The energy storage unit can be utilized for energy storage, reducing wind and solar energy fluctuations, and enabling the safe usage of electricity, depending on the system operational status.

3) The CER can implement arbitrary energy conversions between power, heat, and cooling energy, as well as input efficient combined cooling, heat, and power supply, depending on the demand for various energy types on the user side. This can help to increase the overall efficiency of energy utilization.

4) The energy router input unit is connected to a sizable power grid, and the device can transfer power to or withdraw power from the grid based on the energy status on both the source and the user's side, maintaining the stability of the users' power supply.

Compared with the single energy conversion function electric-to-electric of the general system, the CER can absorb, convert, store and output various forms of energy from heat, cooling and power, which emphasizes the energy consumption of IES. Additionally, the capacity of the

CER for large-scale energy storage and energy conversion can promote the absorbing additional energy and at regulating energy on both the source and user sides.

3.3 The Importance of AA-CAES for the CER

One of the core goals of the EI is to achieve clean production and utilization of energy. Specifically, this involves researching the characteristics and principles of intermittent and low-energy-density renewable energy sources during the processes of conversion, storage, and reuse. The objective is to transform low-controllability and fluctuating renewable energy (such as wind energy and solar energy) into controllable and conventional energy forms (such as thermal energy, electrical energy). At the same time, the aim is to minimize and avoid the emissions of various pollutants to the greatest extent possible during the transformation process [110]. Analogous to information processing units on the Internet, the CER is also a typical example of an information-physical coupling system. it encompasses information system components such as network communication, state, measurement, data conversion, and analysis, as well as core functional modules of the energy network that involve energy input, storage, conversion and transmission.

Another significant component of the future EI should be the clean energy. Therefore, the energy supply comes from renewable sources like the solar and wind with the characteristics of intermittent and fluctuation. However, the large-scale integration of renewable energy sources into the grid can maintain the stable operation of the power grid. ESS technologies can enhance the capability of the power system to accommodate large-scale wind and solar power generation, enabling smooth, reliable, secure, and stable power supply from wind and solar power systems to the users, to further improve the safety, economy, and flexibility of grid

operation. As a crucial component of the EI for energy consumption and conversion, efficient and clean high-capacity energy storage technologies are indispensable.

Due to limitation of PHS are complex geographical conditions and a single energy conversion function (only electric-to-electric energy conversion), PHS cannot fully achieve the energy storage demands for the future EI. Compared with PHS, AA-CAES also has the merits of large capacity, high efficiency, clean and environmental protection [38]. It not only can use the underground salt cavity, mines, caves and other special geological conditions for air storage, but it also can use SPT and air storage tanks as air storage medium. Therefore, less restricted by geographical conditions and system adaptability is greatly increased. In addition, through compression heat recycling, AA-CAES abandoned the conventional CAES of fuel through compression heat recycling. As a clean large-scale energy storage technology, it executes a system operation process with the features of non-combusting and zero carbon emission. In the interim, AA-CAES can obtain the decoupling of power energy storage and high-pressure air heat energy storage, and can combine cooling, heat, and electricity which can effectively fulfil the demands of multiple energy storage and conversion output of energy routers in the future.

3.4 Coupling Architecture and Working Mode

Based on the above analysis, the architecture of the CER proposed in this chapter is shown in Figure 3.2. The system is built based on AA-CAES technology and consists of an energy input unit, a conversion unit, a storage unit, an output unit and control unit. It is worth mentioning that pressurized water's role is to ensure that the water flow during compression heat transfer reaches a preset value, thus functioning as heat transfer and storage. From the general

modelling theory of information physical coupling system, the CER should follow the following three principles.

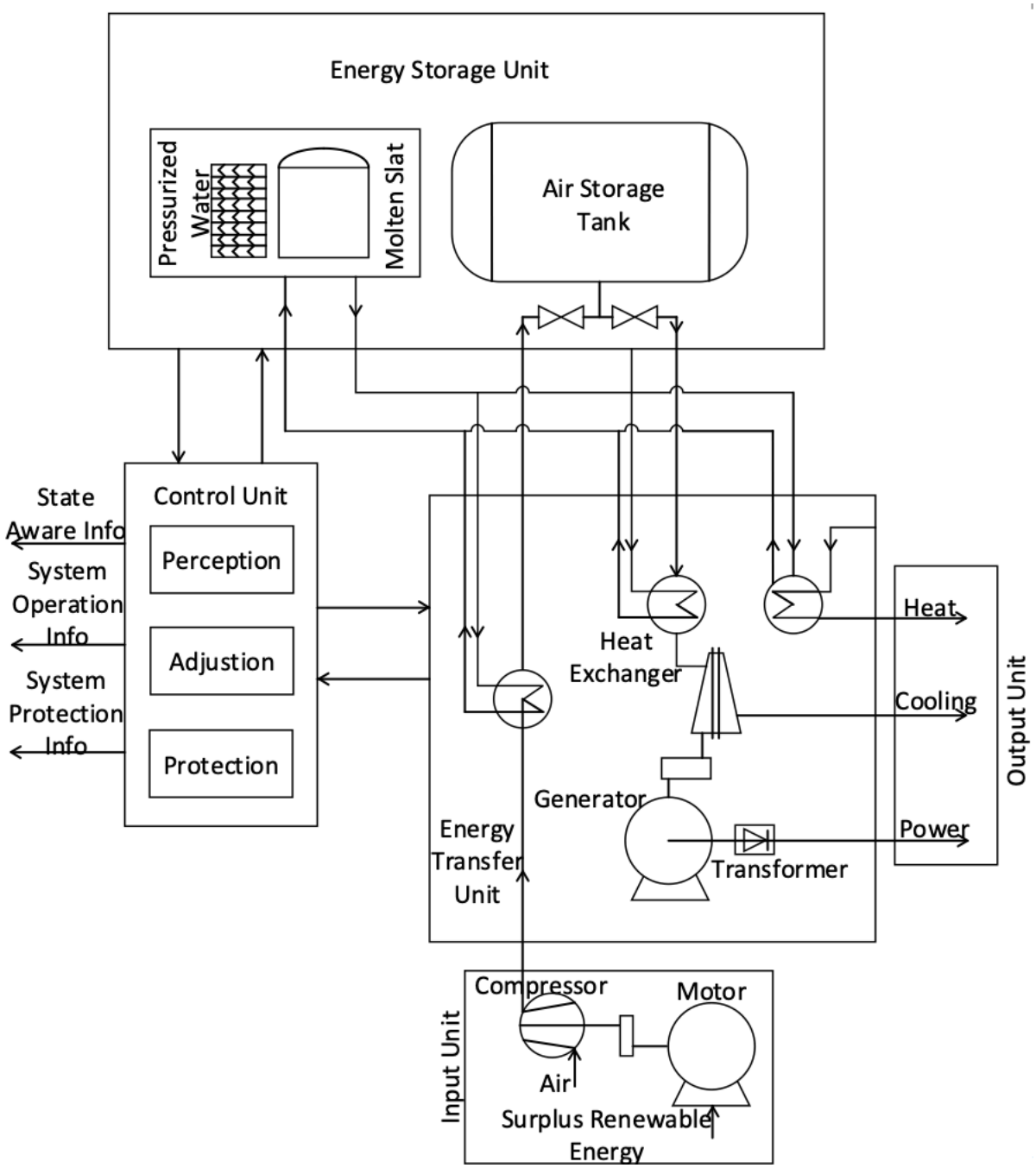

Figure 3.2. Initial concept diagram of the CER from information router

First, the CER network simultaneously interfaces with the information and energy which the information network's input interface includes energy supply, demand and market price. The CER can collect the information of environment changes, market fluctuation and network control dynamic of the energy router to support response analysis of data, model change and control process. In the meantime, the CER also continuously outputs information to outside, including its status, control, protection information, data reflecting its mode, function and capability. It can achieve comprehensive utilization and active matching by users and regulators in the EI.

Second, a neural network-like information gathering and processing system is required in CER to accomplish real-time sensing and management of various energy processing mitigation. This will enable flexible and high-quality information and energy application functions.

In addition, considering that energy routers have different operation modes and can provide customizable energy supply forms, it is necessary to configure an embedded high-performance information processing unit. The unit can analyze and make decisions based on real-time information on process changes from information and energy network. On the premise of maintaining efficient, safe and reliable energy transformation, it can adjust all kinds of parameter for the system operation and realize the comprehensive optimization decision-making and control process supported by multiple clean energy sources and information.

The CER can connect the energy supply and demand, and then transfer a steady and distant energy supply on the demand side. Furthermore, by connecting the information network and energy network through a control unit, it becomes possible to perceive and analyze information such as energy price fluctuations, energy demand signals, and energy prediction at both the

supply and demand. The control unit can integrate and optimize this information to provide control instructions for system operations. The CER can also effectively adapt to demand and supply requirements in the energy network and increase the overall efficiency of energy use through the factual transmission of information and the quick adjustment and transformation of the system operation mode.

As a result, Figure 3.3 depicts the following overview of the core operational principle of the CER based on AA-CAES: The control unit of the CER can realize the bidirectional flow of energy and the real-time measurement of the energy situation at both ends of the process by connecting to the information network, and then balance the energy fluctuation at both ends of the source and use [112]. Among these, the bidirectional energy flow of the CER has clean energy input and clean energy output, it can realize the function of the absorption of energy and the supply of energy. Off-peak electricity, wind and solar power, and other clean energy sources can be input into the energy processing unit. In the energy conversion unit, these energy sources can drive the operation of an air compressor. The obtained high-pressure air and compression heat can be stored separately in the air storage tank and the cascade thermal storage system (CTS). During the storage progress, the compressors divide the electric energy into thermal and other forms of energy (potential energy). The thermal energy is subsequently stored in the CTS using a thermal storage medium, while other forms of energy (potential energy) is stored in the air storage tank using compressed air instead. When energy is output, air turbine of the energy storage unit can produce electricity, and the output unit generates electric energy to meet the demand for the power grid and users. The compressed heat stored in the heat storage system is transmitted to the intake air of each stage of the turbine due to increase the thermal efficiency of the system circulation during operation. To jointly operate

the turbine and supply the regional energy network (REN) during peak shaving, the CTS provides high grade thermal energy coupled to the compressed air in the air storage tank for power generation. Additionally, the industrial user and residential can achieve cooling energy from the low-temperature air produced during the air expansion process.

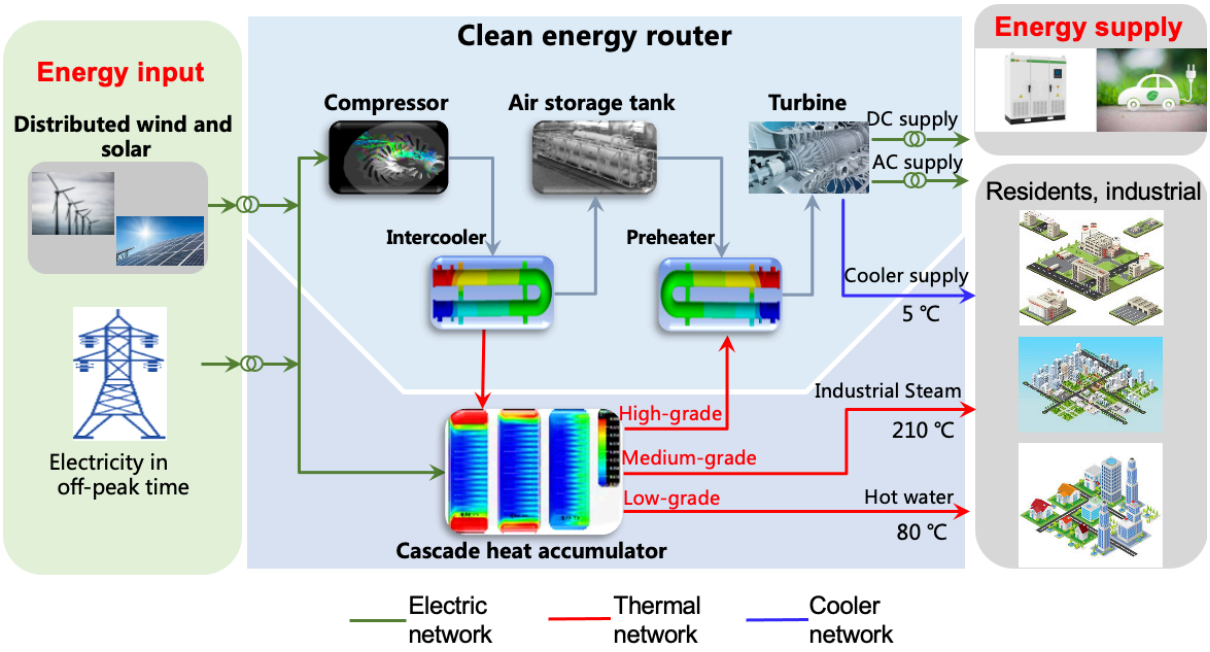

Figure 3.3. The concept diagram of the CER

The CER has an energy storage mode that can be turned on during off-peak hours, it can store the electricity through high pressure and store the thermal energy through the CTS for eight hours. CTS primary function is to offer better-quality thermal energy during high demand periods and to provide REN with industrial steam and hot water on a constant basis. Electric heating transforms the low-grade heat generated during the storage of electric energy into high-grade heat energy, which is then transferred through CTS. When peak regulation is required on the power grid, high-grade heat energy can be applied to preheat the input air of turbines and then generates high-grade electric energy. When the moderate heat energy of AA-CAES is returned to CTS, it still has sufficient heat energy. For the entire CTS system, it can apply low

grade heat to continuously deliver hot water at 80℃ for 24 hours and medium grade heat to continuously supply steam at 210℃ for 16 hours.

Summary

This chapter describes the origin of the CER. The main inspiration comes from the multiple communication modes of information routers, which provide a great convenience for enriching and utilizing information. The main function of the router is to absorb fluctuating renewable energy such as wind and solar through the input unit and use its core ESS technology as the medium – the CER for storage. The CER can implement the arbitrary conversion of various types of energy, including power, heat, and cooling energy, depending on the needs of various forms of energy on the user side. Additionally, the AA-CAES with large-scale energy storage features is chosen for the CER to provide the clean and effective operation of the system.

CHAPTER 4 MODEL OF CER AND IMPLEMENTATION

4.1 Introduction

In the application background of the power system and IES with the high proportion of renewable energy, the internal components of AA-CAES will work in the non-rated condition to varying degrees in response to the changing demand for renewable energy and electric heating load. The AA-CAES power plant will operate off-design in response to the frequent fluctuations in heating load demand if it is integrated into a complete energy system with several complimentary energies. Therefore, it is essential to thoroughly analyze the operating characteristics of each fundamental component and establish the corresponding quasi-steady-state thermodynamic simulation model to obtain the requirements of the external environment for the operation of AA-CAES under off-design conditions and study the heat transfer and adiabatic operation of internal components on the overall operating characteristics of AA-CAES.

The flow of this chapter is arranged as follows. In Section 4.2, the core of the CER including various conventional components is introduced to provide a basis for studying the thermodynamic simulation model of system off-design conditions. In section 4.3, based on the first law of thermodynamics, the simulation models of heat exchange and adiabatic conditions of AA-CAES components are established. In Section 4.4, a thermodynamics analysis model of CAES based on exergy equilibrium was established. In Section 4.5, based on the

thermodynamic simulation model constructed in the previous two sections, the internal thermodynamic characteristics and external energy supply characteristics of the CER are analyzed.

4.2 The Core of the CER

Most current studies use a fixed efficiency model to describe the functional transformation relationship of internal components, and some literatures also establish simulation models based on the rated conditions. This is in terms of modelling and simulation analysis of the thermodynamic characteristics of AA-CAES. AA-CAES is a form of physical energy based on a CAES system that produces no combustion or carbon emissions with advantages of AA-CAES include its large-scale, good performance, and cleanliness. This chapter proposes a 7-stage compression and 2-stage expansion of the AA-CAES system to obtain the optimal performance. It is worth mentioning that first five stages of the compressor unit are centrifugal compressors with separator shafts, and the last two stages are single-shaft piston compressors. In addition, the thermal energy storage system consists of three parts, which are low temperature thermal energy storage, medium temperature thermal energy storage and high temperature thermal energy storage. The system is designed based on the industrial and residential energy needs of Yangzhong district, Zhenjiang city, Jiangsu province, China.

Figure 4.1 shows how to complete the energy storage by decoupling the power into thermal and other forms of energy (potential energy) using a compressor and HEX, then coupling the thermal and air potential energy into power using a turbine to achieve the generation of the energy [113][114]. When the grid connection is insufficient, the power in storage progress can employ both wind and solar power plants in addition to power from the grid during off-peak

hours. There is a main supporting like grid peak shaving, the electric energy produced during the energy release process might be used.

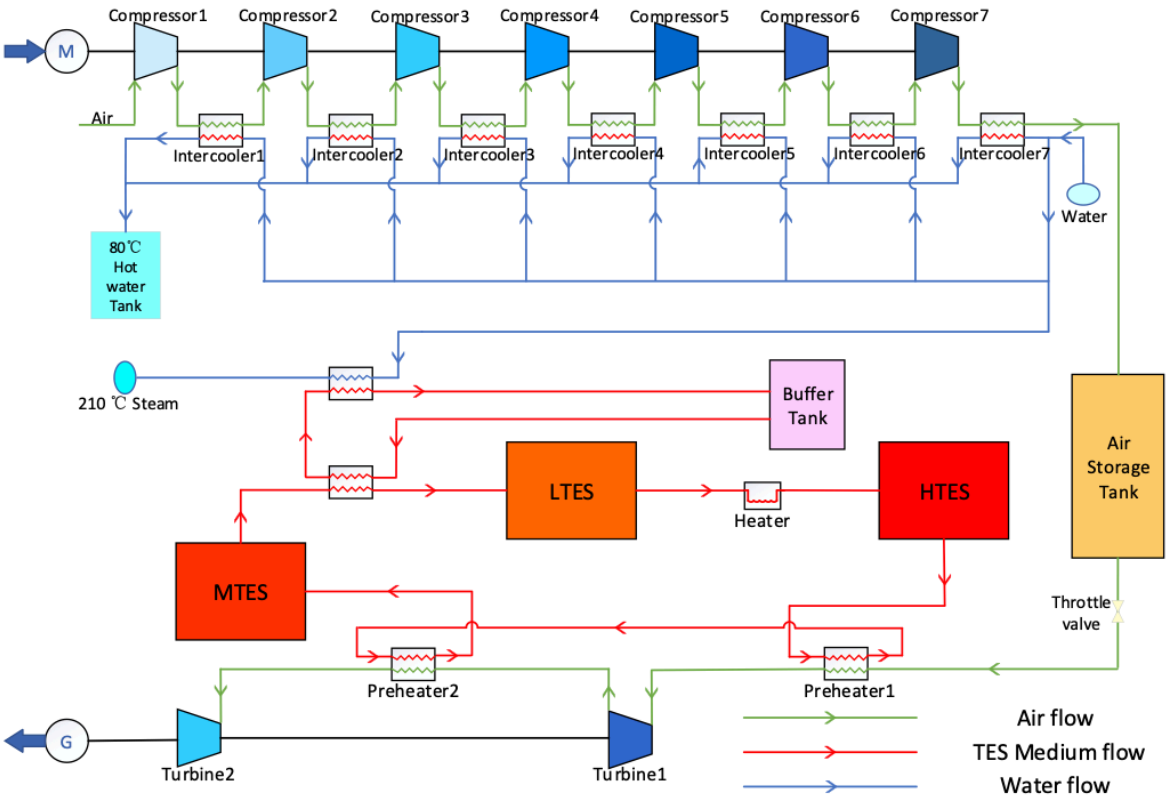

Figure 4.1. AA-CAES detailed schematic diagram

In contrast to existing ESS technologies like PHS and BES, AA-CAES not only offers clean energy storage without making the pollution of the environment (no pollution or carbon emissions), but it also acts as a source of numerous energy reserves. In addition to improving the sustained high-proportion acceptance capacity of renewable energy, it may also become a strategy for the consumption of wind and solar energy while exerting the synergistic effect of multi-energy complementarity. For convenience of analysis, the realization form of the thermodynamic properties of AA-CAES analysis, modeling, and operation problems in using the following assumptions:

1) Assume air as an ideal gas and it satisfies the ideal air equation of state.

2) The specific heat capacity of air and heat transfer medium and heat storage medium is constant.

3) Energy loss between compressor and motor, turbine and generator are not considered.

4) The HEX is a counter-current type HEX, and the heat leakage loss is ignored.

5) The compressor flow and turbine flow in the energy storage process is constant.

6) Ignoring the power consumption of the heat storage medium and heat-carrying fluid booster pump in the compression heat collection and heat recovery system.

7) The air throttling process at the inlet and outlet of the air storage tank is an adiabatic process.

8) Ignore the heat dissipation and pressure loss of relevant pipelines.

4.3 Thermodynamic Model of Off-design conditions based on Heat Balance

Under the specified operating conditions, a thermodynamic simulation model of AA-CAES is suggested in this section. Based on the AA-CAES process, the compressor, HEX, thermal storage, air storage tank, and turbine modules are presented in the quasi-steady-state thermodynamic simulation of the AA-CAES system.

4.3.1 Compressor Module

(1) Rated Condition Model

The i-th stage compressor's isentropic outlet temperature is

$$T_{c,i}^{out,is} = T_{c,i}^{in}\left(\beta_{c,i}\right)^{\frac{k-1}{k}} \tag{4.1}$$

where k: the adiabatic index (1.4), $T_{c,i}^{in}$: the compressor's inlet air temperature at the i-th stage, $\beta_{c,i}$ is the pressure ratio at the i-th stage, and $\eta_{c,i}$ is the compressor isentropic efficiency at the i-th stage.

The compressor's isentropic efficiency at the i-th stage is

$$\eta_{c,i} = \frac{T_{c,i}^{out,is} - T_{c,i}^{in}}{T_{c,i}^{out} - T_{c,i}^{in}} \tag{4.2}$$

The i-th stage compressor's outlet temperature at the is

$$T_{c,i}^{out} = \frac{1}{\eta_{c,i}} T_{c,i}^{in}\left(\left(\beta_{c,i}\right)^{\frac{k-1}{k}} + \eta_{c,i} - 1\right) \tag{4.3}$$

The compressor's actual output temperature at the i-th stage is

$$p_{c,i}^{out} = p_{c,i}^{in}\beta_{c,i} \tag{4.4}$$

where $p_{c,i}^{in}$: the compressor inlet air pressure at the i-th stage, $p_{c,i}^{out}$: the compressor outlet air pressure at the i-th stage, the compressor's power consumption at the i-th stage is

$$W_{c,i} = \dot{m}_c c_p^a\left(T_{c,i}^{out} - T_{c,i}^{in}\right) \tag{4.5}$$

where $\dot{m}_c$: the compressor mass flow rate, and c_p^a: the constant pressure-specific heat of the air.

The total power consumption of compressor is

$$W_c = \sum_{i=1}^{N_c} W_{c,i} \tag{4.6}$$

where N_c: the stage of the compressor, and $W_{c,i}$: the compressor' actual power at the i-th stage.

When back-pressure becomes stable, Formula (4.5) can be used to calculate the compressor power consumption. When back pressure is continuously rising, however, Formula (4.5) should be integrated by the full unstable storage progress.

$$W' = \int_{p_1}^{p_2} \frac{1}{\eta_c} \frac{kV_{AST}\dot{m}_c}{k-1} \frac{T_{in}}{T_{cav}} \left[\left(\frac{p_{out}}{p_{in}} \right)^{\frac{k-1}{k}} - 1 \right] dp_{AST} \tag{4.7}$$

where p_{AST} is the pressure of the air storage tank, V_{AST} is the volume of the air storage tank, and p_1 and p_2 are the lower and upper limits of pressure, respectively.

Part of the load characteristics of the compressor are excluded in the following study, quasi-steady-state heat at rated working condition can be equated by (4.3) - (4.5).

(2) Off-design Model

In the off-design operating mode caused by some internal components, the compressor efficiency changes most obviously. The operation efficiency (isentropic efficiency) of the compressor at the rated design point can reach 87%-90%, while the compression efficiency drops to 65%-70% at 50% load and even less than 50% at 30% load [115]. To explain how the

compressor's isentropic efficiency changes, which are often brought on by air mass flow rate and compressor speed deviations from rated settings.

$$\eta_{c,i} = (\eta_{c,i})_0 - \alpha_c\left((\beta_{c,i})_0 - \beta_{c,i}\right)^2 \tag{4.8}$$

where α_c is a constant, and $(\cdot)_0$ is the parameter of the compressor under the off-design condition, which is the same as the following. It can be seen from Equation (3.8) that this approach can only express the relationship between isentropic efficiency and the change of ratio, but it is difficult to reveal the physical nature of pressure ratio and isentropic efficiency change caused by non-rated mass flow of compressed air. Literature [116] provides a typical regression method for compressor characteristic parameters, which can be used for the construction of the air turbine thermodynamic simulation model. The analytical expressions of the characteristic curves of the compressor and turbine are given in this chapter, which provides a basis for studying the characteristic of the compressor. This section introduces the analytical expression of the compressor characteristic [117].

where the actual pressure ratio and isentropic efficiency of the compressor can be expressed, respectively.

$$\frac{\beta_{c,i}}{(\beta_{c,i})_0} = a_{1,i}(\dot{G}_{c,i})^2 + a_{2,i}\dot{G}_{c,i} + a_{3,i} \tag{4.9}$$

$$\frac{\eta_{c,i}}{(\eta_{c,i})_0} = \left[1 - c\left(1 - \dot{n}_{c,i}\right)^2\right]\left(\dot{n}_{c,i}/\dot{G}_{c,i}\right)\left(2 - \left(\dot{n}_{c,i}/\dot{G}_{c,i}\right)\right) \tag{4.10}$$

where $\left(a_{1,i}, a_{2,i}, a_{3,i}\right)$ are effect factors of rotational speed on pressure ratio, it can be expressed as actual pressure ratio and isentropic efficiency of the compressor can be expressed, respectively.

$$a_{0,i} = \left[b_1 \left(1 - \frac{b_2}{\dot{n}_{c,i}} \right)^2 + \dot{n}_{c,i} \left(\dot{n}_{c,i} - b_2 \right)^2 \right] \tag{4.11}$$

$$a_{1,i} = \frac{\dot{n}_{c,i}}{a_{0,i}} \tag{4.12}$$

$$a_{2,i} = \frac{\left(b_1 - 2 b_2 \dot{n}_{c,i}^2 \right)}{a_{0,i}} \tag{4.13}$$

$$a_{3,i} = \frac{b_2^2 \dot{n}_{c,i}^2 - b_1 b_2 \dot{n}_{c,i}}{a_{0,i}} \tag{4.14}$$

where b_1, b_2, b_3 are constant coefficient and can be valued as $b_1 = 1.8, b_2 = 1.4, c = 0.3$ or $b_1 = 3.6, b_2 = 1.06, c = 0.3$. The actual compressor can be fitted by its characteristic diagram effect factor of rotational speed on pressure ratio, but it needs to meet $\sqrt[3]{b_1} \leq \frac{2b_2}{3}$. Meanwhile, dimensionless reduced order flow rate and reduced order speed can be defined as

$$\dot{G}_{c,i} = \left[\dot{m}_c \frac{\left(T_{c,i}^{in} \right)^{0.5}}{p_{c,i}^{in}} \right] / \left[\dot{m}_c \frac{\left(T_{c,i}^{in} \right)^{0.5}}{p_{c,i}^{in}} \right]_0 \tag{4.15}$$

$$\dot{n}_{c,i} = \left[n_c \left(T_{c,i}^{in} \right)^{-0.5} \right] / \left[n_c \left(T_{c,i}^{in} \right)^{-0.5} \right]_0 \tag{4.16}$$

where n_c is the rotational speed of the compressor, it can be defined as $n_c(t) = (n_c)_0$. The actual pressure ratio and the actual isentropic efficiency can be achieved through the equations (4.8) - (4.16). The actual power consumption, actual outlet temperature and outlet pressure of 1st stage compressor can be obtained under the conditions of given actual inlet temperature and actual inlet pressure.

4.3.2 HEX Module

In these circumstances, the heat transfer coefficient has a simple impact on the HEX heat transfer coefficient. Therefore, this section constructed the design model of the HEX charging process under changeable conditions from the heat transfer equation in reference [118].

(1) HEX on the Compression Side

Calculations can be made to determine the heat transfer fluid's (HTF) and the HEX's outlet air temperatures, respectively.

$$T_{c,HX,i}^{a,out} = T_{c,HX,i}^{a,in} - \frac{\phi_{c,i}^{HX}}{(c_p^a \dot{m}_{c,i}^a)} \tag{4.17}$$

$$T_{c,HX,i}^{HTF,out} = T_{c,HX,i}^{HTF,in} + \frac{\phi_{c,i}^{HX}}{(c_p^{HTF} \dot{m}_{c,i}^{HTF})} \tag{4.18}$$

where $T_{c,HX,i}^{a,in}$ is the HEX's inlet temperature on the compression side at the i-th stage, $T_{c,HX,i}^{HTF,in}$ is the HTF' inlet temperature on the compression side at the i-th stage, $\dot{m}_{c,i}^a$ is the compressor's mass flow at the i-th stage, c_p^{HTF}: the constant pressure-specific heat for the HTF, and $\phi_{c,i}^{HX}$: the actual heat capacity for the HTF during the storage progress.

$$\phi_{c,i}^{HX} = \varepsilon_{c,i} \cdot C_{c,i}^{min}(t)\left(T_{c,HX,i}^{a,in} - T_{c,HX,i}^{HTF,in}\right) \tag{4.19}$$

where $\varepsilon_{c,i}$: the HEX's heat transfer coefficient during the storage progress.

$$\varepsilon_{c,i} = \frac{1-exp[-NTU_{c,i}(1-C_{c,i}^{HX})]}{1-C_{c,i}^{HX} exp[-NTU_{c,i}(1-C_{c,i}^{HX})]} \tag{4.20}$$

where $NTU_{c,i}$ and $C_{c,i}^{HX}$: the heat transfer unit and the heat capacity ratio of the HEX during the storage progress [119], respectively.

$$NTU_{c,i} = \frac{UA}{C_{c,i}^{min}} \tag{4.21}$$

$$C_{c,i}^{HX} = \frac{C_{c,i}^{min}}{C_{c,i}^{max}} \tag{4.22}$$

where $C_{c,i}^{min}$ and $C_{c,i}^{max}$: the maximum and minimum heat capacities of the HEX during the storage progress, respectively, and U and A: the heat exchange coefficient and the size of heat exchange, respectively.

$$C_{c,i}^{min} = \left(\dot{m}_c c_p^a, \dot{m}_{c,i}^{HTF} c_p^{HTF}\right)_{min} \tag{4.23}$$

$$C_{c,i}^{max}(t) = \left(\dot{m}_c(t) c_p^a, \dot{m}_{c,i}^{HTF}(t) c_p^{HTF}\right)_{max} \tag{4.24}$$

where $\dot{m}_{c,i}^{HTF}$: the HTF's mass flow at i-th stage and can be defined as

$$\dot{m}_{c,i}^{HTF} = \frac{\dot{m}_c c_p^a \left(T_{c,HX,i}^{a,in} - T_{c,HX,i}^{a,out}\right)}{c_p^{HTF}\left(T_{c,HX,i}^{HTF,out} - T_{c,HX,i}^{HTF,in}\right)} \tag{4.25}$$

In practice, the HEX operates when large amounts of compressed air are considered to flow through the HEX [111]. The majority of the present models, on the other hand, presume that the HEX efficiency is constant without pressure loss. Since the HEX is one of the essential elements of AA-CAES, pressure loss has a direct impact on the system overall effectiveness. On the compression side, the HEX's pressure retention coefficient is represented as

$$\eta_{c,HX,i}^{p} = 1 - \frac{0.0083\varepsilon_{c,i}}{1-\varepsilon_{c,i}} \tag{4.26}$$

During the storage progress, the HEX's outlet pressure is

$$p_{c,HX,i}^{out} = \eta_{c,HX,i}^{p} p_{c,HX,i}^{in} \tag{4.27}$$

where $p_{c,HX,i}^{in}$: the HEX's inlet air pressure at the i-th stage during the storage progress.

(2) HEX on the Expansion Side

The outlet temperature of the HEX and the HTF during the generation progress can be formulated similarly to the HEX on the compression side.

$$T_{e,HX,i}^{a,out} = T_{e,HX,i}^{a,in} + \frac{\phi_{e,i}^{HX}}{(c_p^a \dot{m}_e^a)} \tag{4.28}$$

$$T_{e,HX,i}^{HTF,out} = T_{e,HX,i}^{HTF,in} - \frac{\phi_{e,i}^{HX}}{(c_p^{HTF} \dot{m}_{e,i}^{HTF})} \tag{4.29}$$

where $T_{e,HX,i}^{a,in}$: the HEX's inlet temperature at the i-th stage on the expansion side, $T_{e,HX,i}^{HTF,in}$: the the HTF's inlet temperature at the i-th stage during the generation progress, $\dot{m}_e^a$ is the i-th stage of the turbine's mass flow, $\dot{m}_{e,i}^{HTF}$ is the HTF's mass flow during the generation progress, and $\phi_{e,i}^{HX}$ is the HTF's actual heat capacity during the generation progress.

$$\phi_{e,i}^{HX} = \varepsilon_{e,i} \cdot C_{e,i}^{min}(t)\left(T_{e,HX,i}^{a,in} - T_{e,HX,i}^{HTF,in}\right) \tag{4.30}$$

where $\varepsilon_{e,i}$: the HEX's heat transfer coefficient during the generation progress.

$$\varepsilon_{e,i} = \frac{1-exp[-NTU_{e,i}(1-C_{e,i}^{HX})]}{1-C_{e,i}^{HX} exp[-NTU_{e,i}(1-C_{e,i}^{HX})]} \tag{4.31}$$

where $NTU_{e,i}$ and $C_{e,i}^{HX}$: the heat transfer unit and the heat capacity ratio at the i-th stage of HEX during the generation progress, respectively.

$$NTU_{e,i} = \frac{UA}{C_{e,i}^{min}} \tag{4.32}$$

$$C_{e,i}^{HX} = \frac{C_{e,i}^{min}}{C_{e,i}^{max}} \tag{4.33}$$

where $C_{e,i}^{max}$ and $C_{e,i}^{min}$: the maximum and minimum heat capacities of the HEX during the generation progress, respectively.

$$C_{e,i}^{min} = \left(\dot{m}_e c_p^a, \dot{m}_{e,i}^{HTF} c_p^{HTF}\right)_{min} \tag{4.34}$$

$$C_{e,i}^{max}(t) = \left(\dot{m}_e c_p^a, \dot{m}_{e,i}^{HTF} c_p^{HTF}\right)_{max} \tag{4.35}$$

where $\dot{m}_{e,i}^{HTF}$: the HTF's mass flow at the i-th stage and it can be calculated by

$$\dot{m}_{e,i}^{HTF} = \frac{\dot{m}_e c_p^a \left(T_{e,HX,i}^{a,in} - T_{e,HX,i}^{a,out}\right)}{c_p^{HTF}\left(T_{e,HX,i}^{HTF,out} - T_{e,HX,i}^{HTF,in}\right)} \tag{4.36}$$

The pressure retention coefficient of the HEX during the generation progress while considering the pressure loss characteristics of the HEX can be written as

$$\eta_{e,HX,i}^{p} = 1 - \frac{0.0083\varepsilon_{e,i}}{1-\varepsilon_{e,i}} \tag{4.37}$$

The HEX's outlet pressure during the generation progress is

$$p_{e,HX,i}^{out} = \eta_{e,HX,i}^{p} p_{e,HX,i}^{in} \tag{4.38}$$

where $p_{e,HX,i}^{in}$: the HEX's inlet air pressure at the i-th stage during the generation progress.

The mass flow rate and temperature of the HTF which using the equation of conservation of mass can be determined, respectively.

$$\dot{m}^{HTF} = \sum_{i=1}^{N} \dot{m}_i{}^{HTF} \tag{4.39}$$

$$T_{HX}^{Merge} = \frac{\sum_{i=1}^{N} \dot{m}_{HX,i}^{HTF} T_{HX,i}^{HTF,out}}{\sum_{i=1}^{N} \dot{m}_{HX,i}^{HTF}} - T_{HX,i}^{HTF,in} \tag{4.40}$$

Overall, the equations of the HEX on compression and expansion side (4.17) - (4.40), the inlet temperature and pressure of each stage depend on the parameters of each stage of compressor and turbine. At the same time, the mass flow on the air side is the same as the air mass flow of the corresponding compressor and turbine.

4.3.3 Thermal Storage System Module

The types of thermal storage system can be classified as high-temperature [120], medium-temperature [121], and low-temperature thermal storage tanks [122] according to the compressor grade change and compressor outlet compressed air temperature change. Thermal storage technology is consisted of four categories: MSTS [123], double-tank liquid thermal storage [124], concrete thermal storage [115], and phase-change material thermal storage [121]. These classifications are based on the heat storage device heat storage medium. The thermal storage medium's temperature can be described as

$$\left(\rho_{TES} V_{TES} c_p^{TES}\right) \frac{dT_{TES}}{dt} = \dot{m}_c^{HTF} c_p^{HTF} \left(T_c^{TES,in} - T_{TES}\right)$$

$$-\dot{m}_e^{HTF} c_p^{HTF} \left(T_{TES} - T_e^{TES,in}\right) - Q \tag{4.41}$$

where ρ_{TES}: the density of the heat storage medium density, V_{TES}: the volume of the heat storage medium volume, c_p^{TES}: the constant pressure-specific heat of the thermal energy storage, $T_c^{TES,in}$: the heat storage medium inlet temperature during the storage progress, $T_e^{TES,in}$: the heat storage medium's inlet temperature ring the generation progress, and Q is the heat transfer with the surrounding air, which can be formulated by

$$Q = U_{TES} A_{TES} (T_{TES} - T_{env}) \tag{4.42}$$

where U_{TES} and A_{TES}: the heat transfer coefficients between the heat storage tank and the environment and the heat storage tank external surface area (U_{TES} is 0 when the heat transfer loss is not considered), and T_{env}: the environment temperature.

4.3.4 Air Storage Tank Module

In the AA-CAES system, the air storage tank is the main equipment to realize the transfer of power across time and space. The air storage approaches to the air storage tank mainly involve constant pressure air storage tank [125] and constant capacity air storage tank [128]. This chapter focused on the fixed-volume air storage tank which is common and less dependent on geographical conditions. This type of the air storage tank includes pressure vessels including pressure vessels, salt cavern air storage, SPT etc. In figure 4.1, the pressure vessel is used as the air storage tank in the pressure vessel. To accurately replicate the instantaneous temperature and pressure of the air storage tank, the authors of this study chose to use an air storage tank with a constant volume and less dependence on the geography around it. Both the generalized air state equation and the conservation of air mass are terms that can be defined.

For constant volume air storage, most studies assume constant temperature air storage. In fact, when the CAES power plant is running, the constant exchange of heat between the air inside and outside the building causes both the temperature and the pressure in the air storage tank to change all the time. This has an effect on thermodynamic parameters, such as the back-pressure of the final stage compressor, when compressed energy is stored. When compressed energy is released, it changes the temperature and pressure of the air that comes into the turbine. If the effect of heat exchange is not taken into account correctly in the thermodynamic analysis of the CAES system, there will be some errors. In the literature, there are two analytical solutions to the problem of the change in temperature and pressure in the air storage tank of CAES. The isothermal solution and the approximate solution of average density are examples of these solutions. These two analytical solutions are derived from the mass conservation equation, energy conservation equation and surrounding rock conduction equation. Then, the approximate solution is obtained by Laplace transform, but it is difficult to calculate the integral because of the large amount of calculation. Therefore, assume some condition such as temperature to a constant value simplifies the calculation process. Based on the temperature and pressure dynamic models [101][115], a general thermodynamic simulation is established in this chapter.

(1) Consider Air Storage for HEX

First, the air storage tank of CAES can be regarded as a control volume system, and the air storage tank's walls and ports serve as the system's borders. Air leakage is disregarded when the air storage tank's surrounding rock is salt rock or limited permeability rock. Based on the

CAES system's operational condition, the air storage tank air mass flow model is created. The air storage tank air mass flow model is

$$a\dot{m}_c(t) = \dot{m}_{in}(t) + \dot{m}_{out}(t) \tag{4.43}$$

where $a\dot{m}_c$ for import and export air mass flow rate, $\dot{m}_{in}$ is inlet air mass of the air storage tank, $\dot{m}_{out}$ is outlet air mass of the air storage tank, air mass flow rate of air accumulator a as the running state of the CAES system. a = 1, a = 0, a= -1 represent the charge compression process, storage and power generation (static) process, as shown in figure 4.2.

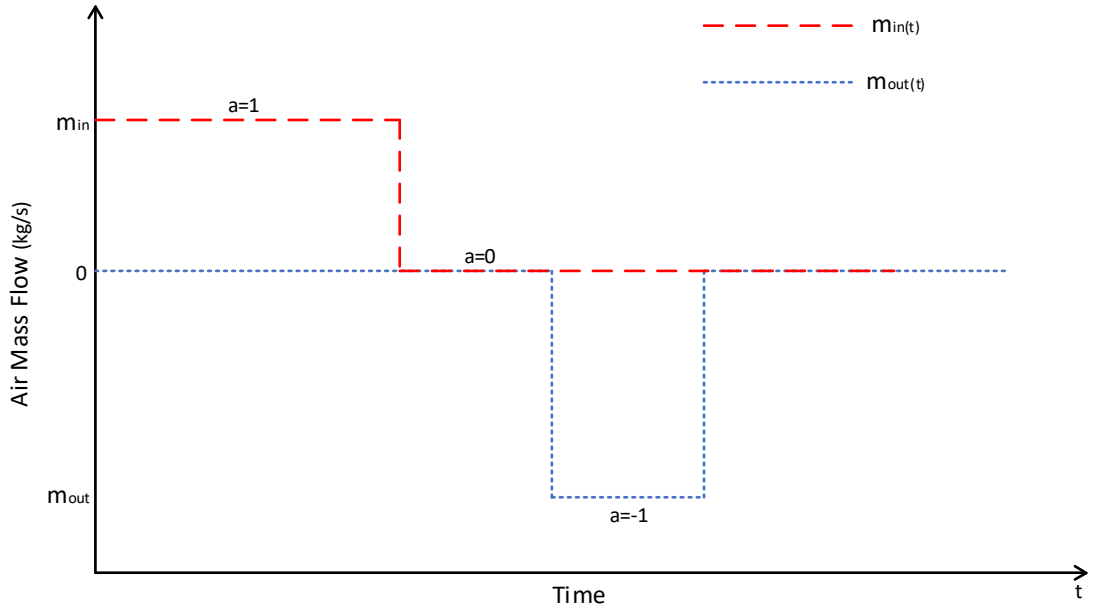

Figure 4.2. The change diagram of air mass flow in air storage tank of AA-CAES

The air mass conservation model and energy conservation model of air storage room are established based on the aerodynamic principle of the air storage tank. The air mass conservation model and energy conservation model are respectively specified as

$$V\frac{d\rho}{dt} = a\dot{m}_c \tag{4.44}$$

$$V_{cav}\rho c_v \frac{dT}{dt} = \dot{m}_{in}\left(h_i - h + ZRT - \rho \frac{\partial u}{\partial \rho}|_T\right) + \dot{m}_{out}\left(ZRT - \rho \frac{\partial u}{\partial \rho}|_T\right) + \dot{Q} \quad (4.45)$$

where V: he capacity of the air storage tank, ρ: the air density, c_v: the constant volume heat capacity for air, T: the temperature of the air storage tank, h_i: the enthalpy for injection of air from the storage tank in t time, h is the enthalpy for injection of current air from storage tank at t time, Z: the air's compressibility factor, R: the air constant, u: the internal energy for air, Q: the heat transfer efficiency between the air storage tank and environment. The generalized air state equation is

$$p = Z\rho RT \quad (4.46)$$

Furthermore, the first heat conduction model is established based on the thermal coupling effect between the air in the air storage tank and the surrounding rock of the air storage tank, and the second heat conduction model is established based on the thermal coupling effect inside the surrounding rock of the air storage tank. The first and second heat conduction model are

$$\dot{Q} = h_c A_c (T_{RW} - T) \quad (4.47)$$

$$\rho_R c_R^p \frac{dT_R}{dt} = \frac{1}{r}\frac{\partial}{\partial r}\left(k_R r \frac{\partial T_R}{\partial r}\right) \quad (4.48)$$

The heat conducting conditions of surface of the air storage tank

$$r = R_w \quad (4.49)$$

$$-K_R r \frac{\partial T_R}{\partial r} = h_c (T - T_{RW}) \quad (4.50)$$

$$r \to \infty \quad (4.51)$$

$$T_R = T_0 \tag{4.52}$$

where h_c: the air storage tank's average heat transfer coefficient, A_c: the air storage tank's surface area of the of the surrounding rock, T_{RW}: the surrounding rock's surface temperature, ρ_R: the air storage tank's surrounding rock density, c_R^p: the specific heat at constant pressure of the air storage tank surrounding rock, T_R: the air storage tank' surface internal temperature, k_R: the thermal conductivity of the air storage tank of the surrounding rock and r is the radius of the air storage tank.

It is difficult to figure out the temperature and pressure of the air in the air storage tank because the equations should be solved at the same time. It is reasonable to assume that the temperature of the cave wall stays the same to avoid figuring out the heat conduction equation for the rock around the cave if the air temperature change in the air storage tank is small or if the heat transfer coefficient and thermal transfer efficiency of the rock, as defined by Kushnir [127]. Due to the cave wall's temperature will not change (mean that heat will be transferred quickly to distant rocks). Assumed that the air around us is a perfect gas, the compression factor $Z = 1$ and $\rho \frac{\partial u}{\partial \rho} = 0$, formula (3.45) can be expressed as

$$V_{cav}\rho c_v \frac{dT}{dt} = \dot{m}_{in}(h_i - h + RT) + \dot{m}_{out}(RT) + h_c A_c (T_{RW} - T) \tag{4.53}$$

The air mass flow during AA-CAES operation can be described as constant. Consequently, in the air storage tank, the air temperature's ordinary differential equation for is

$$T=\begin{cases}\left(T_0+\frac{m_cC_pT_i+h_cA_cT_{RW}}{m_c(R-C_p)-h_cA_c}\right)e^{\frac{m_c(R-C_p)-h_cA_c}{V\rho_{av}c_v}(t-t_0)}-\frac{m_cC_pT_i+h_cA_cT_{RW}}{m_c(R-C_p)-h_cA_c}, a=1\\ (T_0-T_{RW})e^{\frac{-h_cA_c}{V\rho a_vc_v}(t-t_0)}+T_{RW}, a=0\\ \left(T_0+\frac{h_cA_cT_{RW}}{m_cR-h_cA_c}\right)e^{\frac{m_cR-h_cA_c}{V\rho a_vc_v}(t-t_0)}-\frac{h_cA_cT_{RW}}{m_cR-h_cA_c}, a=-1\end{cases} \quad (4.54)$$

where T_{i}: the air storage tank's inlet temperature at the i-th stage, T_0: the beginning air temperature, and ρ_{av}: the average air density for the operation period. The air temperature at the conclusion of the preceding phase must be utilized as the beginning temperature for succeeding phases to determine the air temperature for the whole operating cycle. For instance, the temperature solution for the following storage cycle can be defined as follows when the air temperature at the conclusion of the charging cycle is T_1.

$$T=\begin{cases}\left(T_1+\frac{m_cC_pT_i+h_cA_cT_{RW}}{m_c(R-C_p)-h_cA_c}\right)e^{\frac{m_c(R-C_p)-h_cA_c}{V\rho_{av}c_v}(t-t_1)}-\frac{m_cC_pT_i+h_cA_cT_{RW}}{m_c(R-C_p)-h_cA_c}, a=1\\ (T_0-T_{RW})e^{\frac{-h_cA_c}{V\rho a_vc_v}(t-t_1)}+T_{RW}, a=0\\ \left(T_0+\frac{h_cA_cT_{RW}}{m_cR-h_cA_c}\right)e^{\frac{m_cR-h_cA_c}{V\rho a_vc_v}(t-t_1)}-\frac{h_cA_cT_{RW}}{m_cR-h_cA_c}, a=-1\end{cases} \quad (4.54)$$

Overall, the air pressure can be achieved by equation (3.46) when it gets the air temperature. Therefore, air temperature and pressure can be simplified to define separately.

(2) Isothermal Air Storage Tank

For the underground salt cave air storage and other small air storage methods, the heat loss between storage tanks and the surface of the tank is not obvious, it can be easily controlled implementation way of heat preservation and heat insulation. Therefore, to further simplify the constant volume and capacity adiabatic model is based on the constant capacity model. The

constant volume isothermal model assumes that the air temperature in the air storage does not change with time, and can be expressed as

$$a\dot{m}_c(t) = \dot{m}_{in}(t) + \dot{m}_{out}(t) \tag{4.56}$$

$$P = \begin{cases} P_{cav,0} + \frac{m_i(t)R_gT_0}{V}, a = 1 \\ P_{cav,0} + \frac{m_e(t)R_gT_0}{V}, a = -1 \end{cases} \tag{4.57}$$

$$T = T_0 \tag{4.58}$$

(3) Adiabatic Air Storage Tank

$$a\dot{m}_c(t) = \dot{m}_{in}(t) + \dot{m}_{out}(t) \tag{4.59}$$

$$T = \begin{cases} \left(T_1 + \frac{m_cC_pT_i}{m_c(R-C_p)}\right)e^{\frac{m_c(R-C_p)}{V\rho a_v c_v}(t-t_0)} - \frac{m_cC_pT_i}{m_c(R-C_p)}, a = 1 \\ (T_0 - T_{RW})e^{\frac{-h_cA_c}{V\rho a_v c_v}(t-t_0)} + T_{RW}, a = 0 \\ \left(T_0 + \frac{1}{m_cR}\right)e^{\frac{m_cR}{V\rho a_v c_v}(t-t_0)} - \frac{1}{m_cR}, a = -1 \end{cases} \tag{4.60}$$

$$p = Z\rho RT \tag{4.61}$$

4.3.5 Throttle Valve Module

For ideal air, throttle valve (TV) throttle air mass flow rate before and after the same temperature and pressure, only so can be treated as isenthalpic, flow through the inlet side TV of the air storage tank can be satisfied as

$$\dot{m}_{c,TV}^{in} = \dot{m}_{c,TV}^{out} \tag{4.62}$$

$$T_{c,TV}^{in} = T_{c,TV}^{out} \tag{4.63}$$

Similarity to flow through the inlet side TV of the gas storage tank, flow through the outlet side TV of the air storage tank

$$\dot{m}_{e,TV}^{in} = \dot{m}_{e,TV}^{out} \tag{4.64}$$

$$T_{e,TV}^{in} = T_{e,TV}^{out} \tag{4.65}$$

4.3.6 Air Turbine Module

(1) Rated Condition Model

The turbine' isentropic outlet temperature at the i-th stage is

$$T_{e,i}^{out,is} = T_{e,i}^{in} / \left(\beta_{e,i}\right)^{\frac{1-k}{k}} \tag{4.66}$$

where $T_{e,i}^{out,is}$: the turbine isentropic outlet temperature at the i-th stage during the generation progress, $T_{e,i}^{in}$: the turbine's inlet temperature at the i-th stage during the generation progress, $\beta_{e,i}$: the turbine's pressure ratio the i-th stage during the generation progress.

The i-th stage of the turbine's isentropic efficiency is

$$\eta_{e,i} = \frac{T_{e,i}^{in} - T_{e,i}^{out}}{T_{e,i}^{in} - T_{e,i}^{out,is}} \tag{4.67}$$

where $\eta_{e,i}$: the turbine's isentropic efficiency, thus the turbine's actual outlet temperature at the i-th stage is

$$T_{e,i}^{out} = T_{e,i}^{in}\left(1 - \eta_{e,i} + \eta_{e,i}\left(\beta_{e,i}\right)^{\frac{1-k}{k}}\right) \tag{4.68}$$

The turbine's actual power generation at the i-th stage is

$$W_{e,i} = \dot{m}_e c_p^a \left(T_{e,i}^{in} - T_{e,i}^{out}\right) \tag{4.69}$$

The total power generation of turbine is

$$W_e = \sum_{i=1}^{N_e} W_{e,i} \tag{4.70}$$

where $\dot{m}_e$: the turbine mass flow rate, c_p^a: the constant pressure-specific heat of the air and N_e is the stage of turbine.

The turbine's actual outlet temperature at the i-th stage is

$$p_{e,i}^{out} = \frac{p_{e,i}^{in}}{\beta_{e,i}} \tag{4.71}$$

where $p_{e,i}^{in}$, $p_{e,i}^{out}$ are the inlet and outlet air pressure of turbine, respectively.

Similarity to the compressor, the quasi-steady-state thermodynamic model of the rated condition can be used to demonstrate it from equations (4.68) – (4.71).

(2) Off-design Model

The isentropic efficiency of the air turbine fluctuates with the operating state under the off-design situation, much like the operation characteristics of the compressor. The isentropic efficiency of the turbine can reach 85% to 90% under the rated condition, while the isentropic efficiency drops to 65% to 75% under the 50% load condition [111]. As the air storage pressure drops during the expansion energy release, the air temperature and pressure at the air storage tank's outlet will change as well. For this reason, the analytical expression of the turbine under

the off-design condition proposed in [67] is used to establish the complete module of turbine expansion.

The characteristic of isentropic efficiency should be satisfied as [116][125]

$$\frac{\eta_{e,i}}{(\eta_{e,i})_0} = \left[1 - b_0\left(1 - \dot{\eta}_{e,i}\right)^2\right]\left(\dot{\eta}_{e,i}/\dot{G}_{e,i}\right)\left(2 - \left(\dot{\eta}_{e,i}/\dot{G}_{e,i}\right)\right) \tag{4.72}$$

where b_0 is a constant and typical value is 0.3 [96].

The dimensionless order reduction flow rate and order reduction speed are

$$\dot{G}_{e,i} = \left[\dot{m}_e \frac{\left(T_{e,i}^{in}\right)^{0.5}}{p_{c,i}^{in}}\right] / \left[\dot{m}_e \frac{\left(T_{e,i}^{in}\right)^{0.5}}{p_{c,i}^{in}}\right]_0 \tag{4.73}$$

$$\dot{n}_{e,i} = \left[n_{e,i}\left(T_{e,i}^{in}\right)^{-0.5}\right] / \left[n_{e,i}\left(T_{e,i}^{in}\right)^{-0.5}\right]_0 \tag{4.74}$$

The actual turbine expansion ration can be expressed by [125]

$$\frac{\dot{m}_e}{(\dot{m}_e)_0} = \alpha_i \sqrt{\frac{(T_{e,i}^{in})_0}{T_{e,i}^{in}}} \sqrt{\frac{{\beta_{e,i}}^2 - 1}{({\beta_{e,i}}^2)_0 - 1}} \tag{4.75}$$

where α_i is the impact factor that characterized the influence of the change of rotation speed on the expansion ratio, it should be formulated by

$$\alpha_i = \sqrt{1.4 - 0.4\frac{n_{e,i}}{(n_{e,i})_0}} \tag{4.76}$$

The actual expansion ratio and isentropic efficiency can be obtained by the equations (4.72) – (4.76). at the same time, the actual outlet temperature and pressure of the turbine at the i-th stage should be achieved under the conditions of the actual inlet temperature and pressure.

4.4 Thermodynamic Model based on Exergy Balance

AA-CAES has typical multi-energy flow coupling characteristics, mainly manifested as the coupling between the internal air compression thermal energy and pressure potential energy double energy flow and the external cooling, heat and electricity multi-energy flow coupling. Exergy theory could provide a new perspective for analyzing the characteristics of the exergy flow of AA-CAES. Although the thermodynamic simulation model based on the exergy balance in this section is difficult to give the difference between exergy flow, exergy theory could provide a new perspective for analyzing the characteristics of the exergy flow of AA-CAES.

4.4.1 Compressor Module

Exergy input into the i-stage compressor is the power consumption and can be demonstrated by

$$Ex_{c,t}^{in}(t) = W_{c,i}(t) \tag{4.77}$$

The output exergy of the compressor at the i-th stage is

$$Ex_{c,t}^{out}(t) = \dot{m}_c(t)\left[c_p^a\left(T_{c,i}^{out}(t) - T_{c,i}^{in}(t)\right)\right] - T_0\left(c_p^a \ln\frac{T_{c,i}^{out}(t)}{T_{c,i}^{in}} - R_g \ln\frac{P_{c,i}^{out}(t)}{P_{c,i}^{in}}\right) \tag{4.78}$$

The exergy destruction of the i-th stage compressor is

$$Lx_{c,i}(t) = Ex_{c,t}^{in}(t) - Ex_{c,t}^{out}(t) \tag{4.79}$$

4.4.2 HEX Module

(1) HEX Exchanger on the Compression Side

The input exergy of the stage of compression supply by high-temperature air and the output exergy was carried away by heat carrier fluid. Therefore, the exergy of the i-th stage HEX is

$$Ex_{HX,t}^{c,in}(t) = \dot{m}_c(t)\left[c_p^a\left(T_{HX,i}^{a,in}(t) - T_{HX,i}^{a,out}(t)\right) - T_0 c_p^a \ln\frac{T_{HX,i}^{a,in}(t)}{T_{HX,i}^{a,out}(t)}\right] \tag{4.80}$$

The output exergy of the i-th stage HEX was carried away by heat carrying fluid, it can be expressed by

$$\begin{aligned} Ex_{HX,t}^{c,out}(t) &= \dot{m}_{c,i}^{HTF}(t)\left[\left(h_{HX,i}^{HTF,out}(t) - h_0^{HTF}\right) - T_0\left(s_{HX,j}^{HTF,out}(t) - s_0^{HTF}\right)\right] \\ &\quad - \dot{m}_{c,i}^{HTF}(t)\left[\left(h_{HX,i}^{HTF,in}(t) - h_0^{HTF}\right) - T_0\left(s_{HX,i}^{HTF,in}(t) - s_0^{HTF}\right)\right] \\ &= \dot{m}_{c,i}^{HTF}(t)\left[\left(h_{HX,i}^{HTF,out}(t) - h_{HX,i}^{HTF,in}(t)\right) - T_0\left(s_{HX,i}^{HTF,out}(t) - s_{HX,i}^{HTF,in}(t)\right)\right] \end{aligned} \tag{4.81}$$

The exergy destruction of the i-th stage HEX is

$$Lx_{HX,i}^{c}(t) = Ex_{c,t}^{in}(t) - Ex_{c,t}^{out}(t) \tag{4.82}$$

(2) HEX on the Expansion Side

The input exergy of the stage of compression supply by high-temperature heat exchange fluid and the output exergy was carried away by air. Therefore, the exergy of the i-th stage HEX is

$$Ex_{HX,t}^{e,in}(t) = \dot{m}_{e,i}^{HTF}(t)\left[\left(h_{HX,e,i}^{HTF,in}(t) - h_0^{HTF}\right) - T_0\left(s_{HX,e,j}^{HTF,in}(t) - s_0^{HTF}\right)\right]$$
$$- \dot{m}_{e,i}^{HTF}(t)\left[\left(h_{HX,e,i}^{HTF,out}(t) - h_0^{HTF}\right) - T_0\left(s_{HX,ei}^{HTF,out}(t) - s_0^{HTF}\right)\right]$$
$$= \dot{m}_{e,i}^{HTF}(t)\left[\left(h_{HX,e,i}^{HTF,in}(t) - h_{HX,i}^{HTF,out}(t)\right) - T_0\left(s_{HX,e,i}^{HTF,in}(t) - s_{HX,e,i}^{HTF,out}(t)\right)\right] \quad (4.83)$$

The output exergy of the i-th stage HEX was carried away by air, it can be demonstrated by

$$Ex_{HX,t}^{e,out}(t) = \dot{m}_{e,i}(t)\left[c_p^a\left(T_{HX,i}^{a,e,out}(t)\right) - T_{HX,i}^{a,e,in}(t) - T_0 c_p^a \ln\frac{T_{HX,i}^{a,e,out}(t)}{T_{HX,i}^{a,e,in}(t)}\right] \quad (4.84)$$

The exergy destruction of the i-th stage HEX is

$$Lx_{HX,i}^{c}(t) = Ex_{c,t}^{in}(t) - Ex_{c,t}^{out}(t) \quad (4.85)$$

4.4.3 Throttle Valve Module

The input exergy of TV is exergy of inlet air and the output exergy is exergy of outlet air, the equation is

$$Lx_{TV}^{c} = Ex_{c,TV,t}^{in} - Ex_{c,TV,i}^{out} \quad (4.86)$$

For the inlet of TV, the input exergy of TV is output exergy of last stage HEX air and the expression is

$$Lx_{TV}^{e} = Ex_{e,TV,t}^{in} - Ex_{e,TV,i}^{out} \quad (4.87)$$

4.4.4 Air Turbine Module

Exergy of turbine is provided by air and the output exergy is output work. As a result, the inlet exergy of the i-th stage turbine is

$$Ex_{e,t}^{in}(t) = \dot{m}_e(t)\left[c_p^a\left(T_{e,i}^{in}(t)\right) - T_{e,i}^{out}(t) - T_0\left(c_p^a \ln\frac{T_{e,i}^{in}(t)}{T_{e,i}^{out}(t)} - \right)\right] \quad (4.88)$$

The output exergy of the i-th stage turbine is

$$Ex_{e,t}^{out}(t) = W_{e,i}(t) \quad (4.78)$$

The exergy destruction of the i-th stage turbine is

$$Lx_{e,i}(t) = Ex_{e,i}^{in}(t) - Ex_{e,i}^{out}(t) \quad (4.79)$$

4.5 The Experiment and Validation of the CER

At present, there is feasible AA-CAES thermodynamic simulation software, most of them which can only analyze the performance of the system at a specific operating point Simulation is difficult to give the dynamic characteristics of the whole system during operation (heat storage system, air storage, so it is not convenient to analyze the coupling relationship between the internal thermodynamic parameters of AA-CAES within a cycle, and it is also difficult to match the real operating situation of AA-CAES. Based on the AA-CAES off-design thermodynamic simulation model given above, this section focuses on heat exchange and adiabatic of the system, discusses the necessity of the off-design operating model research, and verifies the accuracy of the proposed model combined with the overall operation process of the AA-CAES system.

4.5.1 The Design Parameters of the CER

A typical AA-CAES system operational characteristics are now analyzed in this part using the developed thermodynamic quasi-steady-state simulation model. In Figure 4.1, the system diagram is displayed. Tables 4.1 to 4.6 display the thermodynamic design parameters for the compressor, turbine, HEX, and other system components.

Table 4.1 The parameters of each stage compressor

Stage	Pressure [MPa]		Temperature [℃]		Adiabatic efficiency %	Mass flow [kg/s]
	Inlet	Outlet	Inlet	Outlet		
1	0.0995	0.24	20	120	83.85	7.389
2	0.2182	0.4315	40	120	84.2	7.389
3	0.411	0.8134	40	120	84.3	7.38
4	0.7747	1.532	40	120.1	84.19	7.341
5	1.459	2.882	40	120	84.04	7.319
6	2.771	5.465	40	120	83.82	7.308
7	5.306	10.2	40	121	79.3	7.303

Table 4.2 The parameters of each stage turbine

Stage	Pressure [MPa]		Temperature [℃]		Adiabatic efficiency %	Mass flow [kg/s]
	Inlet	Outlet	Inlet	Outlet		
1	3.846	0.8614	300	124.8	87.87	14.458
2	0.8204	0.1025	200	9.997	89.83	14.458

Table 4.3 The parameters of each stage intercooler

Stage	Air Temperature [℃]		Water temperature [℃]		Mass flow [kg/s]
	Inlet	Outlet	Inlet	Outlet	
1	120	40	15.01	80	2.178
2	120	40	15.01	80	2.267
3	120	40	15.01	80	2.524
4	120.1	40	15.01	80	2.352
5	120	40	15.01	80	2.274
6	120	40	15.01	80	2.259
7	121	40	15.01	80	2.327

Table 4.4 The parameters of air storage tank

Air storage volume, m^3	36×86.6
Pressure range of air storage, MPa	4-10

Table 4.5 The parameters of each stage preheater

Stage	Air temperature [℃]		TSS temperature [℃]		Mass flow [kg/s]
	Inlet	Outlet	Inlet	Outlet	
1	22.23	300	540.1	464.8	36.97
2	124.8	200	464.8	444.7	36.97

Table 4.6 The parameters of each thermal storage system

	Temperature [℃]	Pressure [MPa]	Medium
Low-temperature thermal energy storage	290	0.1014	Molten-salt
Medium-temperature thermal energy storage	434.7	0.1014	Molten-salt
High-temperature thermal energy storage	550	0.1014	Molten-salt
Water Tank	80	0.4	Water

The system adopts the compression process of multi-stage compression, inter-stage cooling with heat recovery, the heat storage system includes thermal storage medium tanks, the thermal storage medium is water and molten salt, the air storage tank adopts SPT, the regulating valve is located between the air storage tank and the expansion system to guarantee the air pressure entering the expansion system reaches the design value for molten. The expansion process of multi-stage expansion and inter-stage heating is adopted. The high-speed turbine drives the low-speed generator through the compressed air to output electric energy.

4.5.2 The Process of Compression Energy Storage

When the compression process started, the beginning pressure in the air storage tank was 2.82 MPa, and the system's ambient temperature was 293 K. Under the premise that the rated parameters were being used, a comparison was made between the compression process and the

air storage tank's the adiabatic and heat exchange. Figures 4.3 and 4.4 show how the output pressure of all levels of the compressors alter by time as they worked in the different modes of adiabatic and heat transfer of the ATS. This shows that an eight-hour simulation of the air storage method was carried out. During the process, the first 5-stage compressor units ran continuously, the sixth compressor stabilized under changing back-pressure conditions, and the 7th compressor ran continuously under changing back-pressure conditions. Because there were so many stages of compression, the system was able to work better while using less energy. When the heat exchange of the air storage tank was considered, it took the sixth stage compressor 3.4 h to reach stable pressure. However, it only took 2.5 h when the air storage tank was in an adiabatic state. Because adiabatic heat and pressure losses were not considered, the sixth stage attained stable pressure more quickly than it did under heat exchange conditions. When comparing the air storage tank's adiabatic conditions to actual system data, the air storage tank's conditions were more representative of the actual situation.

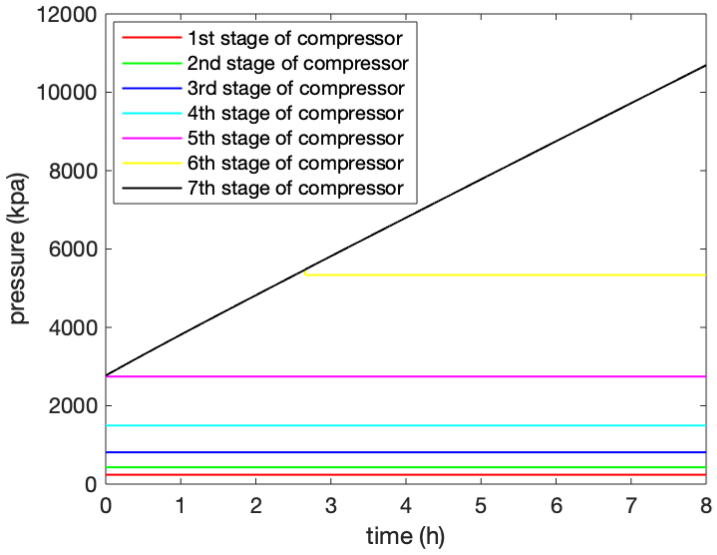

Figure 4.3. Changes in each stage compressor outlet pressure during compression in an adiabatic situation

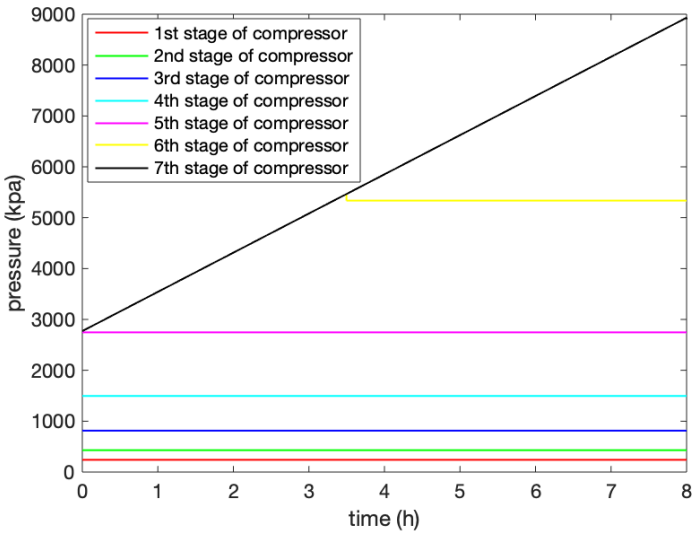

Figure 4.4. Changes in each stage compressor outlet pressure during compression in a heat exchange situation

Each stage's power consumption for the two modes of adiabatic and heat exchange of the air storage tank during the storage progress is shown in Figures 4.5 and 4.6 which a) is original and b) details of each stage. The varying back-pressure times of the 6th and 7th phases, which are identical to the pressure change curves in figures 4.3 and 4.5, are the key indicators of the altering power consumption characteristics.

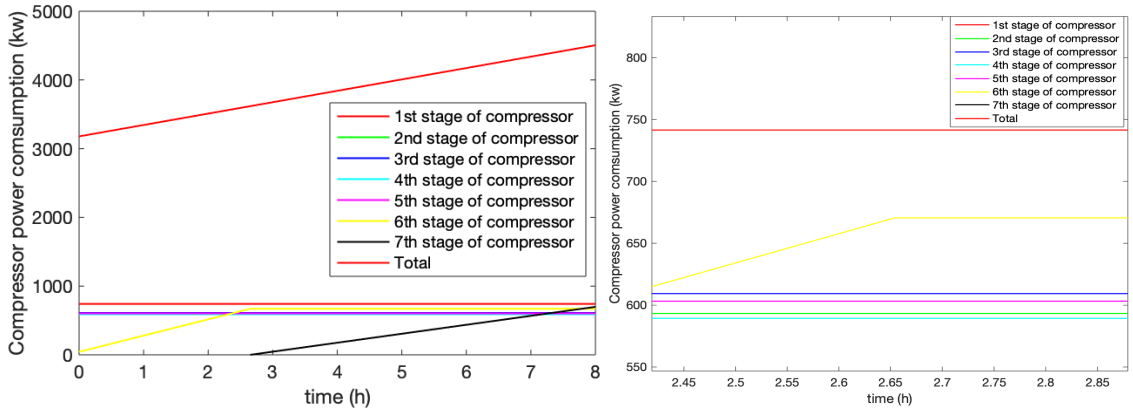

a) Original b) details

Figure 4.5. Under adiabatic conditions, the power consumption of the compressors at all levels

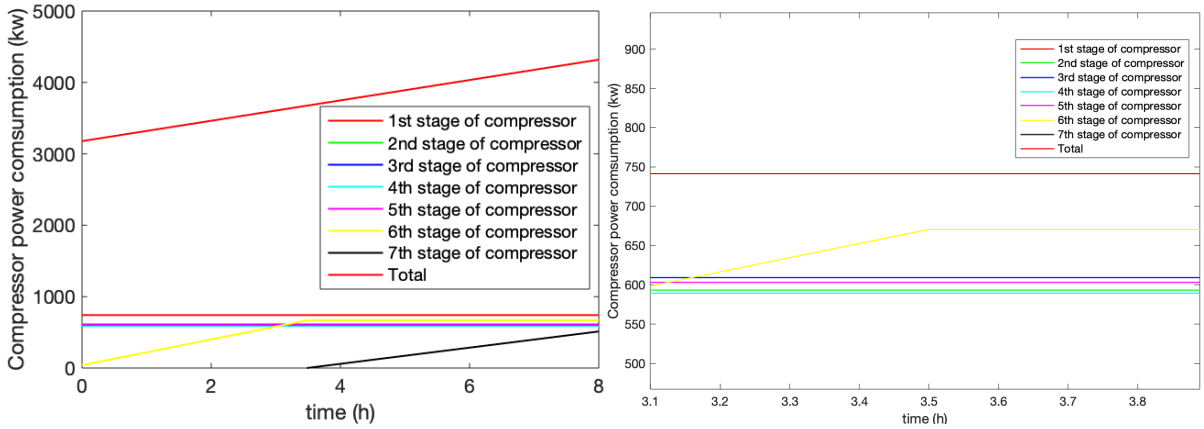

a) Original b) details

Figure 4.6. Under heat exchange conditions, the power consumption of the compressors at all levels

Figure 4.7 depicts the heat exchange on the HEX's compression side. Through the heat exchange between the water and the HEX, the system produced 80 °C hot water after storing air for 8 h. Electric heating utilized the 80 °C hot water that was left after 16 h. Electric heating might supply 16 h of 210 ℃ industrial steam at once to meet local industrial demand. When the power generator is running, the cooling energy that remains after powering the generator can be used to meet the region's cooling needs (air conditioners, refrigerators, etc.). The aggregate effectiveness of the electric, heating, and cooling systems was 93.6%. This not only assures a clean and secure energy supply, but it also shows how effectively and economically the system is operating. The optimal distribution of a range of energy resources may be achieved, user demand can be met, and user energy efficiency can be increased by comprehensive utilization of the CER.

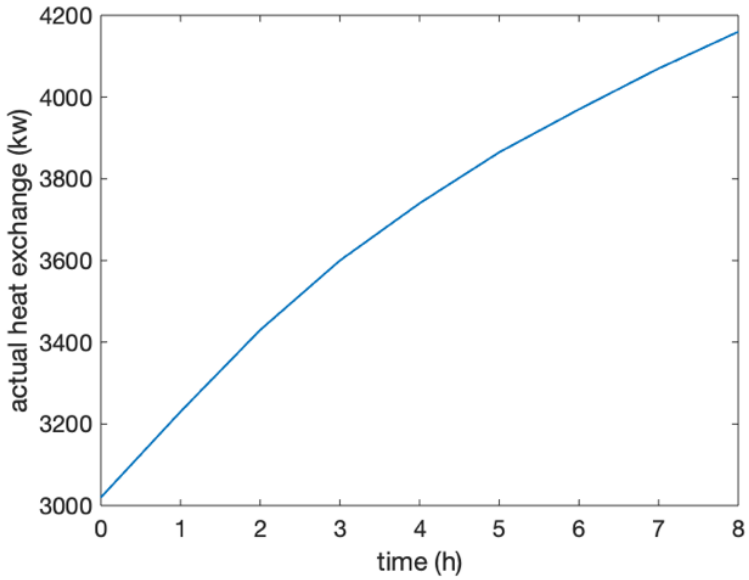

Figure 4.7. The heat exchange amount of the HEX in the compression process

4.5.3 The Process of Expansion Energy Release

Figure 4.8 illustrates the evolution of the expansion process through the fluctuation in output pressure that happens across all turbine stages. The adiabatic and heat exchange conditions of the air storage tank had no effect on the outlet pressure on the expansion side as the inlet pressure of the turbine expansion generator was controlled by the TV to meet the required pressure value. Both the output pressure of the first-stage turbine and the outlet pressure of the second-stage turbine are within the system's design parameters. The 1st stage expansion generator's outlet pressure was immediately transferred to the 2nd stage expansion generator's input pressure, resulting in the 2nd stage expansion generator commencing to generate power.

As illustrated in Figure 4.9, the temperature of the medium-temperature MSTS device has grown following the completion of heat recovery from the expansion generator. When the 4 h generating procedure, the rate of change in temperature of the adiabatic heat exchange and the external heat exchange of the air storage tank are both displayed. In order for the model to be

accurate, the heat exchange that occurs within the medium-temperature thermal storage unit must be precise.

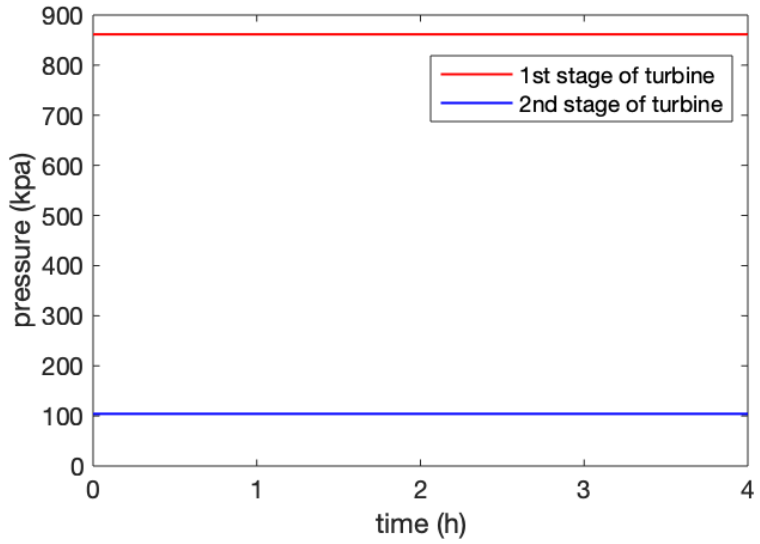

Figure 4.8. Changes in each stage turbine outlet pressure during the expansion process

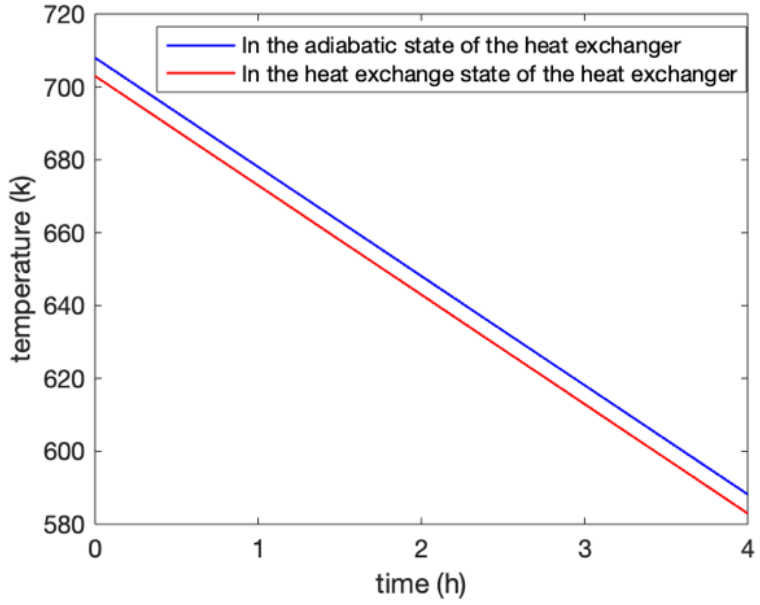

Figure 4.9. Variation in temperature of the thermal storage unit for molten salt at medium temperatures

4.5.4 The Whole System Operation Process

By simulating the compressed air storage tank's temperature and pressure variations over a period of 24 h as shown in figure 4.10, the system integrity was checked. With a shift in time, the pressure grew to 8.92 MPa with eight hours. After two hours of idle time, the pressure remained essentially constant. The pressure in the air storage tank dropped to 2.82 MPa after four hours of power production and stayed there for the next 10 hours of inactivity. After the temperature changed to 42.8 °C in 8 h, then it stabilized. After two hours, the temperature during idle time steadily decreased to 40.5 °C. After the power generation, the temperature fell once again to 36.8 °C; ultimately, it steadily increased to 40.5 °C in the last 2 h.

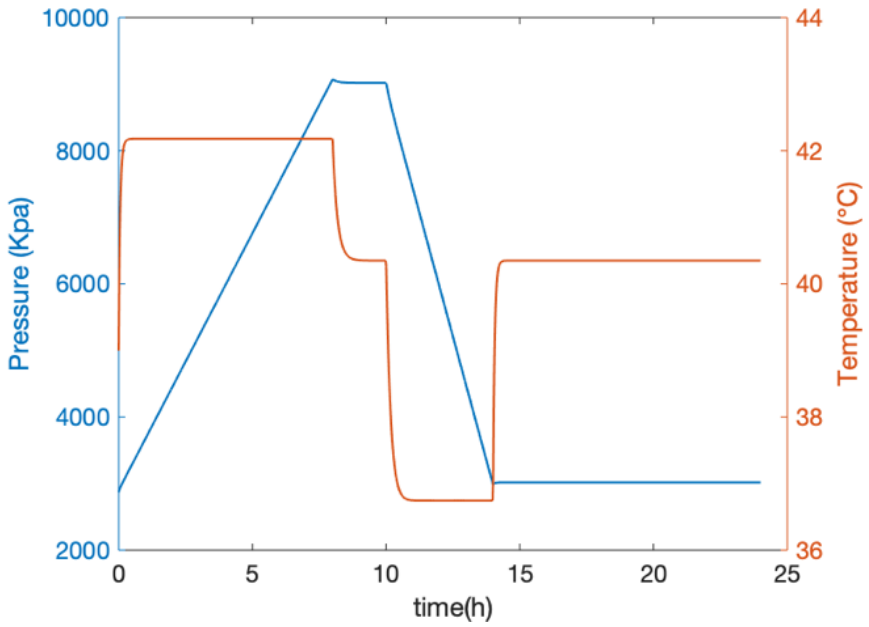

Figure 4.10. Under adiabatic conditions, the power consumption of the compressors at all levels

Two scenarios allow for the analysis of the system's overall efficiency: the first is the electric-to-electric efficiency (EXE), and another one is the round-trip efficiency (RTE), which combines cooling, heating, and electricity. As illustrated in figure 4.11, the system employed

compressed air as the medium to store power for eight hours, followed by two hours of idle time. It then used heated high-pressure air from a HEX to power the generator to provide electricity for 4 hours when it needed. The ratio between power generation and consumption was used to calculate the efficiency of the power exchange, which was found to be 56.5%.

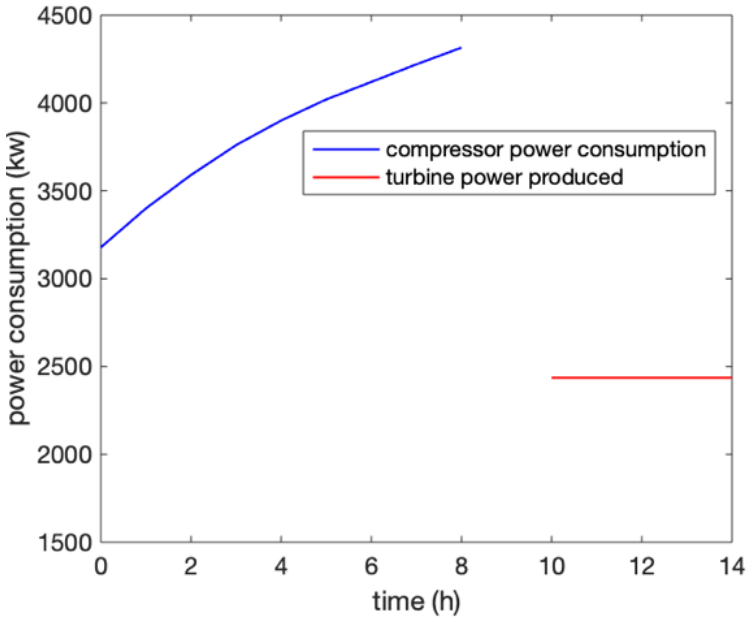

Figure 4.11. The compression and expansion processes use and produce energy

Summary

This chapter analyzes a CER based on AA-CAES as a solution for the consumption and storage of abandoned renewable energy such as wind and solar power, and off-peak electricity. The CER combines cooling, heating and electric energy which can transform stored electric energy into various types of clean energy such as high-grade electric energy, cooling energy, and different cascade thermal energy. The effectiveness of the simulation and verification of the system were demonstrated, with results showing the impact of the adiabatic and heat exchange conditions of the air storage tank on the outlet pressure change of the compressor. Under heat

exchange conditions, the sixth sage of the compressor reached stable pressure in 3.4 h compared to 2.5 h under adiabatic conditions. However, the heat exchange conditions of the air storage tank were closer to the actual situation, as confirmed by comparison with actual system data. The adiabatic and heat exchange conditions of the air storage tank did not affect the outlet pressure of the turbine for the design requirements during the discharging process. The model's accuracy depends on considering the heat exchange of the medium-temperature thermal storage unit. Finally, the overall performance was analyzed based on the power exchange efficiency (56.5%) and the overall efficiency (93.6%) with the consideration of the comprehensive energy utilization rate of the combination of cooling, heat, and electric energy.

CHAPTER 5 SOLAR ENERGY INTERGRATION OF CER

5.1 Introduction

Based on AA-CAES described in chapter 4, this chapter integrates the basis of efficient solar energy heat collection to propose the design process of a solar-thermal assisted AA-CAES (ST-AA-CAES). Under the premise of ensuring the flexible and reliable operation of the system, the comprehensive energy utilization efficiency should be improved as much as possible. The safe, reliable, clean, efficient, and flexible regulation as its core, optimized AA-CAES from four aspects: heat collection, heat storage, air storage and power generation control.

5.2 Process Optimization Objectives

To cope with the problems such as low energy utilization rate and poor energy supply reliability due to high proportion and intermittent renewable energy access to the distributed energy system, this section proposes the process optimization objective of the ST-AA-CAES system with reliability, efficiency, flexibility, and versatility as the core.

(1) Reliability: When the wind and solar power supply are interrupted or faulty, it can ensure the reliable and continuous supply of regional users' energy demand, the cooling, heat, and power generation control subsystem of ST-AA-CAES should have the ability to respond reliably to the change of terminal energy demand. At the same time, ST-AA-CAES also

need to have the function of “buffer storage” of cooling, heat, and power energy to constitute for the lack of reliability of distributed clean power supply.

(2) High efficiency: Efficiency is the basic guarantee for the feasibility and operation economy of ST-AA-CAES. ST-AA-CAES has the input attribute of multi-type and multi-grade energy carriers, so it needs to have the modulation and storage ability of multi-energy flow carriers such as cooling, heat and power. When measuring its efficiency, we should not only pay attention to the electricity-to-electricity conversion efficiency, but also focus on the utilization efficiency of comprehensive energy (cooling, heat and electricity). To improve the energy efficiency of ST-AA-CAES, joint optimization should be carried out in the overall process, component structure configuration, component parameters and other aspects. As far as the process optimization objective concerned in this chapter is concerned, achieving “temperature matching and cascade utilization” is an effective measure to improve the energy efficiency of ST-CAES. For example, in the conventional AA-CAES process, high-grade solar thermal source is introduced, high-temperature thermal energy is used for coupled power generation with air, medium-temperature thermal energy is used for heating and industrial steam, and low-temperature compression heat is used for user heating and hot water supply.

(3) Flexibility: Similarity with the AA-CAES system, the users’ demand for comprehensive energy is complementary in time, so ST-AA-CAES needs to have the ability to flexibly adjust the comprehensive output power. ST-AA-CAES should meet the energy demand of users for comprehensive energy in different seasons. A typical way is to adjust the heating

ratio of heat storage materials in the heat tank to realize the flexible supply and deployment of different forms of energy.

(4) Cleanliness: Based on the CER with AA-CAES as the core, ST-AA-CAES should maintain its cleanliness characteristics while improving the overall efficiency. Therefore, during the process optimization, renewable energy (such as wind, solar, geothermal) should be introduced into the input of ST-AA-CAES as much as possible, and zero emission should be achieved in the internal energy conversion and storage (such as pressure potential energy and compressive heat energy).

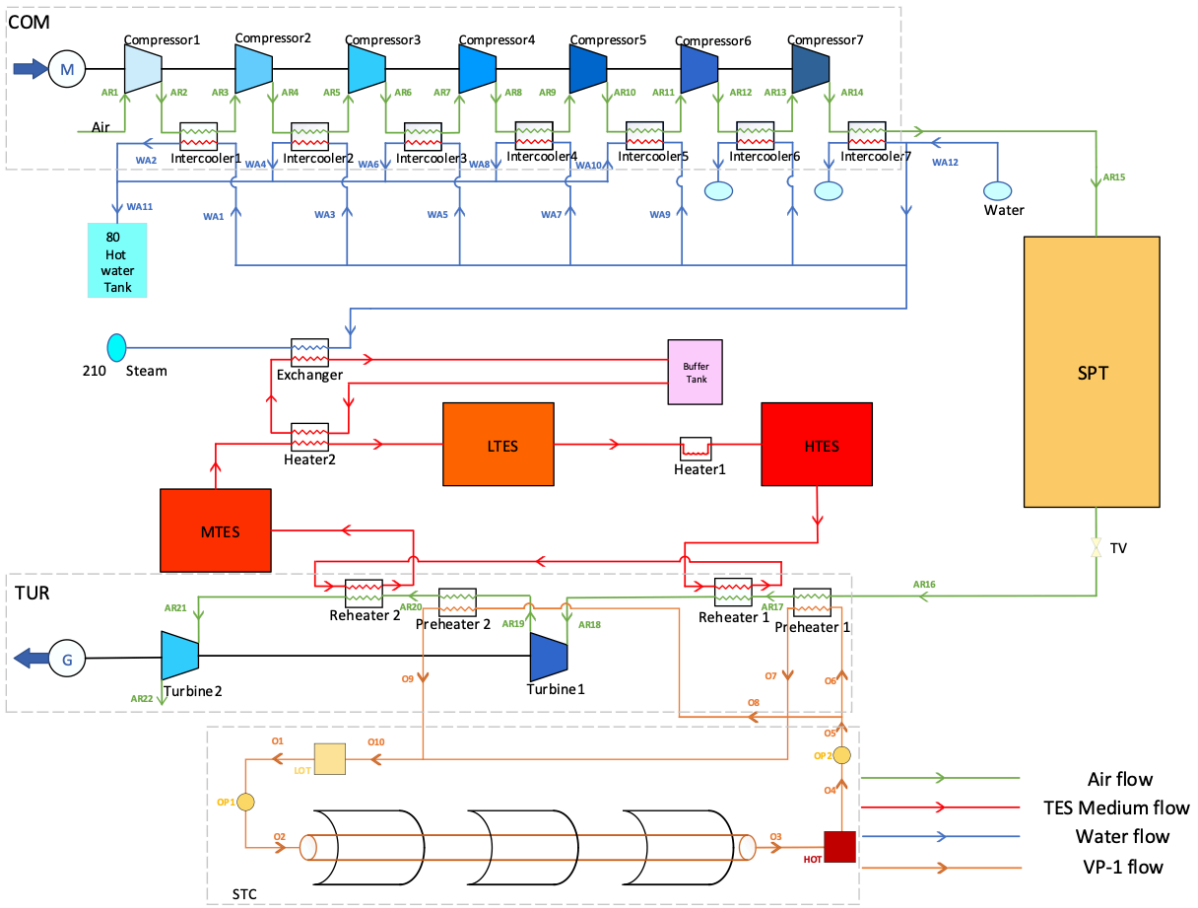

Figure 5.1. The overall structure of ST-AA-CAES

Moreover, the overall process optimization of ST-AA-CAES should have the following characteristics: If multiple clean energy sources such as wind energy and solar energy are accepted at the input end, multi-energy supply such as cooling, heat and electricity is provided at the output end, and energy conversion and storage can be realized internally, so as to realize multi-energy supply and multi-energy storage, the overall structure of ST-AA-CAES is shown in Figure 5.1. It consists of a seven-stage air compressor and a two-stage air turbine to achieve the performance of the system. There are five main subsystems for the system, a compression system, a turbine system, a SPT, a MSTS and a solar and thermal collection and storage (STC).

5.3 The Core Design Process of the System

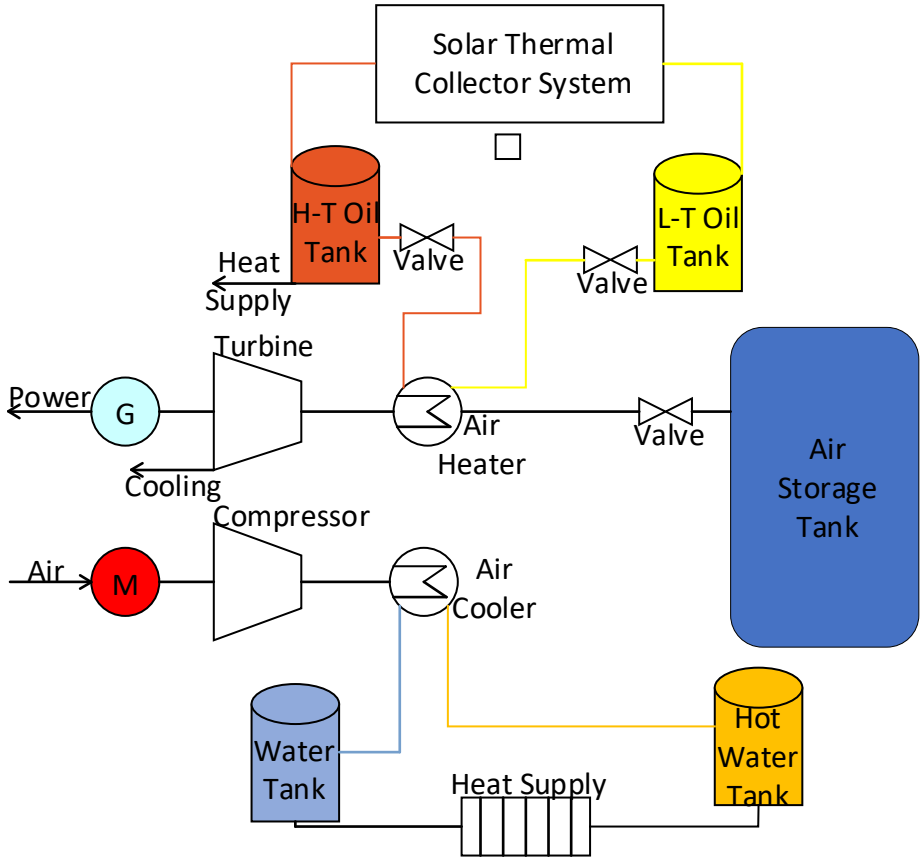

Figure 5.2. The design process of ST-AA-CAES

The system flow is composed of the high-pressure air storage system, air compression subsystem, expansion power generation subsystem, MSTS subsystem and STC subsystem. The flow is shown in Figure 5.2. Compared with AA-CAES described in chapter 4, its main difference is the addition of a STC and this section focuses on the operating principle of STC and how to integrate with the AA-CAES system.

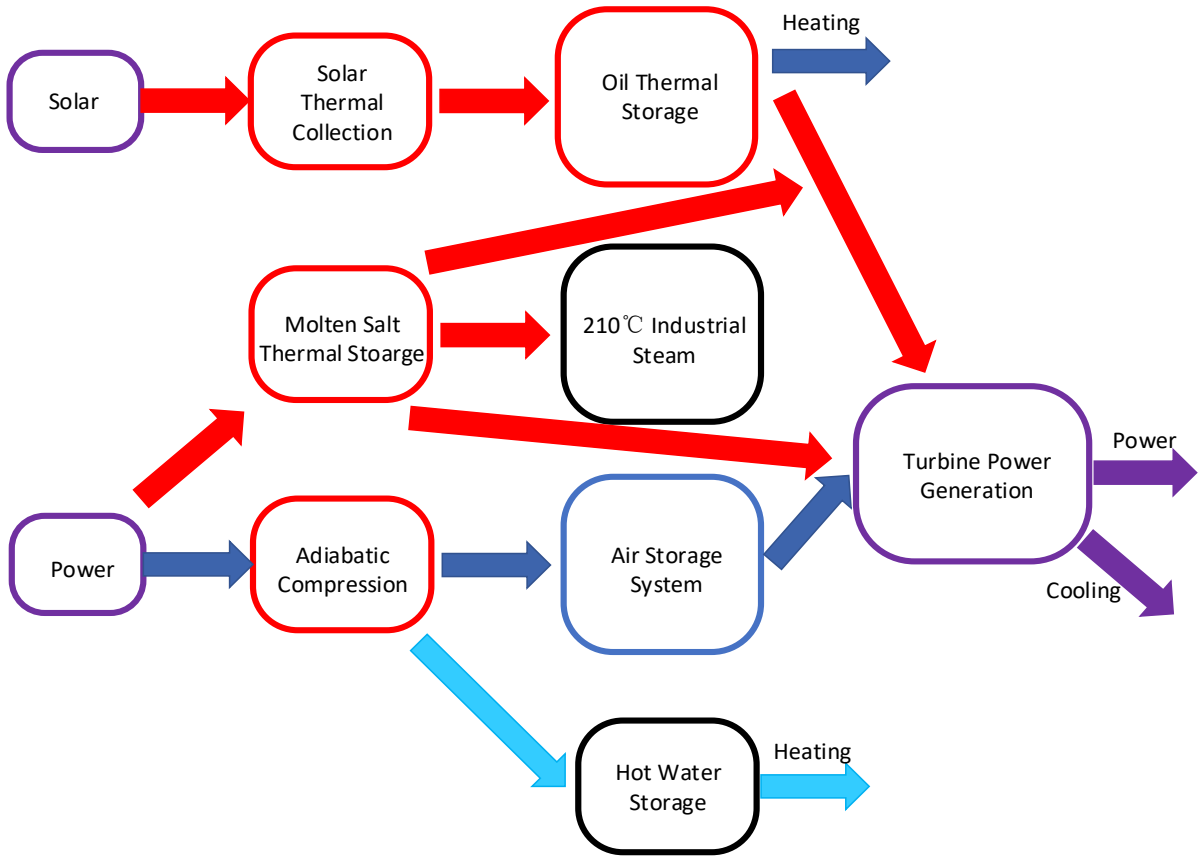

Figure 5.3. The diagram schematic of energy flow conversion of ST-AA-CAES

Based on the AA-CAES process, ST-AA-CAES coupled solar energy heat harvesting and low exergy loss heat storage technology, and its design concept is coupled with the technical trend of the multi-energy coordination and multi-technology coupling of the CER. It can not only realize the absorption and storage of solar, electricity and heat, but also realize supply of power,

cooling and heat. The conversion, cascade utilization and flexible supply of electric energy. Specifically, when ST-AA-CAES is storing energy, the air compression subsystem converts electric energy into molecular potential energy and compressed thermal energy for decoupling storage, and the solar energy is pooled and stored in the STC subsystem. According to the load demand for cooling-heat-electricity energy, by adjusting the storage high-temperature heat conduction oil used in the proportion of the power supply, heating and cooling, respectively for coupling power and high-temperature heating. Meanwhile, TES can be used to store the low-grade heat to the user, it can store and transfer characteristics as shown in figure 5.3.

5.3.1 STC

CAES is limited by the high-temperature compressor, usually the exhaust temperature is not high, which affects the heat storage temperature and limits the energy storage efficiency. ST-AA-CAES improves the two key factors of heat source and heat storage medium by introducing the external solar heat source, improving heat transfer and heat storage working medium to improve heat storage temperature and capacity, and then improving the work capacity and energy storage efficiency of high-pressure air.

The STC adopts solar thermal power generation technology with high technical maturity and tower thermal collecting and parabolic trough collector (PTC) technology with operation experience. The thermal collecting methods include trough heat collection and tower beam-down heat collection [128], whose principle is shown in figure 5.4. ST-AA-CAES with a STC does not depend on the supplementary combustion of the compressor and realizes the goal of clean energy. The process of collection and recovery of compression heat is completely

decoupled with the characteristics of high-grade thermal energy that can be used for coupled energy release power generation.

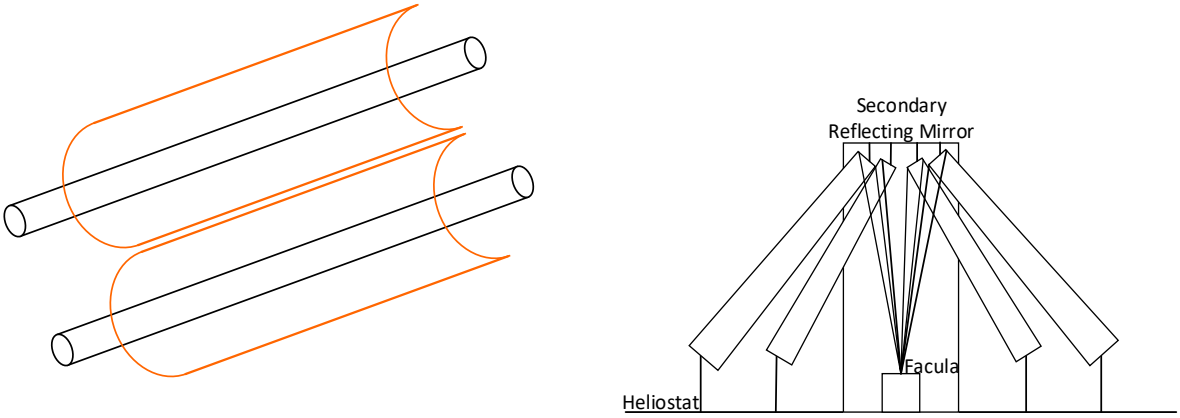

a) Trough heat collector b) Beam-down heat collector

Figure 5.4. Schematic diagram of STC system

In the selection of thermal storage medium of the STC system, heat transfer oil and molten salt both have good heat transfer and storage performance [129]. Among them, heat transfer oil is generally used for occasions below 400 ℃ with the configuration of the special pressure valve and other equipment. For molten salt, it has the advantages of an off-design working temperature range and convenient application that can be applied on the high-temperature thermal storage part of AA-CAES. However, the thermal storage method of molten salt should be equipped with a heat tracing device to avoid the melting salt solidification due to the characteristics of molten salt (should be more than 290℃), and a large amount of energy is needed to maintain the molten salt to maintain liquid static [130]. The STC is used in the power generation unit rather than in the uninterrupted cycle. Therefore, the heat transfer oil without temperature interference can be selected for use in the STC system.

5.3.2 The Model of STC

The SCT subsystem consists of a solar collector, heat storage tank, oil-air HEX and auxiliary components. This section establishes the mathematical model of each part. The STC system in ST-AA-CAES adopts the configuration mode of a beam-down tower heat collecting system and trough heat collecting double tank [131], in which the tower heat collecting model can be found in the literature [132][133]. The mathematical model of the PTC system is divided into two parts: solar thermal collecting and heat storage of the hot tank [134]. The structure of the PTC system is shown in figure. 5.5.

The direct normal exposure (I_{DNI}) by converging direct solar radiation and heats the HTF to realize the transfer of solar energy to HTF [135]. The output temperature of HTF can be calculated according to the law of energy conservation as follows [134]

$$\dot{V}_{HTF}\rho_{HTF}c_{HTF}\left(T_{HTF}^{out}-T_{HTF}^{in}\right)=Q_{SF} \tag{5.1}$$

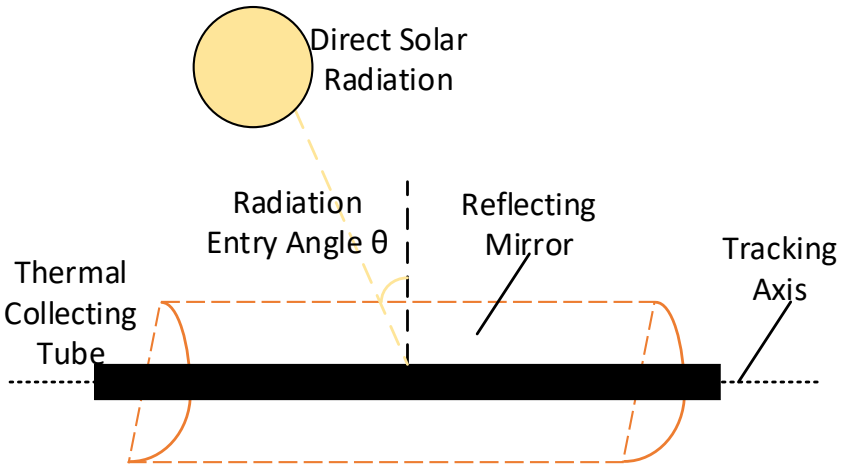

Figure 5.5. The structure diagram of the PTC system

The solar thermal energy absorbed by the heat collection link through direct solar irradiation can be uniformly expressed as:

$$Q_{SF} = Q_S - Q_{Loss} = \eta_{SF} A_{SF} I_{DNI} - Q_{Loss} \tag{5.2}$$

where Q_S, Q_{SF} are the input and absorb of solar thermal power, respectively. $\dot{V}_{HTF}, \rho_{HTF}, c_{HTF}$ are the volume flow of HTF, the density of HTF and specific heat capacity at constant pressure, respectively. I_{DNI} is the surface of direct solar radiation (unit: W/m^2), A_{SF} is the mirror field area of the PTC, Q_{Loss} is the convection loss of heat collecting link, η_{SF} is the efficiency with which solar radiation is converted into heat, its value is closely related to mirror field layout, heat transfer process, heat absorption process, external ambient temperature and other factors. Assuming that the external ambient temperature is unchanged, the calculation can be simplified as follow: The solar thermal energy absorbed by the heat collection link through direct solar irradiation can be uniformly expressed as

$$\eta_{SF} = \eta_{SF,opt} \eta_{SF,ab} \tag{5.3}$$

where $\eta_{SF,opt}$ and $\eta_{SF,ab}$ are the optical efficiency of the heat mirror field and the absorption efficiency of the PTC.

(1) Optical Efficiency Analysis of Heat Collecting Mirror Field

The optical efficiency of the trough concentrator selected for the STC system is

$$\eta_{SF,opt} = \cos\theta \cdot IAM \cdot L_{endloss} \cdot \alpha_{shadow} \cdot \mu_{SF} \tag{5.4}$$

where θ is the solar radiation' incident angle, IAM is the incident angle correction coefficient which is used to correct the difference in the concentrating ability of different incident angles,

$L_{endloss}$ is the endless heat loss the collector tube, α_{shadow} is the performance degradation coefficient of shade between groove collector array, μ_{SF} is the available concentrating area per unit area which is related to the arrangement density of the concentrating array.

The results can be achieved from the performance test of the PTC mode by San Diego Energy Laboratory, the incident angle correction coefficient IAM is

$$IAM = 1 + 0.000884\frac{\theta}{\cos\theta} - 0.00005369\frac{\theta^2}{\cos\theta} \tag{5.5}$$

The shielding coefficient between collector arrays can be expressed as

$$\alpha_{shadow} = \frac{L_{Row}}{W}\frac{\cos\xi}{\cos\theta} \tag{5.6}$$

where L_{Row} is the groove collector of row spacing, W is the width of light collector, ξ is the solar zenith angle, the endless heat loss the collector tube can be expressed as

$$L_{endloss} = 1 - \frac{f_{tub}\tan\theta}{L_{tub}} \tag{5.7}$$

where f_{tub} is the focal line length of the PTC, L_{tub} is the collector length.

(2) Analysis of Absorbed Heat Loss in Heat Collecting Mirror Field

The relationship between the absorption heat loss of the collector tube

$$Q_{loss,ab} = \left(1 - \eta_{SF,ab}\right)Q_{SF} \tag{5.8}$$

According to different physical mechanisms, the heat loss absorbed by the heat collecting link can be divided into heat conduction loss, heat convection loss and heat radiation loss [136]. The research results of San Diego Energy Laboratory show that three different types of

absorbed heat loss are related to the temperature and solar radiation intensity of HTF, which can be expressed as the following polynomial function through actual data fitting.

$$Q_{loss,ab} = Q_{cond} + Q_{conv} + Q_{rad} = \int_{T_{HTF}^{in}}^{T_{HTF}^{out}} [(a_0 + a_1 T + a_2 T^2 + a_3 T^3) + I_{DNI}(b_0 + b_1 T^2)]\, dT \quad (5.9)$$

where Q_{cond}, Q_{conv}, Q_{rad} are heat transfer loss, heat convection loss and heat radiation loss, respectively. T_{HTF}^{in} and T_{HTF}^{out} are the inlet temperature and outlet temperature of the heat collecting tube, respectively. The diagram of the STC system is shown in Figure 5.6.

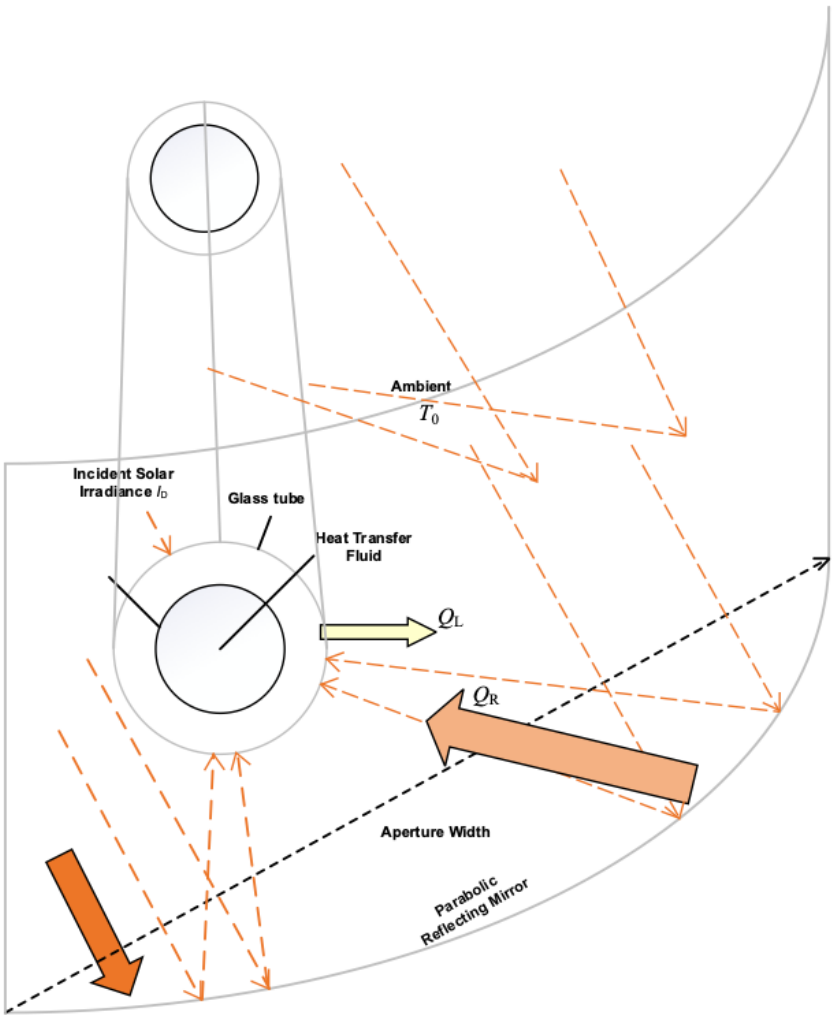

Figure 5.6. The STC system's organizational diagram

To simplify the analysis, the glass tube and width of the collecting tube cannot be considered, the heat loss between the heat collecting tube and the glass surface is neglected, and the equations from the Newton's heat loss can be expressed as

$$\begin{cases} Q_{conv} = Q_{conv1,2} + Q_{conv2,amb} \\ Q_{conv1,2} = h_d(T_1 - T_2)A_{ab} \\ Q_{conv2,amb} = h_c(T_2 - T_{amb})A_g \end{cases} \tag{5.10}$$

where $Q_{conv1,2}$ represents the heat convective consumption between the absorber tube's surface and the inner glass tube, $Q_{conv2,0}$ represents the thermal convection loss. The surfaces of the absorber and glass tubes, respectively, are designated as A_{ab} and A_g The surface temperatures of the absorption tubes and glass tubes are T_1 and T_2, respectively, and h_d is the convective heat transfer coefficient of the heat collection pipe. h_c is the heat transfer coefficient between the glass tube and environment.

According to the operating characteristics of the PTC, the external tube has a higher temperature than the glass tube and their direct thermal radiation should be considered

$$Q_{rad} = Q_{rad1,2} + Q_{rad2,0} \tag{5.11}$$

$$Q_{rad1,2} = \frac{\sigma\left(T_1^4 - T_2^4\right)}{\frac{1}{\varepsilon_1} + \frac{(1-\varepsilon_2)D_1}{\varepsilon_2 D_2}} A_{ab} \tag{5.12}$$

where the Stefan-Boltzmann constant is σ, diameters of the outer and inner glass tube are D_1 and D_2, respectively. T_1 and T_2 are the external surface and inner glass tube surface temperatures of the receiver. ε_1 and ε_2 are the emissivity of the chosen coating and glass tube. The thermal radiation can be defined as

$$Q_{rad2,0} = \sigma\varepsilon_2(T_2^4 - T_{amb}^4)A_g \tag{5.13}$$

The modelling of three tanks depends on dynamic mass balance and dynamic energy balance scheme which can be achieved by the following equation [137]

$$\rho_{HTF} \frac{dV_{HTF}}{dt} = m_{in} - m_{out} \tag{5.14}$$

where the HTF's volume in the tank is V_{HTF}, the density of HTF is ρ_{HTF}. Meanwhile, the energy balance can be expressed by

$$\rho_{HTF} C_{HTF} \frac{d(V_{HTF} T)}{dt} = C_{HTF}(T_{in} m_{in} - T m_{out}) - \mathcal{U} A_t (T - T_0) \tag{5.15}$$

where the HTF's volume in the tank is V_{HTF}, the density of HTF is ρ_{HTF}. Meanwhile, the energy balance can be expressed by

$$\rho_{HTF} C_{HTF} \frac{d(V_{HTF} T)}{dt} = C_{HTF}(T_{in} m_{in} - T m_{out}) - \mathcal{U} A_t (T - T_0) \tag{5.15}$$

where $\mathcal{U}$ and A_t are the surface area of the heat-transfer tank and its surface area's heat-transfer coefficient, respectively. It is assumed that heat transfer cannot result in heat transfer over the entire tank since the volume of HTF varies. The primary PTC parameters are presented in Table 5.1 to further demonstrate the energy balance for the HTF.

The optical efficiency of the mirror and field area are the major design elements that determine how much thermal energy is captured under specific sun irradiation circumstances [136]. The glass envelope transmittance, optical intercept factor, and cosine loss correction all have an impact on optical efficiency. In the meantime, the cosine loss correction factor is related to the tracking accuracy [138]. So as the efficiency of optical increases, the efficiency of the thermal collection also increases.

Table 5.1 Rated parameters of PTC

Main Parameters	Data
Optical efficiency	75%
Length of reflector (m)	64.15
Rank number	10
Aperture stance (m)	2
Emissivity of absorber tube	0.15
Type of mirror	White float glass
Specular reflectivity	0.93

Exergy analysis and exergy destruction are adopted from the above thermodynamic model of ST-AA-CAES, SPT model and second principle of thermodynamics for overall and each subsystem. In general, the exergy of enthalpy h can be formulated by

$$Ex_i = m_i[(h_i - h_0) - T_0(s_i - s_0)] \tag{5.17}$$

where m is the mass flow rate, s is the entropy of flow, i and o are state and ambient situations, respectively. The compression heat's thermal exergy should be estimated as follow

$$Ex_{heat} = Ex_{WA11} - Ex_{WA12} \tag{5.18}$$

The exergy supply for turbine system can be expressed by

$$Ex_{HTF} = Ex_{O5} - Ex_{O10} \tag{5.19}$$

5.3.3 Performance Criteria of ST-AA-CAES

There are two types of operating modes for the proposed ST-AA-CAES: energy storage and energy release. Compared to the traditional CAES, the operating mode includes the storage of electricity through compressed air, preheating the molten slat and solar energy to store heat. STC and MSTS can be operated independently. Therefore, the processes of operating modes

can be processed simultaneously. When the demand side needs energy, the high-pressure air in the SPT should be preheated by the STC system and then heated by the MSTS system to reach the expected temperature to drive the turbine for power generation. The heat energy is directly provided by the thermal energy storage system such as 80℃ hot water, 210 ℃ industrial steam and heating supplier. Where ESE can be described as

$$\eta_{ESE} = \frac{W_{TUR}}{W_{COM}} \tag{5.20}$$

In the complete charging and discharging cycle mode - RTE, the total heat and energy production of the turbine is taken as the numerator and the energy consumption of the compressor and heat storage of molten salt are taken as the denominator. The equation can be expressed as follow

$$\eta = \frac{W_{TUR}+Q_c+Q_{heat}}{W_{COM}+E_{TES}} \tag{5.21}$$

where Q_c is the cooling energy from the expansion process, the exergy efficiency can be depicted by

$$\eta_{EXE} = \frac{W_{TUR}+Ex_{heat}}{W_{COM}+Ex_{HTF}} \tag{5.22}$$

For each subsystem j, the exergy destruction and exergy efficiency should be estimated by:

The energy balance for each tank is

$$L_j = E_{j,in} - E_{j,out} \tag{5.23}$$

$$\eta_{EXE,j} = \frac{E_{j,out}}{E_{j,in}} \tag{5.24}$$

The exergy flows of subsystem of the ST-AA-CAES are provided in Table 5.2.

Table 5.2 Equations of exergy flow

Subsystem	Ex_{in}	Ex_{out}
Air compressor	$W_{COM} + Ex_{AR3} + Ex_{AR5} + Ex_{AR7} + Ex_{AR9} + Ex_{AR11} + Ex_{AR13}$	$Ex_{AR2} + Ex_{AR4} + Ex_{AR6} + Ex_{AR8} + Ex_{AR10} + Ex_{AR12} + Ex_{AR14}$
HEX of Compression system	$Ex_{AR2} + Ex_{AR4} + Ex_{AR6} + Ex_{AR8} + Ex_{AR10} + Ex_{AR12} + Ex_{AR14} + Ex_{WA1} + Ex_{AR3} + Ex_{WA5} + Ex_{WA7} + Ex_{WA9}$	$Ex_{AR3} + Ex_{AR5} + Ex_{AR7} + Ex_{AR9} + Ex_{AR11} + Ex_{AR13} + Ex_{WA2} + Ex_{WA4} + Ex_{WA6} + Ex_{WA8} + + Ex_{WA10}$
STC	Ex_{Qu}	$Ex_{O3} - Ex_{O2}$
Air turbine	$Ex_{AR18} + Ex_{AR21}$	$W_{TUR} + Ex_{AR19} + Ex_{AR22}$
HEX of turbine system	$Ex_{AR16} + Ex_{AR17} + Ex_{AR19} + Ex_{AR20} + Ex_{O5}$	$Ex_{AR17} + Ex_{AR18} + Ex_{AR20} + Ex_{AR21} + Ex_{O10}$
SPT	Ex_{AR15}	Ex_{AR16}

5.4 The Optimization Approach of Process and Main Parameters

In this chapter, the process optimization method of the ST-AA-CAES system is proposed. On this basis, the main parameter range of ST-AA-CAES is given, which provides the theoretical basis for subsequent thermodynamic analysis.

5.4.1 The Optimization Approach of Process

The specific optimization method is divided into four parts, as follows and the logical structure is shown in Figure 5.7:

1) From the perspective of meeting the regional load demand, the initial thermodynamic parameters of the expansion generation subsystem are configured according to the rated demand power, including the mass flow of turbine, inlet temperature, expansion stage and ratio.

2) The period of energy release generation and the mass flow rate of the turbine as rated parameters, the pressure operating range of the air storage tank, the mass flow rate and the density of storage air are determined.

3) Based on the above initial design parameters, the parameter ranges of the air compression subsystem, regenerative heating subsystem and STC system are determined.

4) The comprehensive energy efficiency of the system was evaluated, and the value range of the final parameters was determined after several iterations of revision, aiming at optimal energy efficiency.

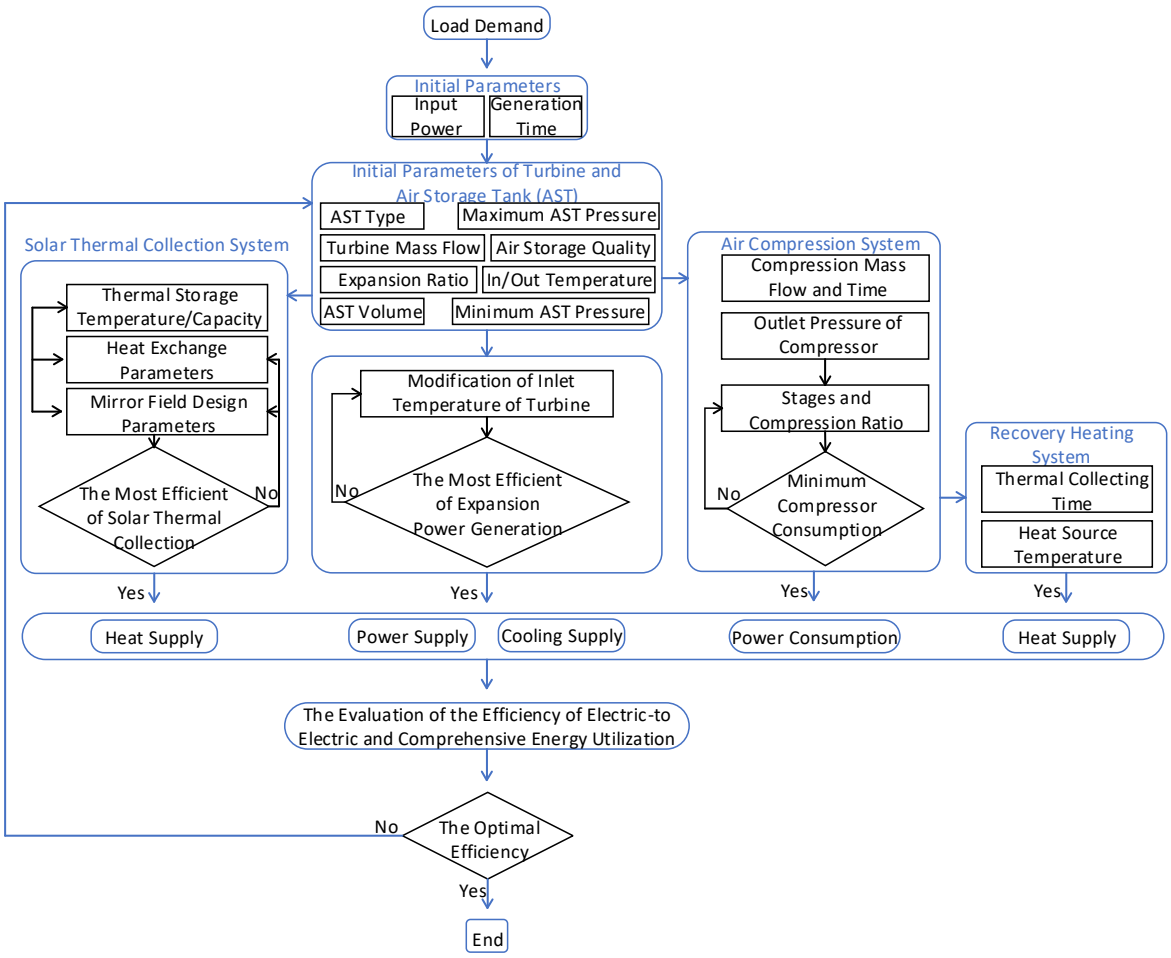

Figure 5.7. The logical optimization structure of ST-AA-CAES

5.4.2 The Range of Main Parameters

The combination of design and optimization process, the main parameters range of ST-AA-CAES can be shown in Table 5.3.

Table 5.3 The main parameters of ST-AA-CAES

Main Parameters	Unit	Value
The stage of compression	Stage	7
The stage of expansion	Stage	2
Inlet temperature of air turbine	k	573
Compressor isentropic efficiency, $\eta_{c,i}$	%	0.84
Turbine isentropic efficiency, $\eta_{e,i}$	%	0.9
Compressor air mass flow	t/h	26.6
Turbine air mass flow	t/h	52.05
Air mass flow of thermal storage medium,	t/h	36.97
At constant pressure: Specific heat capacity of air	J/kg· k	1005
Water's specific heat capacity	J/kg· k	4200
Heat transfer coefficient between air and the outside of the tank	W/$(m^2 \cdot k)$	287
The operation of STC	h	4
80℃ Hot water supply	h	8
210℃ Industrial steam supply	h	16
Heat collection efficiency	%	66.8
Environment temperature	k	293
Environment pressure	MPa	0.1
Air storage pressure	MPa	10
Inlet pressure of expansion	MPa	4

5.5 The Experimental and Verification of ST-AA-CAES

5.5.1 Exergy Analysis

For exergy analysis, Table 5.4 illustrates the key simulation results of the ST-AA-CAES system in typical operating scenarios. At the same time, the flow parameters of air, oil (Therminol VP-1) and water are listed in Table 5.5 and Table 5.6, respectively. Based on the parameters from the above table, EXE, RTE and exergy efficiency of the system are 56.5%, 95.5%, and 55.9%,

respectively. The temperature of water increases from 15.01℃ to 80℃. The STC needs about 4h to increase the temperature of VP-1 from 105.3℃ to 250℃ under the average situation. Since the efficiency of the expansion generator depends on the temperature of the high-pressure air, it is critical for the VP-1 temperature given by the solar energy absorbed and stored. The performance improvement of ST-AA-CAES mainly depends on two key technologies: first, utilize thermal energy storage system to store the compression heat through the water medium and use ambient power to heat molten salt to store the heat; second, the utilization of the STC system to store the solar heat VP-1 medium. Efficient storage and utilization of compression heat can improve the power generation efficiency and meet the thermal energy demand for users, such as hot water and user thermal supply etc.

Table 5.4 Results of the ST-AA-CAES system simulation run under typical operating circumstances

Main Data	Unit	Value
MSTS mass flow	kg/s	36.97
VP-1 mass flow	kg/s	8.522
Water mass flow	kg/s	2.27
Electric to electric	%	56.5
Round-trip efficiency	%	95.5
Exergy efficiency	%	55.9
Power consumption of compression	kW	4315
Power generation of expansion	kW	2436
PTC power collection	kW	2122

Table 5.5 The thermodynamic analysis results of air

Stream	T (℃)	P (MPa)	h (kJ/kg)	s (kJ/kg.k)	Ex (kJ/kg)	m (kg/s)
AR1	20	0.0995	419.41	3.8687	0.00	7.39
AR2	120	0.24	520.14	3.9116	88.17	7.39
AR3	40	0.2182	439.29	3.7090	66.69	7.39
AR4	120	0.4315	519.92	3.7425	137.50	7.39
AR5	40	0.411	438.90	3.5261	119.92	7.39
AR6	120	0.8134	519.47	3.5592	190.79	7.38
AR7	40	0.7747	438.15	3.3420	173.16	7.34

AR8	120.1	1.532	518.75	3.3753	243.99	7.34
AR9	40	1.459	436.87	3.1565	226.24	7.32
AR10	120	2.882	517.15	3.1890	296.98	7.32
AR11	40	2.771	434.18	2.9644	279.88	7.31
AR12	120	5.465	514.48	2.9969	350.62	7.31
AR13	40	5.306	429.40	2.7634	334.00	7.30
AR14	121	10.2	511.28	2.8061	403.36	7.30
AR15	40	10	421.36	2.5563	386.68	7.30
AR16	40	4	431.82	2.8519	310.49	14.46
AR17	150	4	547.29	3.1680	333.28	14.46
AR18	200	3.846	704.62	3.4976	393.99	14.46
AR19	124.8	0.8614	524.31	3.5550	196.97	14.46
AR20	150	0.8614	550.04	3.6177	204.23	14.46
AR21	200	0.8204	601.35	3.7463	217.83	14.46
AR22	10	0.1025	409.34	3.8252	2.67	14.46

Table 5.6 The thermodynamic analysis results of water and Therminol VP-1

Stream	T (℃)	P (MPa)	h (kJ/kg)	s (kJ/kg.k)	Ex (kJ/kg)	m (kg/s)
WA1	15.01	0.52	412.53	3.3634	0.00	2.18
WA2	80	0.40	478.67	3.6456	-15.19	2.18
WA3	15.01	0.52	412.53	3.3634	0.00	2.27
WA4	80	0.40	478.67	3.6456	-15.19	2.27
WA5	15.01	0.52	412.53	3.3634	0.00	2.52
WA6	80	0.40	478.67	3.6456	-15.19	2.52
WA7	15.01	0.52	412.53	3.3634	0.00	2.35
WA8	80	0.40	478.67	3.6456	-15.19	2.35
WA9	15.01	0.52	412.53	3.3634	0.00	2.27
WA10	80	0.40	478.67	3.6456	-15.19	2.27
WA11	80	0.40	478.67	3.6456	-15.19	11.69
WA12	15	0.40	412.86	3.4396	-21.65	14.58
O1	105.3	0.1014	0.1009	-2.754	11.72	8.52
O2	105.6	0.4372	0.787105	-2.75278	12.14	8.52
O3	250	0.1014	243.1709	-2.21482	94.12	8.52
O4	250	0.24	243.2409	-2.21499	94.24	8.52
O5	250	0.1034	243.1719	-2.21482	94.13	8.52
O6	250	0.1014	243.1719	-2.21482	94.13	6.9
O7	100	0.1034	-7.2053	-2.77313	10.21	6.9
O8	250	0.1014	243.1719	-2.21482	94.13	1.62
O9	127.6	0.1034	32.09951	-2.67157	19.23	1.62
O10	105.3	0.104	0.102984	-2.75369	11.72	8.52

Based on the above data in Table 5.5 and Table 5.6 with formulas 5.22 and 5.23, the performance of each subsystem in CER can be analyzed for exergy destruction and efficiency. The exergy efficiencies of all subsystems are provided in Figure 5.8. The exergy efficiency of the STC system is lower than the rest subsystems due to its basic characteristics such as some internal factors (optical efficiency, mass flow, mirror field area etc) and external factors (weather: rainy and cloudy days) [139]. In addition, the enthalpy efficiency of HEX of turbine system and air turbine is relatively low because of the high-temperature difference during the discharge process of high-pressure air.

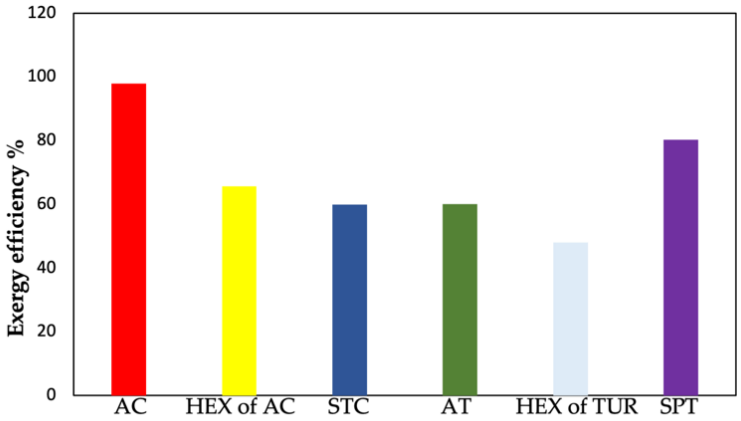

Figure 5.8. Exergy efficiencies of each subsystem of the ST-AA-CAES system

The energy destruction in the CER system is shown in Figure 5.9. The parabolic mirror surface and absorption tube external heat conduction, convection, and radiation cause numerous irreversible losses throughout the operation of the STC system [140], resulting in the exergy destruction of the system being 15.29%. Because it spends a long period to achieve the objective temperature, therefore, the STC exergy destruction during this process can be ignored in the overall analysis. Because of the irreversible heat loss of the process of heat transfer, HEX

of turbine system and HEX of compression system have relatively more exergy destruction of the CER.

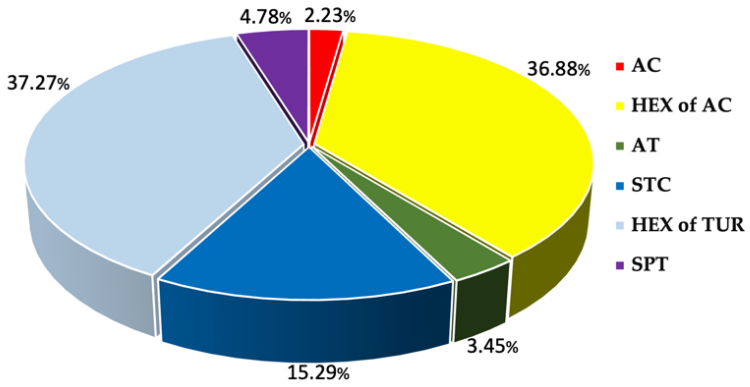

Figure 5.9. Exergy destruction of each subsystem of the ST-AA-CAES system

Some main simulation results can be compared between ST-AA-CAES in [112] and hybrid adiabatic compressed air energy storage (HA-CAES) in Table 5.7. First, the RTE and EXE for each system are 95.5% and 55.9% respectively. In comparison to the AA-CAES system, the key distinction between ST-AA-CAES and it is that the STC can be used as an extra subsystem to gather and store solar energy. The primary distinction between the HA-CAES system and ST-AA-CAES is that thermal energy storage system is not included in the air turbine's output power and is therefore susceptible to changes in solar radiation. Although the HA-CAES system has relatively higher exergy efficiency, it depends on the fuel combustion of fossil fuel which could cause the environment and air pollution, it is contrary to the development of zero carbon emission in the current world. Compared to the above ST-AA-CAES and HA-CAES systems, ST-AA-CAES not only store compression heat through the TES to improve the power generation efficiency and thermal supply, but it also collects the solar energy through the STC system to reduce power consumption in the MSTS system and further enhance the overall efficiency and flexibility.

Table 5.7. Performance of ST-AA-CAES in comparison

Parameters	Unit	ST-AA-CAES	AA-CAES	Hybrid A-CAES
With/without TES	/	Yes	Yes	No
Inlet temperature of air turbine	℃	300	300	900
Electric-to electric efficiency	%	56.5	56.5	/
Round-trip efficiency	%	95.5	93.6	87
Exergy efficiency	%	55.9	/	80

5.5.2 Analysis of the Influence of Main Parameters of Subsystem Efficiency

To comprehensively analyze factors affecting ST-AA-CAES performance, key parameters of each subsystem are analyzed in this section. The main parameters include the inlet temperature and pressure of the turbine system, the inlet temperature and pressure of air compression system.

5.5.3 The Influence of Turbine

Figure 5.10 shows the relationship between RTE, EXE, and exergy efficiency with the inlet temperature of the turbine expansion system. As can be seen from the figure, the output power of the turbine increases with the increase of the inlet temperature. The power consumption of the compressor and the compression heat collected have no impact on the inlet temperature of the turbine. As a result, RTE, EXE, and exergy efficiency all increased with the increase in turbine intake temperature.

The pressure provided to the turbine intake is one of the important parameters that impacts the thermodynamic performance of the system. There is a close association between the design value and the air storage pipe's lowest air storage pressure. The intake pressure of the turbine

is therefore set to match the minimum storage pressure of the storage line. This aids in reducing throttle loss. It should be noted that the input temperature and inlet pressure affect the turbine generator's output power, necessitating a thorough analysis.

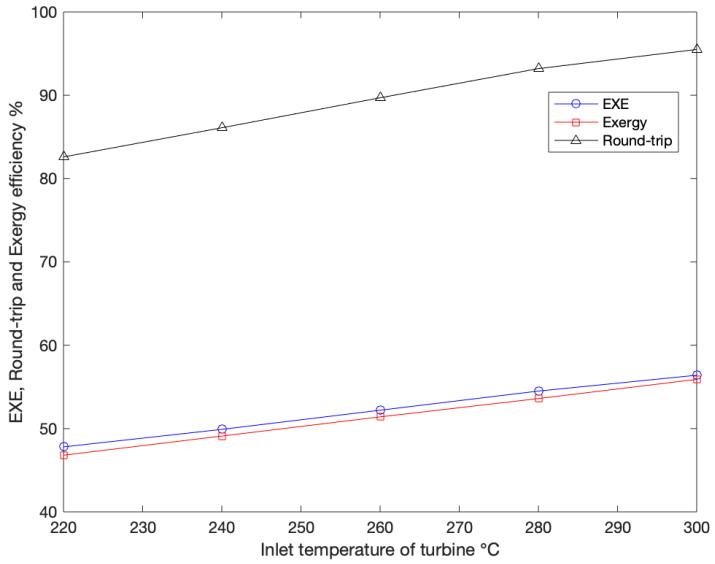

Figure 5.10. The relationship between RTE, EXE efficiency and exergy efficiency with inlet temperature of turbine

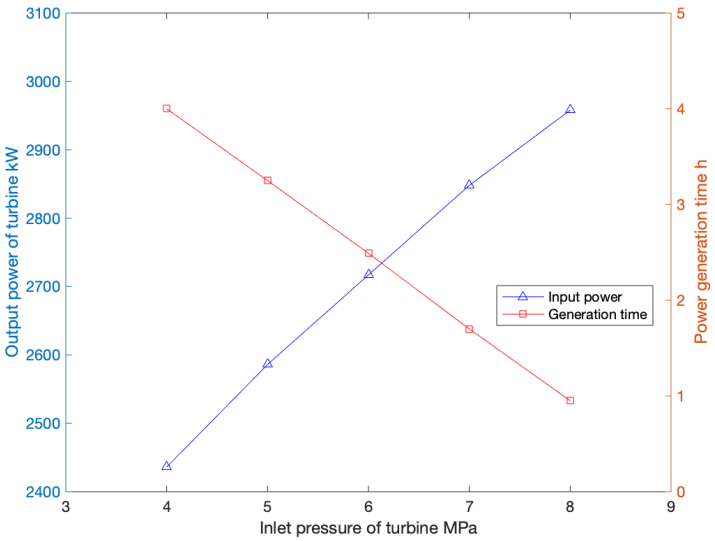

Figure 5.11. The relationship between turbine inlet pressure and output power and generating time

The relationship between the output power and generation time and the turbine's inlet pressure is depicted in Figure 5.11 The figure shows that the turbine's output power increases with increasing input pressure. When the maximum air storage pressure of the air storage tank is fixed, increasing the inlet pressure of the turbine will reduce the energy release generation time and thus reduce the electric energy output. As the running time decreases, the consumption of heat conduction oil VP-1 for heating high-pressure air decreases.

5.5.4 The Influence of Compressor

Figure 5.12 shows the compressor inlet temperature grew with the increase in the compressor power consumption increased while the output power of the expansion generator remained unchanged. When the inlet temperature increased from 20 ℃ to 40 ℃, the RTE, EXE and exergy efficiency decreased by 2.8%, 2.5% and 2.4%, respectively. Overall, the lower inlet temperature (ambient temperature) improves the overall performance of the system.

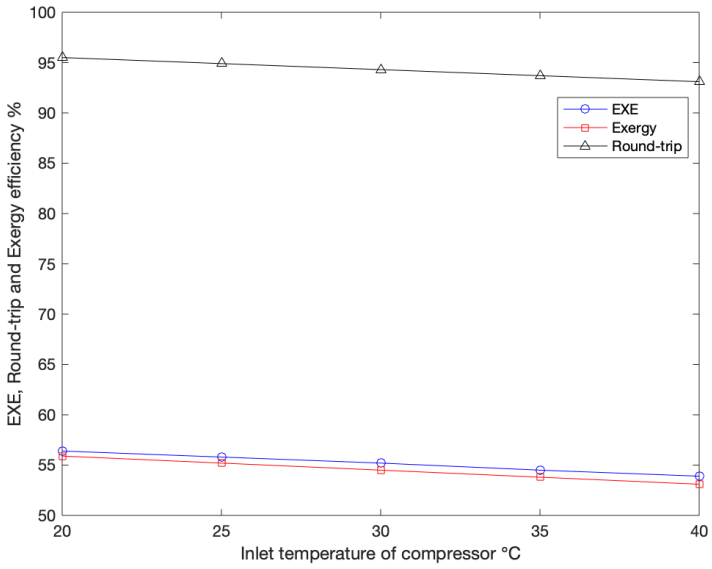

Figure 5.12. Variation of the generating time and power output in relation to the turbine inlet pressure

In the ST-AA-CAES system, increasing the exhaust pressure of the air compressor means increasing the power of the compressor as the back pressure increases, as well as increasing the time of compressed air storage. The relationship between compressor power consumption and air storage time with compressor exhaust pressure is shown in figure 5.13. Under the operating condition of the mass flow rate of 7.389kg/s, the compressor exhaust pressure increases from 6MPa to 10MPa, the charging time increases from 2.97 hours to 8 hours, and the compressed consumption increases by 425kW.

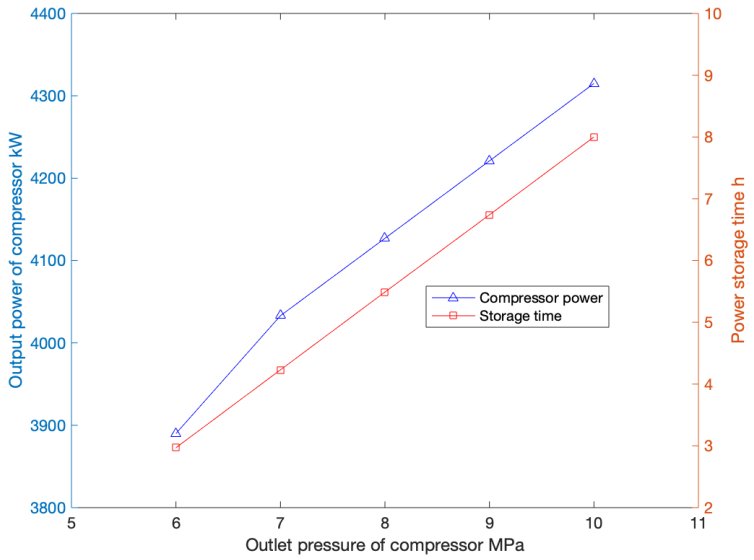

Figure 5.13. The relationship between turbine inlet pressure and output power and generation time fluctuation

Summary

Based on the overall process design in Chapter 4, energy analysis and exergy analysis of ST-AA-CAES are demonstrated in this chapter, and the main factors affecting the overall efficiency of the ST-AA-CAES system, and the comprehensive energy supply capability are discussed. First, EXE, RTE and exergy efficiency are 56.5%, 95.5% and 55.9%, respectively.

Second, the exergy efficiency and destruction of each subsystem are analyzed, it mentioned that HEX of turbine system and HEX of compression system have the lowest exergy efficiency and the greatest exergy destruction. Finally, to improve the efficiency of the HEX on the compression side can reduce the inlet temperature of each stage compressor and the inlet temperature of the air storage tank, and thus reduce the power consumption of the compressor. To enhance the efficiency of the HEX during the generation progress can increase each stage turbine's inlet temperature, thus increasing the output power of the turbine.

CHAPTER 6 ECONOMIC PERFORMANCE OF THE CER

6.1 Introduction

The operation of the CER not only ensure high efficiency and versatility, but also the economic performance of the system is crucial. Therefore, the economics of CER will be demonstrated and analyzed in this chapter. The non-renewable nature of fossil fuels and the high cost of energy production makes it imperative to optimize the use of the power system. Under the condition of considering system constraints (heat and power energy demand), the optimal state is achieved under the condition of minimum generation cost. The purpose of ED is to determine the output of the system under optimal conditions. Therefore, many authors have studied different methods to solve the problem of economic scheduling. Cogeneration optimization of cogeneration units is a challenging optimization problem due to the nonlinear and non-convex characteristics of cogeneration units and the dual dependence of cogeneration units.

CHP units have a significant impact on energy production due to their high efficiency (approximately 90%). The CER proposed in this chapter is the main generation of thermal and electricity in the comprehensive energy supply system (accounting for more than 99%). To simplify the process of calculation of CER, the cooling energy rarely can be ignored in the calculation of optimal economics. ED is used to determine the power and thermal output of the unit to minimize operating costs. Combined heat and power economic dispatch (CHPED)

problem is a challenging non-convex and non-linear optimization problem, the power and thermal demand should be satisfied simultaneously.

In previous research, different mathematical models and approaches were applied to solve the CHPED problem. For example, the CHPED problem was decomposed into a sub-problem constrained by two operating regions which are the demand for heat and power [141][142]. The proposed approach of Lagrange can be used to solve the optimization problem and implement the various heuristic method. At the same time, a penalty function formula of the genetic algorithm proposed in [143] is improved to further reduce the error by the utilization of the variance of the preceding term. PSO was initially created to artistically mimic the ethereal and erratic motions of a swarm of birds. Therefore, studying animal social behaviour and discovering that social sharing of information in groups offers an evolutionary advantage is utilized as the foundation for constructing algorithms. The corresponding glowworm swarm optimization (GSO) as another heuristic optimization approach based on animal search behaviour is implemented in the CHPEP problem [144]. In this chapter, PSO is applied to solve the CHPED problem.

6.2 Application of PSO to CHPEDP

PSO is widely used to solve different power system problems [145]. To find the appreciate fitness values through random numbers, it is based on the objective function and the process of all evolutionary algorithms by the generation of random numbers. In the meanwhile, the position of a particle as a decision variable in PSO can be expressed by position vector X and a velocity vector V in each iteration, the equations as follow

$$X_i^{iter} = \left[x_{i,1}^{iter}, x_{i,2}^{iter}, \ldots, x_{i,N}^{iter}\right] \tag{6.1}$$

$$V_i^{iter} = \left[v_{i,1}^{iter}, v_{i,2}^{iter}, \ldots, v_{i,N}^{iter}\right] \tag{6.2}$$

where N is the total number of decision variables, and the operating principle of iteration is that each particle in each iteration uses its current speed and the experience of other particles to achieve a better position. The mathematical equations can be estimated by

$$v_n^{iter} = \omega \times v_n^{iter-1} + c_1 \times r_1^n \times \left(p_{best_{i,n}}^{iter-1} - x_{i,n}^{iter-1}\right) + c_2 \times r_2^n \times \left(g_{best_{i,n}}^{iter-1} - x_{i,n}^{iter-1}\right) \tag{6.3}$$

$$x_{i,n}^{iter} = x_{i,n}^{iter-1} + v_{i,n}^{iter} \tag{6.4}$$

where the inertia coefficient is ω, r_1^n and r_2^n are the interval (0, 1) for random numbers, $p_{best_{i,n}}^{iter-1}$ and $g_{best_{i,n}}^{iter-1}$ are the best position of i th particle in previous iteration and entire swarm, respectively. The learning components are c_1 and c_2. The predefined range for updated velocities is as follow

$$-v_n^{min} \leq v_{i,n} \leq v_n^{max} \tag{6.5}$$

$$v_n^{max} = \left(x_n^{max} - x_n^{min}\right)/r \tag{6.6}$$

where x_n^{min} and x_n^{max} are the minimum and maximum limits of variables, r is a component for the control of velocity value.

Figure 6.1 illustrates the application of PSO to the CHPED problem and the principle of an evolutionary algorithm to verify the effectiveness of this approach in the power system.

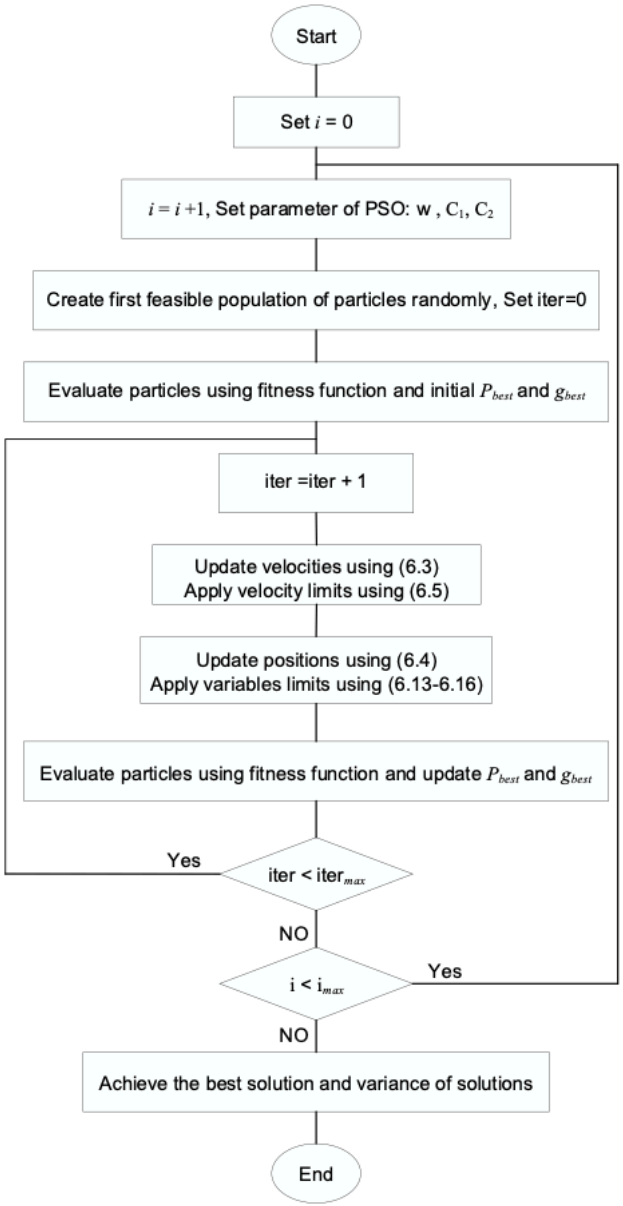

Figure 6.1. Diagram of implementing PSO into CER [145]

6.3 The Optimization Model of the CER Based on PSO

In CER there are three different conditions of operation, including power-only, CHP and heat-only units.

6.3.1 Objective Function

The objective function of CER should be determined to minimize the operation cost.

$$OBJ = \sum_{v=1}^{N_p} C_v\left(P_v^p\right) + \sum_{n=1}^{N_c} C_z(P_z^c, H_z^c) + \sum_{k=1}^{N_k} C_k\left(H_k^h\right) \tag{6.7}$$

where the operation cost of the power-only unit for generating P_v^p MW is $C_v\left(P_v^p\right)$, the operation cost of CHP units (power: P_z^c MW and heat: H_z^c) is $C_z(P_z^c, H_z^c)$, the operation cost of heat-only units (H_k^h) is $C_k\left(H_k^h\right)$ MW. N is the number of each type of unit, v, z and k are indices for each type of unit, respectively. The cost functions of each type of unit can be estimated by [48]

$$C_v\left(P_v^p\right) = \alpha_v\left(P_v^p\right)^2 + \beta_v P_v^p + \gamma_v \quad (\$/h) \tag{6.8}$$

$$C_z(P_z^c, H_z^c) = a_z(P_z^c)^2 + b_z P_z^c + c_z + d_z(H_z^c)^2 + e_z H_z^c + f_z P_z^c H_z^c \quad (\$/h) \tag{6.9}$$

$$C_k\left(H_k^h\right) = \alpha_k\left(H_k^h\right)^2 + b_k H_k^h + c_k \quad (\$/h) \tag{6.10}$$

where α_v, $\beta_v$and γ_v are coefficients of cost function related to power-only units. a_z, b_z, c_z, d_z, e_z and f_z are cost coefficients for CHP units. a_k, b_k and c_k are cost coefficients for heat-only units.

6.3.2 Constraints

The constraints based on demand for power and heat of the system are as follow

$$\sum_{v=1}^{N_p} P_v^p + \sum_{n=1}^{N_c} P_z^c = P_d + P_{loss} \tag{6.11}$$

$$\sum_{n=1}^{N_c} H_z^c + \sum_{k=1}^{N_h} H_k^h = H_d \tag{6.12}$$

where the demand for power and heat are P_d and H_d, respectively. P_{loss} is the transmission loss of the power system. The operating regions of different units should be limited by

$$P_v^{pmin} \le P_v^p \le P_v^{pmax} \;\; v = 1, 2, 3, \dots, N_p \tag{6.13}$$

$$P_z^{cmin} \le P_z^c \le P_z^{cmax}(H_z^c) \;\; n = 1, 2, 3, \dots, N_c \tag{6.14}$$

$$H_z^{cmin}(P_z^c) \le H_z^c \le H_z^{cmax}(P_z^c) \;\; n = 1, 2, 3, \dots, N_c \tag{6.15}$$

$$H_k^{hmin} \le H_k^h \le H_k^{hmax} \;\; k = 1, 2, 3, \dots, N_h \tag{6.16}$$

For power-only units, P_v^{pmin} and P_v^{pmax} are the limitations of the lower and upper generation, respectively. The range of power and heat outputs of CHP units are P_n^{cmin}, P_n^{cmax}, H_n^{cmin} and H_n^{cmax}, respectively. H_k^{hmin} and H_k^{hmax} are limits for heat-only units.

Due to the complex composition of the system, it is mainly divided into seven levels of compression subsystem, two levels of expansion subsystem, thermal energy storage subsystem and heat exchange system between each stage. At the same time, power-heat coupling and material changes at all levels in the system also need to be considered at the same time, its beyond PhD thesis. In general, the economic evaluation of CAES system is based on the design rated energy requirements as the boundary conditions. The system can be regarded as compositing of three parts, including power-only units, CHP units and heat-only units. To simplify the process of calculation, the transmission loss of the system can be ignored, the design process of AA-CAES is based on the power and heat requirements. This has certain guiding significance for the economic performance analysis of the CER which has the characteristic of multi-energy storage and supply. Therefore, this thesis chooses a macroscopic perspective when analyzing the optimization of the multistage AA-CAES system. Based on

the demand for the power and heat are 20 MW and 83.66MW, the cost functions of them are linear as follow

$$C_1(P_1) = 12.5P_1; 0 \leq P_1 \leq 37.5 \tag{6.17}$$

$$C_4(H_4) = 23.4H_4; 0 \leq H_4 \leq 1957.7 \tag{6.18}$$

6.4 Effectiveness of PSO for ST-AA-CAES

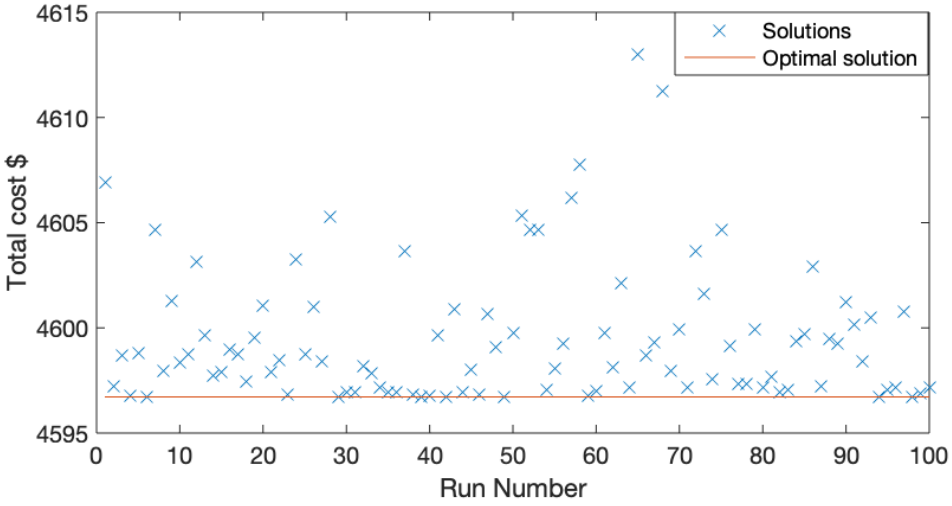

Figure 6.2. Variety solutions and optimal result of PSO

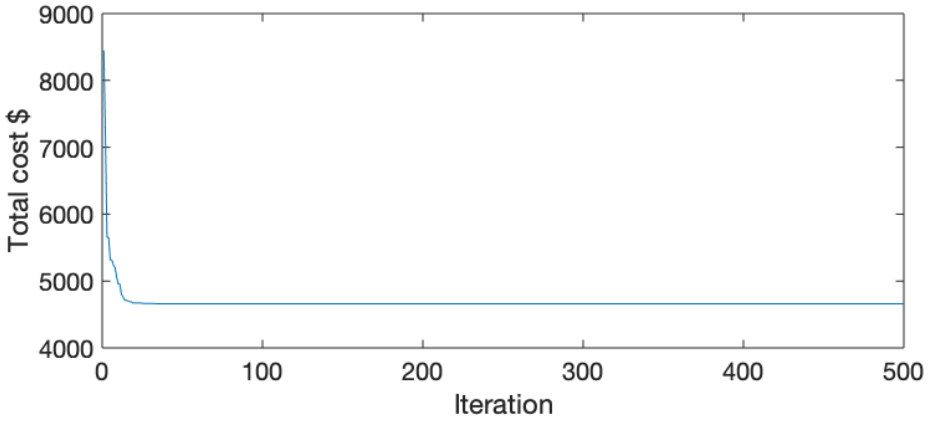

Figure 6.3. Convergence of PSO for the optimal solution

To verify the accuracy of the approach proposed in Section 4, it was set to run 100 times for the random nature of evolutionary is depicted in Figure 6.2. Based on the demand for heat (83.66MW) and power (20MW) as constraints, the results illustrate that the optimal cost of the system is 4596.87 $. Figure 6.3 illustrates the good performance of convergence in this algorithm to further clarify the feasibility of the system.

Table 10 illustrates the cost outcomes obtained from different sensitivity scenarios by considering practical requirements. These scenarios were carefully selected to ensure that they reflect reasonable test conditions, thereby providing stronger support for the effectiveness of our proposed method. The results unequivocally convey a strong message: our method is reliable and has broad applicability in various industrial settings.

Table 6.1 The variable results from sensitivity situations

Case	Changes in power (P) and heat (H) demand	Data ($)
1	P (95%) and H (95%)	4543.97
2	P (95%) and H (100%)	4592.11
3	P (95%) and H (105%)	4641.44
4	P (100%) and H (95%)	4549.31
5	P (100%) and H (100%)	4596.87
6	P (100%) and H (105%)	4643.56
7	P (105%) and H (95%)	4554.63
8	P (105%) and H (100%)	4602.39
9	P (105%) and H (105%)	4651.77

Summary

Because the system is composed of multi-energy storage and multi-energy supply, the economic calculation of the system becomes more complicated. However, the faster speed and better result characteristics of the evolutionary algorithm are more suitable for the economic

evaluation of the system. In this chapter, PSO in MATLAB can be used to solve the economic scheduling problem of this system, and it is evaluated as a CHP system. At the same time, cooling energy can be ignored due to the less amount of production. The results show that the algorithm has good performance and speed in solving CHPED problems to verify the economy of the system.

CHAPTER 7 CONCLUSION

7.1 Contributions and Concluding Remarks

The sustainable consumption of the high proportion of renewable energy requires more flexibility of MPSs. The AA-CAES system naturally has the flexibility of multi-energy supply and multi-energy reserve. The AA-CAES system coupled with solar energy resources is a typical cooling-heat-electricity combined power supply system, which can be used as an EH in the energy system and can effectively improve the comprehensive energy utilization level. This thesis focused on the key issues of comprehensive energy efficiency utilization of AA-CAES, proposed a CER with AA-CAES as the core, and carried out theoretical and simulation analysis from the overall process design, thermodynamic modelling and parameter configuration, turbine expansion power generation control strategy and other aspects. At the same time, the STC composite system is integrated to further improve the overall performance of the system. Therefore, a novel ST-AA-CAES is proposed in this thesis, utilizing the thermal energy storage and solar thermal to improve the system EXE, RTE and exergy efficiency. The economic performance of the system is verified by the PSO. The main achievements of the thesis are summarized as follows:

(1) As the future development direction of the energy industry, EI will change the centralized utilization mode of fossil energy in the traditional energy system, and realize the production, conversion, storage and consumption of safer and more economical clean energy by establishing a distributed comprehensive utilization mode of various forms of energy, thus greatly improving the comprehensive utilization efficiency of energy. To

support the development of a sustainable ecological civilization. Based on the principle and structure of the information router, the concept of the CER with AA-CAES as the core is proposed. Because AA-CAES has the natural endowment of a triple supply of cooling, heat and electricity, the CER based on this technology can not only realize the input and storage of clean energy such as wind, solar, electricity, and heat, but also realize the mutual conversion and output of multiple forms of energy such as high-grade heat, cooling and electricity. Thus, the future EI provides a variety of clean energy coordination and comprehensive utilization of key technology solutions.

(2) An integrated simulation model considering the off-design operating characteristics of AA-CAES was constructed, especially the characterization of the heat exchange and adiabatic conditions of the AA-CAES system. It can convert stored electric energy into high-grade electric energy, cooling energy, cascade thermal energy and other clean energy. Therefore, the validity of the simulation and system verification is verified. Some of the main conclusions of the proposed CER are as follows: The results show the changes in the compressor outlet pressure of air storage tank under the adiabatic and heat exchange conditions. When considering the air storage tank heat exchange, compared with the adiabatic condition of 2.5h, the compressor sixth stage under the adiabatic condition reaches the stable pressure within 3.4h. When compared with the actual data of the system, air storage tank under adiabatic condition is closer to the actual condition. The results of the exhaust process show that the adiabatic heat transfer of air storage tank does not affect the turbine outlet pressure, which meets the design requirements. At the same time, considering the accuracy of the model, it is necessary to consider the heat transfer problem of the medium-temperature regenerative unit. Finally, the efficiency of the system is

analysed from two aspects: first, the ratio of power consumption to power generation is 56.5%. Secondly, from the CER rate combined with cooling, heat and electricity, the overall efficiency of the system reaches 93.6%.

(3) The overall design process of the ST-AA-CAES system coupled with a STC subsystem is proposed. The STC subsystem is integrated into the system in Chapter 4, which further improves the overall performance of the system. Through thermodynamic modelling, the optimal configuration of compression/expansion series and thermodynamic parameter analysis of each subsystem, the main parameters that affect the efficiency of multi-energy flow conversion of each subsystem are revealed. On this basis, the influence laws of key parameters on the EXE, RTE and exergy efficiency of the whole system are described. The theoretical analysis results show that the inlet air temperature of the turbine is a key parameter affecting the system performance, which is closely related to the performance of the STC subsystem and the efficiency of the HEX. As the inlet air temperature increased, the EXE, RTE and exergy efficiency of the system increased significantly.

(4) To accurately verify the economic performance of the system, appropriate algorithm verification can be applied to the system. In this thesis, PSO as an evolutionary algorithm with fast response speed and high accuracy, it can be used to evaluate the economy of the ST-AA-CAES system. According to the requirements of heat energy (83.66MW) and power energy (20MW) of the system, the optimal cost of the system is 4596.87 $.

7.2 Future Works

The application and popularization of ST-AA-CAES in the IES cannot be separated from the improvement of its basic theory. Based on the work in this thesis, the following research can be further carried out: ST-AA-CAES technology involves interdisciplinary fields such as electrical, thermodynamics, heat transfer and fluid mechanics, which makes it difficult to develop a general simulation platform. At present, relevant research are still in the initial stage, and there is no mature overall simulation calculation model covering multiple time scales. In addition, the thermodynamic analysis in Chapter 4 of this thesis is only from the perspective of quasi-steady-state thermodynamic flow, and the performance evaluation of the full dynamic process system is still lacking.

In addition, the purpose of the IES is that have the synergistic effect of multi-energy flow carriers such as heat and power, while the unity and difference between energy flow must be considered in the multi-energy flow synergy. The existing research on the IES mainly introduces the separate study method of energy flow carriers such as electricity and heat into the analysis of the IES. However, this kind of research approach is difficult to describe the differences among various energy flow carriers. The descriptions of differences in energy flow grade can be considered as future research directions.

The model developed in this thesis is currently undergoing industrial scale experimental testing. Implementation of the system requires an area with abundant renewable energy sources such as wind and solar energy, sufficient power generation capacity, and also demand for comprehensive energy supply in both industrial and residential areas. Without these conditions, the system will not be able to fulfill its intended role.

References

[1] Word Wind Energy Association. WWEA Half-year Report 2022: WorldWide Windpower Boom Continues in 2022, 15 Nov 2022.

[2] P. A. Owusu, and S. A. Sarkodie, “A review of renewable energy source, sustainability issues and climate change mitigation,” Cogent Engineering, vol. 3, no. 1, 1167990, 16 Mar 2016.

[3] M. J. B. Kabeyi, and O. A. Olanrewaju, “Sustainable Energy Transition for Renewable and Low Carbon Grid Electricity Generation and Supply,” Front. Energy Res, vol. 9, 743114, 2021.

[4] J. Emblemsvag, “Wind energy is not sustainable when balanced by fossil energy,” Applied Energy, vol. 305, 117748, 2022.

[5] A. Akrami, M. Doostizadeh, F. Aminifar, “Power system flexibility: an overview of emergence to evolution,” Journal of Modern Power Systems and Clean Energy, vol. 7, pp. 987–1007, 2019.

[6] H. Blanco, A. Faaij, “A review at the role of storage in energy systems with a focus on Power to Gas and long-term storage,” Renewable and Sustainable Energy Reviews, vol. 81, no. 1, pp. 1049-1086, 2019.

[7] C. Liu, M.-S. Cheng, B.-C. Zhao, and Z.-M. Dai, “A Wind Power Plant with Thermal Energy Storage for Improving the Utilization of Wind Energy,” Energies, vol. 10, no. 12, p. 2126, Dec 2017.

[8] J. Jurasz, F.A. Canales, A. Kies, M. Guezgouz, A. Beluco, “A review on the complementarity of renewable energy sources: Concept, metrics, application and future research directions,” Solar Energy, vol. 195, pp. 703-724, 2020.

[9] G. Pulazza, N. Zhang, C. Kang and C. A. Nucci, "Transmission Planning With Battery-Based Energy Storage Transportation For Power Systems With High Penetration of Renewable Energy," IEEE Transactions on Power Systems, vol. 36, no. 6, pp. 4928-4940, Nov 2021

[10] H. M. Hussain, A. Narayanan, P. H. J. Nardelli and Y. Yang, "What is Energy Internet? Concepts, Technologies, and Future Directions," IEEE Access, vol. 8, pp. 183127-183145, 2020.

[11] R. Dai, R. Esmaeilbeigi and H. Charkhgard, "The Utilization of Shared Energy Storage in Energy Systems: A Comprehensive Review," IEEE Transactions on Smart Grid, vol. 12, no. 4, pp. 3163-3174, July 2021.

[12] J. McDowall, “Integrating energy storage with wind power in weak electricity grids,” Journal of Power Sources, vol. 162, pp. 959-964, 2020.

[13] Emerging energy storage technologies in Europe. Rapport Frost & Sullivan, 203.

[14] H. Chen, T. N. Cong, W. Yang, C. Tan, Y. Li, Y. Ding, “Progress in electrical energy storage system: A critical review,” Progress in Natural Science, vol. 19, no. 3, pp. 291-312, 2009.

[15] M. Beaudin, H. Zareipour, A. Schellenberglabe, W. Rosehart, “Energy storage for mitigating the variability of renewable electricity sources: An updated review,” Energy for Sustainable Development, vol. 14, no. 4, pp. 302-314, 2010.

[16] X. Luo, J. Wang, M. Dooner, J. Clarke, “Overview of current development in electrical energy storage technologies and the application potential in power system operation,” Applied energy, vol. 137, pp. 511-536, 2015.

[17] J. Kondoh, I. Ishii, H. Yamaguchi, A. Murata, K. Otani, K. Sakuta, N, Higuchi, S. Sekine, M. Kamimoto, “Electrical energy storage systems for energy networks,” Energy Conversion and Management, vol. 41, no. 17, pp. 1863-1874, 2000.

[18] S. M. Shoenung, “Characteristics and technologies for long- vs. short-term energy storage: a study by the DOE energy storage systems program,” Technical report. SAND2001-0765. Sandia National Laboratories. United States Department of Energy, 2021.

[19] B. Paul, “The future of electrical energy storage: the economics and potential of new technologies. Report,” Business Insights (Energy). 2009.

[20] F. A. Farret, M. G. Simões, “Integration of alternative sources of energy,” John Wiley & Sons Inc, pp. 262–300, 2006.

[21] S. J. Andrepont, “Energy storage – thermal energy storage coupled with turbine inlet cooling,” In: 14th annual electric power conf. & exhibition. n.d. Available at: <http://www.turbineinletcooling.org/res ources/papers/Andrepont_2012EP.pdf>.

[22] Piller power systems products. Energy storage. n.d. Available at: <http://www.piller.com/205/energy-storage>.

[23] Beacon power technology. Beacon Power Corporation. n.d. Available at: <http:// beaconpower.com/resource s/>.

[24] T. Fujihara, H. Imano, K. Oshima, “Development of pump turbine for seawater pumped-storage power plant,” Hitachi Rev, vol. 47, pp. 199–202, 1998.

[25] M. P. Moghaddam, M. R. Haghifam, G. R. Yousefi, “Electric energy storage systems in a market-based economy: comparison of emerging and traditional technologies,” Renew Energy, vol. 34, no. 12, pp: 2630–2639, 2009.

[26] A. Abele, E. Elkind, J. Intrator, Washom B, “2020 Strategic Analysis of Energy Storage in California,” University of California, Berkeley School of Law; University of California, Los Angeles; and University of California, San Diego. California Energy Commission, 2011.

[27] Electrical energy storage: white paper. Technical report. Prepared by electrical energy storage project team. International Electrotechnical Commission (IEC), Published December 2011. Available at: <http://www.iec.ch/ whitepaper/pdf/iecWP-energystorage-LR-en.pdf>.

[28] M. Finkenrath, S. Pazzi S, M. DErcole, “Status and technical challenges of advanced Compressed Air Energy Storage (CAES) technology,” International workshop on environment and alternative energy, 2009.

[29] S. Succar, R. H. Williams, A. Cavallo, C. K. Christopher, P. D. Nrel, D. C. Denkenberger, A. Kalinowski, M. J. McGill, R. H. Socolow, I. Vann, “Compressed Air Energy Storage : Theory , Resources , And Applications For Wind Power 8,” 2008.

[30] T. Sannomiya, H. Hayashi, T. Ishii, R. Ikeda, “Test results of compensation for load fluctuation under a fuzzy control by a 1 kW h/1MW SMES,” IEEE Trans Appl Supercond, vol. 11, pp. 1908–1911, 2001.

[31] W. F. Pickard, A. Q. Shen, N. J. Hansing, “Parking the power: strategies and physical limitations for bulk energy storage in supply–demand matching on a grid whose input power is provided by intermittent sources,” Renew Sust Energy Rev, vol. 13, pp. 1934–1945, 2009.

[32] CAP-XX supercapacitors product guide 2013. CAP-XX Ltd. [Online]. Available at: <http://www.cap-xx.com/products/products.php>.

[33] INGRID 39 MWh grid-connected renewable energy storage project. Fuel Cells Bull 2012.

[34] S. Mekhilef, R. Saidur, A. Safari, “Comparative study of different fuel cell technologies,” Renew Sust Energy Rev, vol. 16, pp. 981–989, 2012.

[35] F. Wu, B. Yang, J. Ye, Chapter 2 - Technologies of energy storage systems, Grid-scale Energy Storage Systems and Applications, Academic Press, pp. 17-56, 2019.

[36] M. King, A. Jain, R. Bhakar, J. Mathur, J. Wang, “Overview of current compressed air energy storage projects and analysis of the potential underground storage capacity in India and the UK,” Renewable and Sustainable Energy Reviews, vol. 139, 2021.

[37] A. Z. AL. Shaqsi, K. Sopian, A. Al-Hinai, “Review of energy storage services, applications, limitations, and benefits,” Energy Reports, vol. 6, pp. 288-306, 2020.

[38] B. C. Tashie-Lewis, S. G. Nnabuife, “Hydrogen Production, Distribution, Storage and Power Conversion in a Hydrogen Economy - A Technology Review,” vol. 8, 2021.

[39] O. Smith, O. Cattell, E. Farcot, R. D. Odea, K. I. Hopcraft, “The effect of renewable energy incorporation on power grid stability and resilience,” Science Advances, vol. 8, no. 9, 2022.

[40] B. Yang, J. Wang, Y. Chen, D. Li, C. Zeng, Y. Chen, Z. Guo, H. Shu, X. Zhang, T. Yu, L. Sun, “Optimal sizing and placement of energy storage system in power grids: A state-of-the-art one-stop handbook,” Journal of Energy Storage, vol 32, 2020.

[41] F. R. McLarnon, E. J. Cairns, “Energy storage,” vol. 14, pp: 241-271, 1989.

[42] B. Cleary, A. Duffy, A. OConnor, M. Conlon and V. Fthenakis, "Assessing the Economic Benefits of Compressed Air Energy Storage for Mitigating Wind Curtailment," IEEE Transactions on Sustainable Energy, vol. 6, no. 3, pp. 1021-1028, July 2015.

[43] I. Calero, C. A. Cañizares, K. Bhattacharya, "Compressed Air Energy Storage System Modeling for Power System Studies", IEEE Transactions on Power Systems, vol. 34, no. 5, pp. 3359-3371, 2019.

[44] X. Luo, J. Wang, M. Donner, J. Clarke, C. Krupke, “Overview of Current Development in Compressed Air Energy Storage Technology,” Energy Procedia, vol. 62, pp. 603-611, 2014.

[45] S. Succar, R. Williams, A. Cavallo, C. Christopher, Paul Denholm Nrel, D. Denkenberger, A. Kalinowski, M. McGill, R. Socolow, I. Vann. “Compressed Air Energy Storage: Theory, Resources, And Applications for Wind Power 8.” 2008.

[46] S. Koohi-Fayegh, M.A. Rosen, “A review of energy storage types, applications and recent developments,” Journal of Energy Storage, vol. 27, 2020.

[47] F. W Gay, Means for storing fluids for power generation: U.S. Patent 2433896, 1948.

[48] M. Budt, D. Wolf, R. Span, J. Yan, “A review on compressed air energy storage: Basic principles, past milestones and recent developments,” Applied Energy, vol. 179, pp. 250-268, 2016.

[49] D. R. Mack, "Something new in power technology," IEEE Potentials, vol. 12, no. 2, pp. 40-42, April 1993.

[50] S. Inage, “Prospects for large-scale energy storage in decarbonised power grids,” International Energy Agency, vol. 3, no. 4, 2009.

[51] L. Geissbühler, V. Becattini, G. Zanganeh, S. Zavattoni, M. Barbato, A. Haselbacher, A. Steinfeld, “Pilot-scale demonstration of advanced adiabatic compressed air energy storage, Part 1: Plant description and tests with sensible thermal-energy storage,” Journal of Energy Storage, vol. 17, pp. 129-139, 2018.

[52] H, Guo, Y. Xu, H. Chen, X. Zhou, “Thermodynamic characteristics of a novel supercritical compressed air energy storage system,” Energy conversion and management, vol. 115, pp. 167-177, 2016.

[53] Robert Morgan, Stuart Nelmes, Emma Gibson, Gareth Brett, “Liquid air energy storage – Analysis and first results from a pilot scale demonstration plant,” Applied Energy, vol. 137, pp. 845-853, 2015.

[54] A. Vecchi, Y. Li, Y. Ding, P. Mancarella, A. Sciacovelli, “Liquid air energy storage (LAES): A review on technology state-of-the-art, integration pathways and future perspectives,” Advances in Applied Energy, vol. 3, 2021.

[55] C. Bullough, C. Gatzen, C. Jakiel, M. Koller, “Advanced adiabatic compressed air energy storage for the integration of wind energy,” Proceedings of the European wind energy conference, EWEC, 22-25 Nov 2004.

[56] M. J. Hobson M J. Conceptual design and engineering studies of adiabatic compressed air energy storage (CAES) with thermal energy storage. Pacific Northwest Lab., Richland, WA (USA); Acres American, Inc., Columbia, MD, 1981.

[57] ADELE – adiabatic compressed air energy storage for electricity supply. RWE Power. Report. Published January 2010. <http://www.rwe.com/web/cms/mediablob/en/391748/data/364260/1/rwe-power-ag/innovations/Brochure-ADELE.pdf> [accessed 07.12.22].

[58] T. Wang, X. Yan, H. Yang, X. Yang, T. Jiang, S. Zhao, “A new shape design method of salt cavern used as underground gas storage,” Applied Energy, vol. 104, pp. 50-61, 2013.

[59] K. Zhao, Q. Wanyan, W. Liao, D. Zheng, L. Song, H. Xu, J. Wang, G. Pei, J. Wang, “Quantitative Evaluation Method for Gas Loss in Underground Natural Gas Storage Reconstructed from Abandoned Gas Reservoirs,” Arabian Journal for Science and Engineering, vol. 47, pp. 11587-11597, 2022.

[60] A. Soubeyran, A. Rouabhi, C. Coquelet, “Thermodynamic analysis of carbon dioxide storage in salt caverns to improve the Power-to-Gas process,” Applied Energy, vol. 242, pp. 1090-1107, 2019.

[61] W. Li, G. Chen, S. Ding, Y. Zhang, “A method for assessing the gas capacity based on thermodynamic state analysis for salt cavern during operation,” Journal of Energy Storage, vol. 50, 2022.

[62] X. Shi, Y. Li, C. Yang, Y. Xu, H. Ma, W. Liu, G. Ji, “Influences of filling abandoned salt caverns with alkali wastes on surface subsidence,” Environmental Earth Sciences, vol. 73, pp. 6939-6950, 2015.

[63] K. H. Lux, “Design of salt caverns for the storage of natural gas, crude oil and compressed air: Geomechanical aspects of construction, operation and abandonment,” Geological Society, London, Special Publications, vol. 313. no. 1, pp. 83-128, 2009.

[64] A.A. Solomon, Daniel M. Kammen, D. Callaway, “The role of large-scale energy storage design and dispatch in the power grid: A study of very high grid penetration of variable renewable resources,” Applied Energy, vol. 134, pp. 75-89, 2014.

[65] S. Mei, X. Xue, T. Zhang, X. Zhang, L. Chen, “China’s national demonstration project for compressed air energy storage achieved milestone in industrial operation,” iEnergy, vol. 1, no. 2, 2022.

[66] A. L. Facci, D. Sánchez, E. Jannelli, S. Ubertini, “Trigenerative micro compressed air energy storage: Concept and thermodynamic assessment,” Applied Energy, vol. 158, pp. 243-254, 2015.

[67] M. Cheayb, M. M. Gallego, M. Tazerout, S. Poncet, “A techno-economic analysis of small-scale trigenerative compressed air energy storage system,” Energy, vol. 239, Part A, 2022.

[68] H. Safaei, D. W. Keith, “Compressed air energy storage with waste heat export: An Alberta case study,” Energy Conversion and Management, vol. 78, pp. 114-124, 2014.

[69] H. Daneshi, A. Srivastava, “Security-constrained unit commitment with wind generation and compressed air energy storage,” IET Generation, Transmission and Distribution, vol. 6, no. 2, pp. 167-175, 2012.

[70] T. Nikolakakis, V. Fthenakis, “The value of compressed-air energy storage for enhancing variable-renewable-energy integration: The case of Ireland,” Energy Technology, vol. 5, no. 11, pp. 2026-2038, 2017.

[71] J. Zhan, O. A. Ansari, C. Chung, “Compressed air energy storage-part I: An accurate bi-linear cavern model,” arXiv preprint arXiv: 1709.08272, 2017.

[72] J. Zhan, Y. Wen, O. A. Ansari, C. Chung, “Compressed air energy storage-part II: Application to power system unit commitment,” arXiv preprint arXiv: 1709.08275, 2017.

[73] J. Zhang, K.-J. Li, M. Wang, W. -J. Lee and H. Gao, "A bi-level program for the planning of an islanded microgrid including CAES," 2015 IEEE Industry Applications Society Annual Meeting, pp. 1-8, 2015.

[74] H. Safaei, D. W. Keith, R. J. Hugo, “Compressed air energy storage (CAES) with compressors distributed at heat loads to enable waste heat utilization,” Applied Energy, vol. 103, pp. 165-179, 2013.

[75] H. T. Le, S. Santoso, “Operating compressed-air energy storage as dynamic reactive compensator for stabilising wind farms under grid fault conditions,” IET Renewable Power Generation, vol. 7, no. 6, pp. 717-726, 2013.

[76] G. Li, L. Chen, T. Zheng, S. Mei, Y. Fan, Q. Lu, “Preliminary Investigation on Operation Mode of Compressed Air Energy Storage System as Synchronous Condenser,” Journal of Global Energy Interconnection, vol. 1, no. 3, pp. 348-354, 2018.

[77] X.Wang, L. Duan, Z. Zhu, “Peak regulation performance study of GTCC based CHP system with compressor inlet air heating method,” Energy, vol. 262, Part A, 125366, 2023.

[78] M. Mohammadi, Y. Noorollahi, B. Mohammadi-ivatloo, H. Yousefi, “Energy hub: From a model to a concept – A review,” Renewable and Sustainable Energy Reviews, vol. 80, pp. 1512-1527, 2017.

[79] H. Zhang, A.Tomasgard, B. R. Knudsen, H. G. Svendsen, S. J. Bakker, I. E. Grossmann, “Modelling and analysis of offshore energy hubs,” Energy, vol. 261, Part A, 125219, 2022.

[80] J. Cao, B. Yang, S. Zhu, C. Chen, X. Guan, “Distributionally robust heat-and-electricity pricing for energy hub with uncertain demands,” Electric Power Systems Research, vol. 211, 10833, 2022.

[81] T. Ma, J. Wu, L. Hao, D. Li, “Energy flow matrix modeling and optimal operation analysis of multi energy systems based on graph theory,” Applied Thermal Engineering, vol. 146, pp. 648-663, 2019.

[82] D. Zou, D. Gong, “Differential evolution based on migrating variables for the combined heat and power dynamic economic dispatch,” Energy, vol. 238, Part A, 121664, 2022.

[83] M. Locatelli, F. Schoen, “(Global) Optimization: Historical notes and recent developments,” EURO Journal on Computational Optimization, vol. 9, 100012, 2021.

[84] Hanif D. Sherali, Patrick J. Driscoll, “Evolution and state-of-the-art in integer programming,” Journal of Computational and Applied Mathematics, vol. 124, no. 1-2, pp. 319-340, 2000.

[85] T. Guo, M. I. Henwood and M. V. Ooijen, "An algorithm for combined heat and power economic dispatch," IEEE Transactions on Power Systems, vol. 11, no. 4, pp. 1778-1784, Nov 1996.

[86] A. Rong, H. Hakonen, R. Lahdelma, “An efficient linear model and optimisation algorithm for multi-site combined heat and power production,” European Journal of Operational Research, vol. 168, no. 2, pp. 612-632, 2006.

[87] S. Makkonen, R. Lahelma, “Non-convex power plant modelling in energy optimisation,” European Journal of Operational Research,” vol. 171, no. 3, pp. 1113-1126, 2006.

[88] A. Rong, R. Lahdelma, “An efficient linear programming model and optimization algorithm for trigeneration,” Applied Energy, vol. 82, no. 1, pp. 40-63, 2005.

[89] H. Lund, A. N. Andersen, P. A. Ostergaard, B. V. Mathiesen, D. Connolly, “From electricity smart grids to smart energy systems – A market operation based approach and understanding,” Energy, vol. 42, no. 1, pp. 96-102, 2012.

[90] Theis Bo Harild Rasmussen, Qiuwei Wu, Menglin Zhang, “Combined static and dynamic dispatch of integrated electricity and heat system: A real-time closed-loop demonstration,” International Journal of Electrical Power & Energy Systems, vol. 143, 107964, 2022.

[91] H. Lund, I. R. Skov, J. Z. Thellufsen, P. Sorknæs, A. D. Korberg, M. Chang, B. V. Mathiesen, M. S. Kany, “The role of sustainable bioenergy in a fully decarbonised society,” Renewable Energy, vol. 196, pp. 195-203, 2022.

[92] X. Chen, C. Kang, M. O’Malley, Q. Xia, J. Bai, C. Liu, R. Sun, W. Wang, H. Li, “Increasing the Flexibility of Combined Heat and Power for Wind Power Integration in China: Modeling and Implications,” IEEE Transactions on Power Systems, vol. 30, no. 4, pp. 1848-1857, 2015.

[93] Z. Li, W. Wu, M. Shahidehpour, J. Wang and B. Zhang, "Combined Heat and Power Dispatch Considering Pipeline Energy Storage of District Heating Network," IEEE Transactions on Sustainable Energy, vol. 7, no. 1, pp. 12-22, Jan 2016.

[94] N. Good, E. Karangelos, A. Navarro-Espinosa and P. Mancarella, "Optimization Under Uncertainty of Thermal Storage-Based Flexible Demand Response With Quantification of Residential Users’ Discomfort," IEEE Transactions on Smart Grid, vol. 6, no. 5, pp. 2333-2342, Sept 2015.

[95] J. Huang, Z. Li, Q.H. Wu, “Coordinated dispatch of electric power and district heating networks: A decentralized solution using optimality condition decomposition,” Applied Energy, vol. 206, pp. 1508-1522, 2017.

[96] C. Lin, W. Wu, B. Zhang and Y. Sun, "Decentralized Solution for Combined Heat and Power Dispatch Through Benders Decomposition," IEEE Transactions on Sustainable Energy, vol. 8, no. 4, pp. 1361-1372, Oct 2017.

[97] Pengfei Jie, Zhe Tian, Shanshan Yuan, Neng Zhu, “Modeling the dynamic characteristics of a district heating network,” Energy, vol. 39, no. 1, pp. 126-134, 2012.

[98] Wei Zhong, Encheng Feng, Xiaojie Lin, Jinfang Xie, “Research on data-driven operation control of secondary loop of district heating system,” Energy, vol. 239, Part B, 122061, 2022.

[99] Q. Chen, R. Fu, Y. Xu, “Electrical circuit analogy for heat transfer analysis and optimization in heat exchanger networks,” Applied Energy, vol. 139, pp. 81-92, 2015.

[100] Q. Chen, Y. Wang, Y. Xu, “A thermal resistance-based method for the optimal design of central variable water/air volume chiller systems,” Applied Energy, vol. 139, pp. 119-130, 2015.

[101] A. Rong, R. Lahdelma, “An effective heuristic for combined heat-and-power production planning with power ramp constraints,” Applied Energy, vol. 84, no. 3, pp. 307-325, 2007.

[102] Christopher J. Quarton, Sheila Samsatli, “Power-to-gas for injection into the gas grid: What can we learn from real-life projects, economic assessments and systems modelling?,” Renewable and Sustainable Energy Reviews, vol. 98, pp. 302-316, 2019.

[103] X. Yang, G. Chai, X. Liu, M. Xu, Q. Guo, “Storage-Transmission Joint Planning Method to Deal with Insufficient Flexibility and Transmission Congestion,” Front. Energy Res, 2021.

[104] D. Gielen, F. Boshell, D. Saygin, M. D. Bazilian, N. Wagner, R. Gorini, “The role of renewable energy in the global energy transformation,” Energy Strategy Reviews, vol. 24, pp. 38-50, 2019.

[105] J. Vogel, J. K. Steinberger, D. W. O'Neill, W. F. Lamb, J. Krishnakumar, “Socio-economic conditions for satisfying human needs at low energy use: An international analysis of social provisioning,” Global Environmental Change, vol. 69, 102287, 2021.

[106] Wind energy in Europe. 2021 Statistics and the outlook for 2022-2026. <https://www.anev.org/wp-content/uploads/2022/02/220222-Stats-Outlook.pdf> [accessed 03.09.17]

[107] W. Ding, Z. Yan, R. H. Deng, "A Survey on Future Internet Security Architectures," IEEE Access, vol. 4, pp. 4374-4393, 2016.

[108] Y. Zha, T. Zhang, Z. Huang, Y. Zhang, “Analysis of energy internet key technologies,” Scientia Sinica Informationis, vol. 44, no. 6, June 2014.

[109] J. Cao, K. Meng, J. Wang, M. Yang, “An energy Internet and energy routers,” Scientia Sinica Informationis, vol. 44, no. 6, June 2014.

[110] J. Rifkin, “The third industrial revolution: how lateral power is transforming energy,” New Yorl: Palgrave MacMilla, pp. 88-106, 2011.

[111] L. Chen, T. Zheng, S. Mei, X. Xue, B. Liu, Q. Lu, “Review and prospect of compressed air energy storage system,” Journal of Modern Power Systems and Clean Energy, vol. 4, pp. 529-541, 2016.

[112] C. Ni, X. Xue, S. Mei, X. -P, Zhang, X. Chen, ‘Technological research of a clean energy router based on advanced adiabatic compressed air energy storage system’, Entropy, vol. 20, no. 12, 1440, 2020.

[113] A. Arabkoohsar, M. Dremark-Larsen, R. Lorentzen, G.B. Andresen, “Subcooled compressed air energy storage system for coproduction of heat, cooling and electricity,” Applied Energy, vol. 205, pp. 602-614, 2017.

[114] Sixian Wang, Xuelin Zhang, Luwei Yang, Yuan Zhou, Junjie Wang, “Experimental study of compressed air energy storage system with thermal energy storage,” Energy, vol. 103, pp. 182-191, 2016.

[115] F. D. S. Steta, “Modeling of an advanced adiabatic compressed air energy storage (AA-CAES) unit and an optimal model-based operation strategy for its integration into power markets,” EEH Power Systems Laboratory Swiss Federal Institute of Technology (ETH), 2010.

[116] N. Zhang, R. Cai, “Analytical solutions and typical characteristics of part-load performances of single shaft gas turbine and its cogeneration,” Energy Conversion and Management, vol. 43, no. 9-12, pp. 1323-1337, 2002.

[117] Isil Yazar, Hasan Serhan Yavuz, Arzu Altin Yavuz, “Comparison of various regression models for predicting compressor and turbine performance parameters,” Energy, vol. 140, Part 2, pp. 1398-1406, 2017.

[118] W. Zhang, X. Xue, F. Liu, “Modelling and experimental validation of advanced adiabatic compressed air energy storage with off-design heat exchanger,” IET Renewable Power Generation, vol. 14, no. 3, pp. 389-398, 2020.

[119] L. Geissbühler, V. Becattini, G. Zanganeh, “Pilot-scale demonstration of advanced adiabatic compressed airenergy storage, part 1: Plant description and tests with sensible thermal-energy storage,” Journal of Energy Storage, vol. 17, pp. 129-139, 2018.

[120] C. Jakiel, S. Zuntft, A. Nowi, “Adiabatic compressed air energy storage plants for efficient peak load power supply from wind energy: the european project AA-CAES,” International Journal of Energy Technology and Policy, vol. 5, no.3, pp. 296-306, 2007.

[121] A. Sciacovelli, Y. Li, H.Chen, Y. Wu, J. Wang, S. Garvey, Y. Ding, “Dynamic simulation of Adiabatic Compressed Air Energy Storage (A-CAES) plant with integrated thermal storage –

Link between components performance and plant performance," Applied Energy, vol. 185, Part 1, pp. 16-28, 2017.

[122] S. Wang, X. Zhang, L. Yang, Y. Zhou, J. Wang, "Experimental study of compressed air energy storage system with thermal energy storage," Energy, vol. 103, pp. 182-191, 2016.

[123] S. Mei, R. Li, X. Xue, Y. Chen, Q. Lu, X. Chen, C. D. Ahrens, R. Li, L. Chen, "Paving the way to smart micro energy grid: concepts, design principles, and engineering practices," CSEE Journal of Power and Energy Systems, vol. 3, no. 4, pp. 440-449, Dec 2017.

[124] S. Mei, J. Wang, T. Fang, L. Chen, X. Xue, Q. Lu, Y. Zhou, X. Zhou, "Design and engineering implementation of non supplementary fired compressed air energy storage system: TICC-500," Science China Technological Sciences, vol. 58, no. 4, pp. 600-611, 2015.

[125] R. Li, H. Wang, H. Wang, "Dynamic simulation of a cooling, heating and power system based on adiabatic compressed air energy storage," Renewable Energy 2019.

[126] L. Chen, M. Xie, P. Zhao, "A novel isobaric adiabatic compressed air energy storage (ia-caes) system on the base of volatile fluid," Applied Energy, vol. 210, pp. 198-210, 2018.

[127] R. Kushnir, A. Dayan, A. Ullmann, "Temperature and pressure variations within compressed air energy storage caverns," International Journal of Heat and Mass Transfer, vol. 55, no. 21–22, 2012.

[128] S. A. Kalogirou, "Solar thermal collectors and applications," Progress in Energy and Combustion Science, vol. 30, no. 3, pp. 231-295, 2004.

[129] M. Ebrahimi, A. Keshavarz, "8 - CCHP Thermal Energy Storage," Combined Cooling, Heating and Power, Elsevier, pp. 183-188, 2015

[130] X. Xue, X. Chen, S. Mei, L. Chen, Q. Lin, "Performance of Non-Supplementary Fired Compressed Air Energy Storage with Molten Salt Heat Storage," Transactions of China Electrotechnical Society, vol. 31, no. 14, pp. 11-20, 2016.

[131] M. Raju, S. K. Khaitan, "Modeling and simulation of compressed air storage in caverns: A case study of the Huntorf plant," Applied Energy, vol. 89, no. 1, pp. 474-481, 2012.

[132] X. Li, Y.J. Dai, R.Z. Wang, "Performance investigation on solar thermal conversion of a conical cavity receiver employing a beam-down solar tower concentrator," Solar Energy, vol. 114, pp. 134-151, 2015.

[133] Erminia Leonardi, "Detailed analysis of the solar power collected in a beam-down central receiver system," Solar Energy, vol. 86, no. 2, pp. 734-745, 2012.

[134] Y. S. H. Najjar, J. Sadeq, “Modeling and simulation of solar thermal power system using parabolic trough collector,” Journal of Energy Engineering, vol. 143, no. 2, 04016056, 2016.

[135] M. J. Ahmad, G. N. Tiwari, “Solar radiation models–review,” International journal of energy and environment, vol. 1, no. 3, pp. 513-532, 2010.

[136] M. Eltaweel, A. A. Abdel-Rehim, A. A.A. Attia, “Energetic and exergetic analysis of a heat pipe evacuated tube solar collector using MWCNT/water nanofluid,” Case Studies in Thermal Engineering, vol. 22, 100743, 2020.

[137] L. Szablowski, P. Krawczyk, K. Badyda, S. Karellas, E. Kakaras, W. Bujalski, “Energy and exergy analysis of adiabatic compressed air energy storage system,” Energy, vol. 138, pp. 12-18, 2017.

[138] P. Ktistis, R.A. Agathokleous, S. A. Kalogirou, “A design tool for a parabolic trough collector system for industrial process heat based on dynamic simulation,” Renewable Energy, vol. 183, pp. 502-514, 2022.

[139] J. Farzad, A. Emad, A. Hossein, “Energy and exergy of heat pipe evacuated tube solar collectors,” Thermal Science, vol. 20, pp. 327-335, 2016.

[140] H. Moradi, S. A. A. Mirjalily, S. A. Oloomi, H. Karimi, “Performance evaluation of a solar air heating system integrated with a phase change materials energy storage tank for efficient thermal energy storage and management,” Renewable Energy, vol. 191, pp. 974-986, 2022.

[141] L. Li, D. He, J. Jin, “Multi-objective load dispatch control of biomass heat and power cogeneration based on economic model predictive control’,” Energies, vol. 14, 762, 2021.

[142] V. K. Jadoun, G. R. Prashanth, S. S. Joshi, K. Narayanan, H. Malik, F. P. G. Márquez, “Optimal fuzzy based economic emission dispatch of combined heat and power units using dynamically controlled Whale Optimization Algorithm,” Applied Energy, vol. 315, 119033, 2022.

[143] B. Shi, L. -X. Yan, W. Wu, “Multi-objective optimization for combined heat and power economic dispatch with power transmission loss and emission reduction,” Energy, vol. 56, pp. 135-143, 2013.

[144] Y. -G. Son, B. -C. Oh, M. A. Acquah, R. Fan, D. -M. Kim and S. -Y. Kim, "Multi Energy System With an Associated Energy Hub: A Review," IEEE Access, vol. 9, pp. 127753-127766, 2021.

[145] F. Sohrabi, F. Jabari, P. Pourghasem, “Combined heat and power economic dispatch using particle swarm optimization– optimization of power system problems: methods, algorithms and matlab code,” Springer International Publishing, pp. 127-141, 2020.

PUBLICATIONS

Journal Papers

[1] C. Ni, X. Xue, S. Mei, X.-P, Zhang, X. Chen, 'Technological research of a clean energy router based on advanced adiabatic compressed air energy storage system', Entropy, vol. 20, no. 12, 1440, 2020.

[2] J. Zhai, M. Zhou, J. Li, X.-P. Zhang, G. Li, C. Ni, W. Zhang, "Hierarchical and Robust Scheduling Approach for VSC-MTDC Meshed AC/DC Grid With High Share of Wind Power," IEEE Transactions on Power Systems, vol. 36, no. 1, pp. 793-805, Jan 2021.

[3] X. Chen, J. Zhai, Y. Jiang, C. Ni, S. Wang, P. Nimmegeers, "Decentralized Coordination Between Active Distribution Network and Multi-Microgrids Through a Fast ADMM-based Adjustable Robust Operation Framework," Sustainable Energy, Grids and Networks, vol. 34, 101068, 2023.

[4] C. Ni, L. Chen, X. Chen, J. Zhai, S. Mei, X.-P. Zhang, "Exergy Analysis and Particle Swarm Optimization (PSO) of a Solar-thermal-Assisted Clean Energy Router (CER) Based on Advanced Adiabatic Compressed Air Energy Storage System (AA-CAES)," IET Renewable Power Generation, vol. 17, no. 9, pp. 2302-2314, 2023.

Conference Papers

[5] J. Zhai, C. Ni, P. Nimmegeer, Y. Jiang, "Coordinating Active Distribution Networks with Multi-Microgrids: An ADMM-based Decentralized Adjustable Robust Operation Model," 2022 International Conference on Power Energy Systems and Applications (ICoPESA), pp. 443-447, 2022.